2016

Understanding biofuel production systems from an economic and environmental perspective

Longwen Ou
Iowa State University

Understanding biofuel production systems from an economic and environmental perspective

by

Longwen Ou

A dissertation submitted to the graduate faculty

in partial fulfillment of the requirements for the degree of

DOCTOR OF PHILOSOPHY

Co-majors: Mechanical Engineering; Biorenewable Resources Technology

Program of Study Committee:
Robert Brown, Co-major Professor
Mark Wright, Co-major Professor
Song-Charng Kong
Guiping Hu
Kurt Rosentrater

Iowa State University

Ames, Iowa

2016

DEDICATION

I dedicated this dissertation to my grandparents, my parents, and my brother Longwu Ou. They are the source of my motivation. I will never be able to complete the work without their support.

TABLE OF CONTENTS

ACKNOWLEDGEMENTS

I am more than happy to take this opportunity to express my deep gratitude to all the people that have helped, supported, and encouraged me during my Ph.D. study.

First of all, I would like to thank my co-major professors Dr. Robert Brown and Dr. Mark Wright. I want to thank Dr. Brown for his guidance on my research. I have benefited a lot from his broad perspective and expert knowledge. I also thank Dr. Wright for his patience and for teaching me many useful skills that would be beneficial in my future research.

I would also like to thank my committee members Dr. Song-Charng Kong, Dr. Guiping Hu and Dr. Kurt Rosentrater for their support throughout my Ph.D. study.

In addition, I would like to thank my friends and colleagues Joe Polin, Qi Dang, Wenqin Li, Rajeeva Thilakartne, Tannon Daugaard, Yuan Xue, Fenglei Qi, Denis, Bbosa, Nataliya Apanovich and Mitchell Amundson for their generous help and support. I would also like to thank previous colleagues Kaige Wang, Yanan Zhang, Dr. Tristan Brown and Kwang Ho Kim for their guidance during my Ph.D. program.

At last, I want to give my sincere thanks to my families. Their generous support and encouragement is the source of my power and motivation. I would never be able to complete the work without them.

CHAPTER 1 INTRODUCTION

Biofuels

Biomass is organic materials of recent biological origin [1]. Biomass can be converted to a variety of useful products such as transportation fuels, chemicals, and natural fibers [1]. One thing that differentiate biomass from other renewable energy sources like wind and solar energy is that it can be converted into liquid, commonly called biofuels [1, 2]. Ethanol and biodiesel are the most familiar biofuels in use today [2].

Biochemical & thermochemical routes

There are two main two pathways for converting biomass into biofuels, i.e., biochemical and thermochemical. Biochemical processing of biomass uses enzymes and microorganisms to convert plant polymers into fuels, chemicals, or electric power [3]. Ethanol produced from fermentation is an example of biochemical route. Thermochemical processing of biomass uses heat and catalysts for the same purpose. Typical thermochemical routes include combustion, fast pyrolysis, gasification, hydrothermal liquefaction [3]. Hybrid pathway combines the two to achieve the conversion of biomass into transportation fuels. An example would be ethanol produced from fermentation of syngas produced by biomass gasification.

Biochemical and thermochemical processing of biomass are distinct in many ways. Thermochemical conversion is rapid and takes much shorter time than biochemical conversions. Thermochemical conversion also eliminates the sterilization process which is necessary for most biochemical conversions.

Techno-economic analysis

There are many distinct pathways under investigation for the conversion of biomass into transportation fuels. They all have advantages and disadvantages compared to each other. For example, thermochemical conversion of biomass avoids sterilization step and significantly accelerate the conversion at the cost of higher energy demand and thus higher operation cost when compared to biochemical pathways. It is thus crucial to determine which pathway has the greatest potential of economically competing with petroleum oil.

Techno-economic analysis (TEA) has been utilized as a common tool to compare economic feasibility across various pathways [4-8]. It takes into account all the costs associated with the process of biofuel production and generates a breakeven price for the main product under certain financial assumptions. It is recognized as a powerful tool for evaluating economic feasibility by providing information about composition of capital cost, operation cost and breakeven product price. TEA provides decision makers with valuable information about process economics and facilitates comparison across processes involving distinct technologies and end products.

Generally speaking, TEA compares cost and revenue for a specific process to understand the process economics. Input information for TEA falls into two categories. The first category is process-related, including plant capacity, product yield etc. The information may either come from published literature, or from a detailed process model using commercial software such as Aspen Plus and ChemCAD. Detailed mass and energy balance information is extracted from the modeling results and serves as important input for the subsequent analysis. The second category is economic assumptions that reflects common economic

conditions for the process under investigation. [9] provides useful assumptions for these processes. These assumptions include internal rate of return, interest rate, working capital, etc. The costs associated with a biofuel production system mainly includes capital investment and operation cost. Capital investment comprise investment for purchasing and installing process equipment, contingency, working capital, land cost, etc. [9, 10]. Operating cost includes feedstock cost, cost for utilities such as cooling water and superheated steam, waste disposal, labor cost, and maintenance cost, etc. [9, 10].

Life cycle assessment

Biofuel attracts public attention due to its potential environmental advantages over traditional fossil fuels [11, 12]. Since biomass is capable of fixing atmospheric CO_2 during growth, production and consumption of biofuels effectively create a carbon cycle instead of releasing net carbon dioxide to the atmosphere as occurs in burning fossil fuels [13, 14]. It is hence imperative to quantify emissions from biofuel life cycle so that a comparison between biofuels and fossil fuels can be made. Life cycle analysis (LCA) is a common and powerful tool used for this purpose.

Life cycle assessment (LCA) is an analytical methodology used for quantitative evaluation of energy, materials, wastes and emissions of a product system throughout its full life cycle along with an examination of associated environmental impacts [15]. The basic idea of LCA is to assess all environmental burdens associated with a product or service, from raw materials extraction to waste removal and treatment [16]. It is widely used as a tool of environmental effect assessment and decision making [17]. LCA has been seen both in academic literatures and reports targeting policy makers to describe the environmental impacts

associated with alternative production pathways and comparisons between several potential environment-related policy decisions [18-21].

Components of LCA

A complete LCA consists of four components: (1) goal and scope definition; (2) inventory analysis; (3) life cycle impact assessment (LCIA); and (4) interpretation.

Goal and scope definition plays a central role in LCA [16]. It defines many significant factors of a specific analysis, including the reason of a LCA, the goal, depth, the system to be investigated, system boundaries, functional units, main assumptions, the kind of impact assessment and valuation, etc. [16].

Inventory analysis is the best developed part of LCA. It is also the most scientific and labor-intensive component [16, 22]. Inventory analysis requires that all activities related to the production of one functional unit of the product are analyzed. The activities investigated in inventory analysis include raw material extraction, production of intermediate products, production of the end product, consumption of the product and waste treatment [16]. Outputs of inventory analysis include co-products, emissions to the environment, waste heat and solid wastes [16].

Life cycle impact assessment attempts to examine the potential environmental impacts of a product system [15]. It is performed for comparison among differing product systems as well as a more comprehensive understanding of the system investigated. Impact assessment associates inventory data with particular environmental issues using defined impact categories. The impact categories reflect environmental concerns related with common product systems. A list of impact categories can be found in **Table 1** [16].

In practice, components that are identified to have adverse human and environmental effects for each impact category are targeted for inventory data

collection. The inventory data is converted into a numerical category indicator using simplified assumptions [15]. A simple example of category indicator is carbon dioxide equivalents obtained from all greenhouse gases.

Four steps must be performed in order to convert inventory data into category indicator [16]:

1. Classification: the process of assigning the parameters of the inventory data to the impact categories.
2. Characterization: the process of transforming classified data quantitatively to indicate the contribution of the product system per functional unit to each category.
3. Normalization: calculation of ratio of emission per functional unit to the total (global or national emission).
4. Weighting (Valuation): subjective decision of weighting of each category.

Interpretation aims at a critical evaluation of the LCA. It includes investigating impact assessment with mathematical tools such as sensitivity analysis and linking LCA with corresponding applications such as product development and improvement, strategic planning [16].

Table 1 List of categories [16]

Input related categories ("resource depletion")
Abiotic resources (deposits, flows)
Biotic resources
Land
Output related categories ("pollution")
Greenhouse gases
Depletion of stratospheric ozone
Human toxicological impacts
Ecotoxicological impacts
Photo-oxidant formation
Acidification
Eutrofication (including BOD and heat)
Odor
Noise
Radiation
Casualties

Incorporation of geographic information into LCA

Traditional LCA aims at evaluation total emissions associated with a product system. High level (i.e. country level) average data are usually utilized in the analysis for this purpose. The result of traditional LCA provides information on the environmental effect of a product system. However, regional information is missing from the results. That is to say, traditional LCA calculates the total emission of a product system while providing no information on where and when the emission occurs. In reality these information is valuable for understanding life cycle impact of emissions, especially non-greenhouse-gas emissions [23]. Also site-specific characteristics such as climate, soil type, water availability may have major impacts on the environmental impacts. For these reasons regionalized LCA has been a hot

research topic in recent years where the location of emissions is reported as well as the total amount. Regionalized LCA is able to provide information such as: a) where the process has the least impact; b) optimal production chain design taking into account locally specific technology. Tessum et al. [23] developed a spatially and temporally explicit life cycle inventory of air pollutants for gasoline and ethanol production and consumption. The model is capable of reporting spatial and temporal aspects of emissions. These information is then used as a basis for advanced air dispersion modeling [24-26]. Mutel and Hellweg [27] proposed a generic methodology to couple existing regionalized characterization factors with large life cycle inventory databases to allow for detailed geographic life cycle impact assessment results.

Geographic information systems (GIS) has been integrated into life cycle inventory calculation to utilize geospatial information in LCA [28, 29]. Many of these studies use spatial grids for discretization and refinements of LCA results have been claimed. It is found that appropriate spatial scale is a key to realizing the potential of regionalized LCA [30-32]. Appropriate spatial scales have to be selected in order to minimize spatial uncertainty of LCA results. However, this process leads to a heterogeneity of spatial units when conducting impact assessment, which makes the calculation of the regionalized impact assessment characterization factors more difficult [33].

Uncertainty analysis

Since many of the technologies for which TEA and LCA are conducted are still in early development stage, only limited information about them is available. There is hence intrinsic uncertainty associated with the results. In order for the

results of TEA and LCA to be more robust and informative, it is imperative to report the uncertainty together with the results.

Uncertainties can be classified in many ways. Parameter uncertainty refers to uncertainty in observed or measured values used in a model, considering that parameters may be inherently variable and random. Scenario uncertainty relates to, for example, the normative choices in constructing scenarios and the inherent variability in scenario characteristics given various conditions such as geographical locations or situations. There also exists uncertainty associated with model structure or mathematical representation of the model. [34]

Uncertainty of LCA results has been identified decades ago. Lloyd and Ries summarized common sources of uncertainty in LCA as listed in **Table 2** [34].

Uncertainty of TEA has also attracted attention in recent years. Many researchers incorporated uncertainty analysis into their reports by considering probability distribution of model input parameters [35, 36]. Some analysis report a standard deviation as large as 25% [36]. Brown [37] analyzed probability distribution of the 20-year net present values (NPV) of six thermochemical cellulosic biofuel pathways. The results suggest that asymmetrical probability distributions increase the standard deviation of the NPV cumulative distribution by up to 35% relative to symmetrical distributions. Li et al. [38] compared TEA results of in-situ and ex-situ fast pyrolysis pathways for biofuel production. The results suggest similar breakeven selling price for in-situ and ex-situ catalytic fast pyrolysis but standard deviation of in-situ pathway is higher than that of ex-situ pathway.

Input uncertainty mainly derives from parameter variability. Sensitivity analysis or stochastic modeling are usually used to deal with input uncertainty. In sensitivity analysis, a group of parameter that have high impact on the result is identified first.

One parameter is varied at a time with several values while other parameters remain fixed [36]. The model runs again with the new data set and this process is repeated for each parameter. An alternative is to define a limited number of scenarios with specific but consistent realizations of each parameter and run the model for each scenario [39].

Table 2 Example sources of uncertainty in LCA [34]

Sources of uncertainty	**Parameter**	**Scenario**	**Model**
Random error and statistical variation	Parameter measurement error	Imperfect fit of data to regressions for evaluating trends and forecasting	Measurement error in physical constants or modeled relationships
Systematic error and subjective judgment	Methods for estimating missing data	Developing scenarios based on past trends, using value judgment	Extrapolating relationships from well-studied processes to similar processes
Variability	Inherent geographical, temporal and technological variability in parameter data	Inherent variability in scenario characteristics	Inherent variability in process relationships
Inherent randomness	Simplification of fluctuations in measured variables	A scenario in which simplified characteristics are used	Inconsistent process characteristics
Expert uncertainty	A single parameter value is not widely accepted	Estimates of scenario characteristics	Disagreement about process mechanisms and system behavior
Approximation	Characterizing parameters by a few important properties	Choice of functional unit, allocation rules, system boundaries, cut-off criteria	Simplifications of real-world systems, such as system boundaries

Stochastic modeling is one of the most popular methods employed to integrate uncertainty analysis into TEA and LCA. Stochastic modeling uses results from a large number of runs to investigate model uncertainty. It uses pre-determined probability distribution for each input parameter. Distributions that are used extensively include [39]:

- normal distribution;
- lognormal distribution;
- triangular distribution;
- uniform distribution.

Each input parameter is first sampled from the pre-determined distribution. Usually thousands of samples are required to achieve satisfactory results. The model is then run for each sample combination of input parameters. The results from the runs are then used to infer the true distribution of the result. This method relies on the modern computing power since it requires many times of repetition of calculations with varied input parameters. Random sampling is the most common sampling method used in stochastic modeling, while other advanced sampling techniques such as Latin hypercube sampling were also employed for improved sampling efficiency.

Uncertainty of the output is usually inferred using the results from stochastic modeling. The result may include an average value with boundary values and standard deviation, and cumulative distribution functions and /or probability density functions [34, 38].

Analytical methods can also be used for uncertainty analysis. It quantifies uncertainty of the results by building explicit mathematical expression for the distribution of the results [39]. It is based on a first-order approximation of Taylor

expansion of the underlying model [39]. The method is not widely applied due to its difficulty in implementation [39].

Non-traditional methods have also been employed in LCA uncertainty analysis. However, their applicability compared to the traditional methods is still controversial [34, 40]. Non-traditional methods have not seen many applications in TEA uncertainty analysis.

The objective of this dissertation is to demonstrate a systematic methodology for evaluating economic and environmental performance of a biofuel production system with integrated uncertainty analysis. Chapter 1 introduces basics and fundamentals of related concepts. Chapter 2 demonstrates the TEA methodology with a case study of transportation fuels production from defatted algae hydrothermal liquefaction. Chapter 3 describes a TEA study to analyze the economic feasibility of co-located first and second generation ethanol plants. Chapter 4 evaluates the environmental impact of producing electricity from co-firing bio-oil co-firing fuel (BCF) with traditional coal. Chapter 5 demonstrates uncertainty analysis of TEA results by a case study of transportation fuel production via biomass gasification and mixed alcohol synthesis.

References

[1] Brown RC, Brown TR. Biorenewable resources: engineering new products from agriculture: John Wiley & Sons; 2013.

[2] NREL. Biofuels Basics. Learning About Renewable Energy; 2015.

[3] Brown RC, Stevens C. Thermochemical processing of biomass: conversion into fuels, chemicals and power: John Wiley & Sons; 2011.

[4] Thilakaratne R, Wright MM, Brown RC. A techno-economic analysis of microalgae remnant catalytic pyrolysis and upgrading to fuels. Fuel 2014;128:104-12.

[5] Tzannatos E, Papadimitriou S, Koliousis I. A Techno-Economic Analysis of Oil vs. Natural Gas Operation for Greek Island Ferries. Int J Sustain Transp 2015;9(4):272-81.

[6] Wang T, Long HA. Techno-economic analysis of biomass/coal Co-gasification IGCC systems with supercritical steam bottom cycle and carbon capture. Int J Energ Res 2014;38(13):1667-92.

[7] Wright MM, Brown RC. Comparative economics of biorefineries based on the biochemical and thermochemical platforms. Biofuel Bioprod Bior 2007;1(1):49-56.

[8] Wright MM, Daugaard DE, Satrio JA, Brown RC. Techno-economic analysis of biomass fast pyrolysis to transportation fuels. Fuel 2010;89, Supplement 1(0):S2-S10.

[9] Peters MS, Timmerhaus KD, West RE, Timmerhaus K, West R. Plant design and economics for chemical engineers: McGraw-Hill New York; 1968.

[10] Swanson RM, Platon A, Satrio JA, Brown RC. Techno-economic analysis of biomass-to-liquids production based on gasification. Fuel 2010;89, Supplement 1:S11-S9.

[11] Møller F, Slentø E, Frederiksen P. Integrated well-to-wheel assessment of biofuels combining energy and emission LCA and welfare economic Cost Benefit Analysis. Biomass Bioenerg 2014;60:41-9.

[12] Niven RK. Ethanol in gasoline: environmental impacts and sustainability review article. Renew Sust Energ Rev 2005;9(6):535-55.

[13] Gerpen JV. Biodiesel processing and production. Fuel Process Technol 2005;86(10):1097-107.

[14] Peterson CL, Hustrulid T. CARBON CYCLE FOR RAPESEED OIL BIODIESEL FUELS. Biomass Bioenerg 1998;14(2):91-101.

[15] Owens JW. Life-Cycle Assessment: Constraints on Moving from Inventory to Impact Assessment. Journal of Industrial Ecology 1997;1(1):37-49.

[16] Klöpffer W. Life cycle assessment. Environ Sci & Pollut Res 1997;4(4):223-8.

[17] Plevin RJ, Delucchi MA, Creutzig F. Using Attributional Life Cycle Assessment to Estimate Climate-Change Mitigation Benefits Misleads Policy Makers. Journal of Industrial Ecology 2014;18(1):73-83.

[18] Han J, Elgowainy A, Dunn JB, Wang MQ. Life cycle analysis of fuel production from fast pyrolysis of biomass. Bioresour Technol 2013;133:421-8.

[19] Hsu DD. Life cycle assessment of gasoline and diesel produced via fast pyrolysis and hydroprocessing. Biomass Bioenerg 2012;45:41-7.

[20] Kaltschmitt M, Reinhardt GA, Stelzer T. Life cycle analysis of biofuels under different environmental aspects. Biomass Bioenerg 1997;12(2):121-34.

[21] Lardon L, Hélias A, Sialve B, Steyer J-P, Bernard O. Life-Cycle Assessment of Biodiesel Production from Microalgae. Environmental Science & Technology 2009;43(17):6475-81.

[22] Hunt RG, Sellers JD, Franklin WE. Resource and environmental profile analysis: A life cycle environmental assessment for products and procedures. Environmental Impact Assessment Review 1992;12(3):245-69.

[23] Tessum CW, Marshall JD, Hill JD. A Spatially and Temporally Explicit Life Cycle Inventory of Air Pollutants from Gasoline and Ethanol in the United States. Environmental Science & Technology 2012;46(20):11408-17.

[24] Tessum C, Hill J, Marshall J. Twelve-month, 12 km resolution North American WRF-Chem v3. 4 air quality simulation: performance evaluation. Geoscientific Model Development 2015;8:957-73.

[25] Tessum C, Hill J, Marshall J. InMAP: a new model for air pollution interventions. Geoscientific Model Development Discussions (Online) 2015;8(10).

[26] Tessum CW, Hill JD, Marshall JD. Life cycle air quality impacts of conventional and alternative light-duty transportation in the United States. Proceedings of the National Academy of Sciences 2014;111(52):18490-5.

[27] Mutel CL, Hellweg S. Regionalized Life Cycle Assessment: Computational Methodology and Application to Inventory Databases. Environmental Science & Technology 2009;43(15):5797-803.

[28] Geyer R, Stoms D, Lindner J, Davis F, Wittstock B. Coupling GIS and LCA for biodiversity assessments of land use. Int J Life Cycle Assess 2010;15(5):454-67.

[29] Huijbregts MAJ, Schöpp W, Verkuijlen E, Heijungs R, Reijnders L. Spatially Explicit Characterization of Acidifying and Eutrophying Air Pollution in Life-Cycle Assessment. Journal of Industrial Ecology 2000;4(3):75-92.

[30] Manneh R, Margni M, Deschênes L. Spatial Variability of Intake Fractions for Canadian Emission Scenarios: A Comparison between Three Resolution Scales. Environmental Science & Technology 2010;44(11):4217-24.

[31] McKone TE, Nazaroff WW, Berck P, Auffhammer M, Lipman T, Torn MS, et al. Grand Challenges for Life-Cycle Assessment of Biofuels. Environmental Science & Technology 2011;45(5):1751-6.

[32] Mutel CL, Pfister S, Hellweg S. GIS-Based Regionalized Life Cycle Assessment: How Big Is Small Enough? Methodology and Case Study of Electricity Generation. Environmental Science & Technology 2012;46(2):1096-103.

[33] Rodríguez C, Ciroth A, Srocka M. The importance of regionalized LCIA in agricultural LCA–new software implementation and case study. Proc 9th Int Conf Life Cycle Assess Agri-Food Sector San Francisco; 2014, p. 1120-8.

[34] Lloyd SM, Ries R. Characterizing, Propagating, and Analyzing Uncertainty in Life-Cycle Assessment: A Survey of Quantitative Approaches. Journal of Industrial Ecology 2007;11(1):161-79.

[35] Thilakaratne R, Brown T, Li YH, Hu GP, Brown R. Mild catalytic pyrolysis of biomass for production of transportation fuels: a techno-economic analysis. Green Chem 2014;16(2):627-36.

[36] Zhang Y, Brown TR, Hu G, Brown RC. Techno-economic analysis of monosaccharide production via fast pyrolysis of lignocellulose. Bioresour Technol 2013;127(0):358-65.

[37] Brown TR. A critical analysis of thermochemical cellulosic biorefinery capital cost estimates. Biofuel Bioprod Bior 2015;9(4):412-21.

[38] Li B, Ou L, Dang Q, Meyer P, Jones S, Brown R, et al. Techno-economic and uncertainty analysis of in situ and ex situ fast pyrolysis for biofuel production. Bioresour Technol 2015;196:49-56.

[39] Heijungs R, Huijbregts MA. A review of approaches to treat uncertainty in LCA. Orlando, Fla: Elsevier 2004.

[40] Tan RR, Culaba AB, Purvis MRI. Application of possibility theory in the life-cycle inventory assessment of biofuels. Int J Energ Res 2002;26(8):737-45.

CHAPTER 2 TECHNO-ECONOMIC ANALYSIS OF CO-LOCATED CORN GRAIN AND CORN STOVER ETHANOL PLANTS

A paper published in *Biofuels, Bioproducts and Biorefining*

Longwen Ou, Tristan R. Brown, Rajeeva Thilakaratne, Guiping Hu, Robert C. Brown

Abstract

The goal of this paper is to evaluate the economic performance of co-located corn grain ethanol (Gen 1) and cellulosic ethanol (Gen 2) facilities. We present six scenarios to evaluate the impact of stover-to-grain mass (SGM) ratios on overall minimum ethanol selling price (MESP). For the Gen 1 plant, MESP is $3.18/ gasoline gallon equivalent (GGE) while for the Gen 2 plant it is $5.64/GGE. Co-located Gen 1 and Gen 2 plants operating at the lowest SGM ratio of 0.4 generates the lowest overall MESP of $3.73/GGE as well as the highest MESP for cellulosic ethanol of $7.85/GGE. Co-located plants operating at the highest SGM ratio of 1.0 achieve the highest overall MESP of $3.94/GGE as well as the lowest MESP for cellulosic ethanol of $5.47/GGE. Sensitivity analysis shows that the prices of feedstocks have the greatest impact on the overall MESP.

Introduction

The goal of this paper is to evaluate the economic performance of co-located corn grain ethanol and cellulosic ethanol facilities, which has several advantages over separate facilities. Corn stover is the most abundant agricultural residue available in the U.S. [1], and is expected to be one of the single largest sources of lignocellulosic biomass in the country by the end of the decade [2]. Corn production and stover production occur on the same land and its use effectively increases the amount of biofuel feedstock that can be sustainably harvested per acre of cropland

by 30-51% [3]. Moreover, co-locating cellulosic ethanol and corn ethanol production plants has the potential to reduce the production costs of both pathways due to economies of scale, thus accelerating the commercialization of cellulosic ethanol and making corn ethanol more competitive with fossil fuels. Finally, co-locating the facilities increases the amount of bioenergy derived per acre of land, thereby decreasing the lifecycle emissions of both when measured on the same basis [4]. While such a reduction doesn't benefit the corn ethanol pathway under the revised Renewable Fuel Standard (RFS2) due to its explicit production cap of 15 billion gallons per year (BGY), it could improve public perceptions of the pathway.

Corn ethanol suffers from a number of drawbacks and has come under criticism in recent years. In 2011 nearly 46% of the U.S. corn crop, or 5 billion bushels, was used as corn ethanol feedstock [5]. Despite this high usage rate, fuel ethanol production for the same year equaled only 10% of gasoline production [6]. The diversion of such a large proportion of the U.S. corn crop to fuel ethanol production has driven fears that corn ethanol production causes chronic hunger in developing countries [7] and the destruction of rainforests in Brazil [8]. While more recent analyses have called into question the actual magnitude of these effects [9, 10], the use of corn as a biofuel feedstock has remained controversial.

Cellulosic ethanol has several advantages over corn ethanol from energetic, environmental, and economic perspectives. Cellulosic ethanol can be derived from a variety of lignocellulosic feedstocks including corn stover, switchgrass, hybrid poplar, and wood residues [11]. Lignocellulosic biomass is not a source of human nutrition and can be grown on marginal cropland and forestland, allowing cellulosic ethanol to avoid controversies over "food vs. fuel" and indirect land-use change. Furthermore, cellulosic ethanol has a better net energy balance than corn ethanol and contributes

less to direct-effect greenhouse gas (GHG) emissions than corn ethanol [11, 12]. Cellulosic ethanol has attracted significant attention in U.S. due to these advantages and, based on current construction, will account for nearly half of U.S. cellulosic biofuel capacity by the end of 2014 [13].

Co-locating a first generation (Gen 1) dry mill corn ethanol plant with a second generation (Gen 2) cellulosic ethanol plant is reported to be both technically feasible [14, 15] and capable of reducing cellulosic ethanol production costs [15]. However, the effects of different stover-to-grain mass (SGM) ratios on the economic feasibility of the co-located Gen 1+ Gen 2 plants have not been previously considered. The feedstock type mass ratio is linked to the sustainability of the pathway, since only a fraction of corn stover produced per acre can be sustainably removed for Gen 2 ethanol production, it is important to quantify the impact of changing SGM ratios on the technical and economic feasibility of a Gen 1+ Gen 2 plant as a result. This paper quantifies these feasibilities via a comparative techno-economic analysis of six different process scenarios: a Gen 1 dry mill corn ethanol plant, a Gen 2 cellulosic ethanol plant using corn stover as feedstock, and a Gen 1+ Gen 2 plant under four SGM ratio scenarios of 0.4:1, 0.6:1, 0.8:1, and 1:1. Minimum ethanol selling prices (MESP) are calculated for each scenario.

Methods

Process modeling

The models for the stand-alone Gen 1 and Gen 2 ethanol plants are based on models previously described in the literature [16-19], but with several important differences. First, the models used in the present study were constructed using ChemCAD™ rather than SuperPro Designer® and Aspen Plus™. Different compositions of corn grain and corn stover are assumed (see **Table 1** and **Table 2**).

Moisture content of corn grain is assumed to be 15% while corn stover moisture is assumed to be 20% [17, 20] instead of 25% assumed in a previous National Renewable Energy Laboratory (NREL) model [18].

Table 1 Composition of corn [19]

Component	Mass%
Starch	59.5
Water	15.0
Non-starch polysaccharides	7.0
Other solids	6.7
Protein - insoluble	6.0
Protein - soluble	2.4
Oil	3.4

Table 2 Composition of Corn stover [17, 18]

Components	Composition (%)
Extractives	6.608
Cellulose	26.744
Xylan	17.728
Galactan	1.088
Arabinan	3.264
Mannan	0.464
Lignin	8.552
Ash	4.744
Acetate	4.352
Protein	1.792
Soluble Solids	4.664
Water	20

In this analysis, both kinds of ethanol plants are assumed to have 30-year lifetimes, consistent with the assumption of Humbird et al. [17] but longer than 10-20 year lifetimes assumed by several other studies [16, 18, 19]. Furthermore, a Lang

factor of 5.03 is used for both plants, which is higher than those used in previous reports.

Gen 1 dry mill corn ethanol production

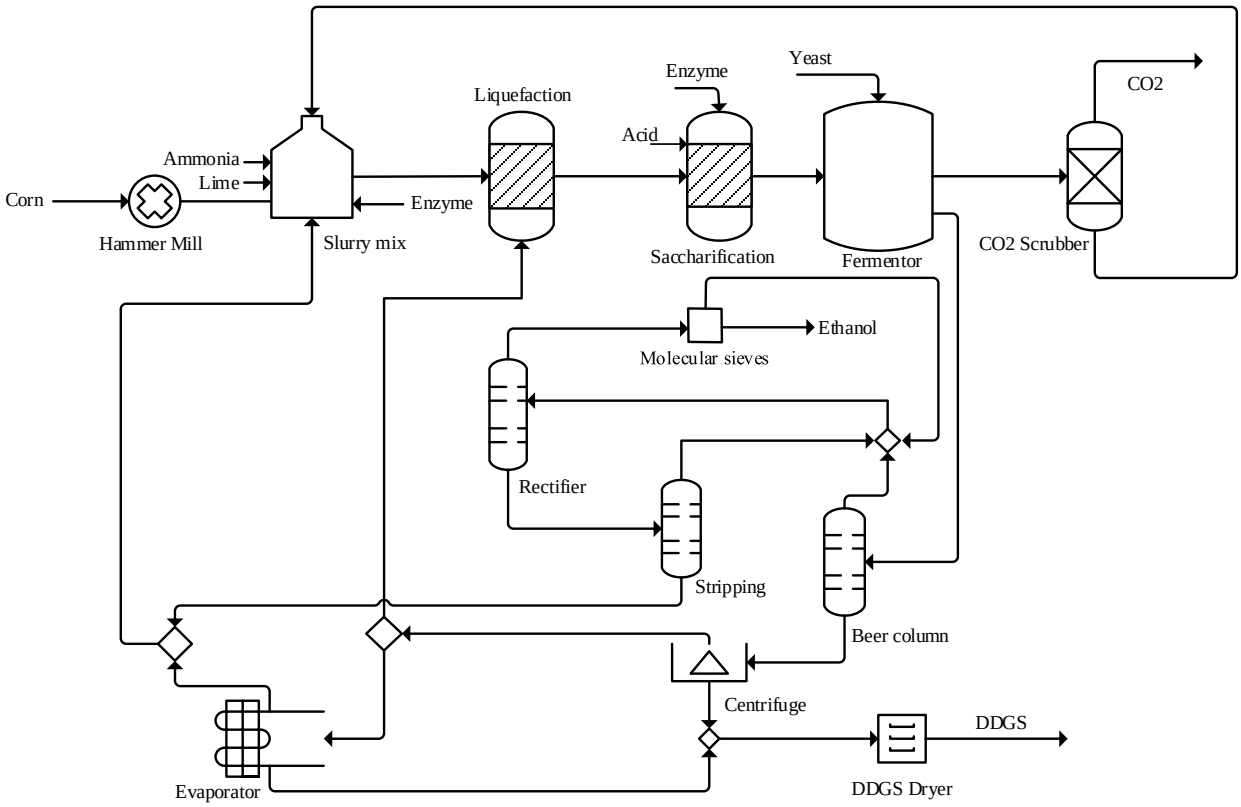

Figure 1 Schematic of a Gen 1 dry mill corn ethanol plant.

Figure 1 is a schematic of the Gen 1 dry mill corn ethanol plant modeled in this study. Corn is received and cleaned using a blower and screens. The cleaned corn is fed to a hammer mill for size reduction. The ground corn is mixed with water, ammonia, lime and enzymes and undergoes liquefaction at 88 oC, where starch is broken down to oligosaccharides. The resulting oligosaccharides are then saccharified to glucose at 61 oC. Sulfuric acid is added to adjust pH in the tank and necessary enzymes are added. The glucose is then fermented to ethanol and carbon dioxide using yeast at 32 oC. Since the conversion of glucose to ethanol produces heat, cooling is necessary in the process of fermentation so that the temperature is

maintained to ensure high yeast activity. After flashing off vapor, the effluent from fermentation goes to a beer column where most of ethanol produced is captured. Rectification is then used to separate water from ethanol. Distillate from the rectifier, which captures more than 99% of the ethanol, feeds the molecular sieves to remove the remaining water, producing 99.6% pure ethanol. The bottoms from the beer column are dewatered by centrifugation. The liquid product is split and used as backset, while the rest goes to an evaporator, where water is recovered. The concentrate from the evaporator is mixed with the solid product from the centrifuge. The mixture is dewatered and concentrated further. The product, known as distiller's dried grains with solubles (DDGS), is sold as an animal feed. Thermal energy for liquefaction of cornstarch, distillation of ethanol, and drying of DDGS in the Gen 1 plant is supplied by natural gas.

Gen 2 ethanol derived from corn stover

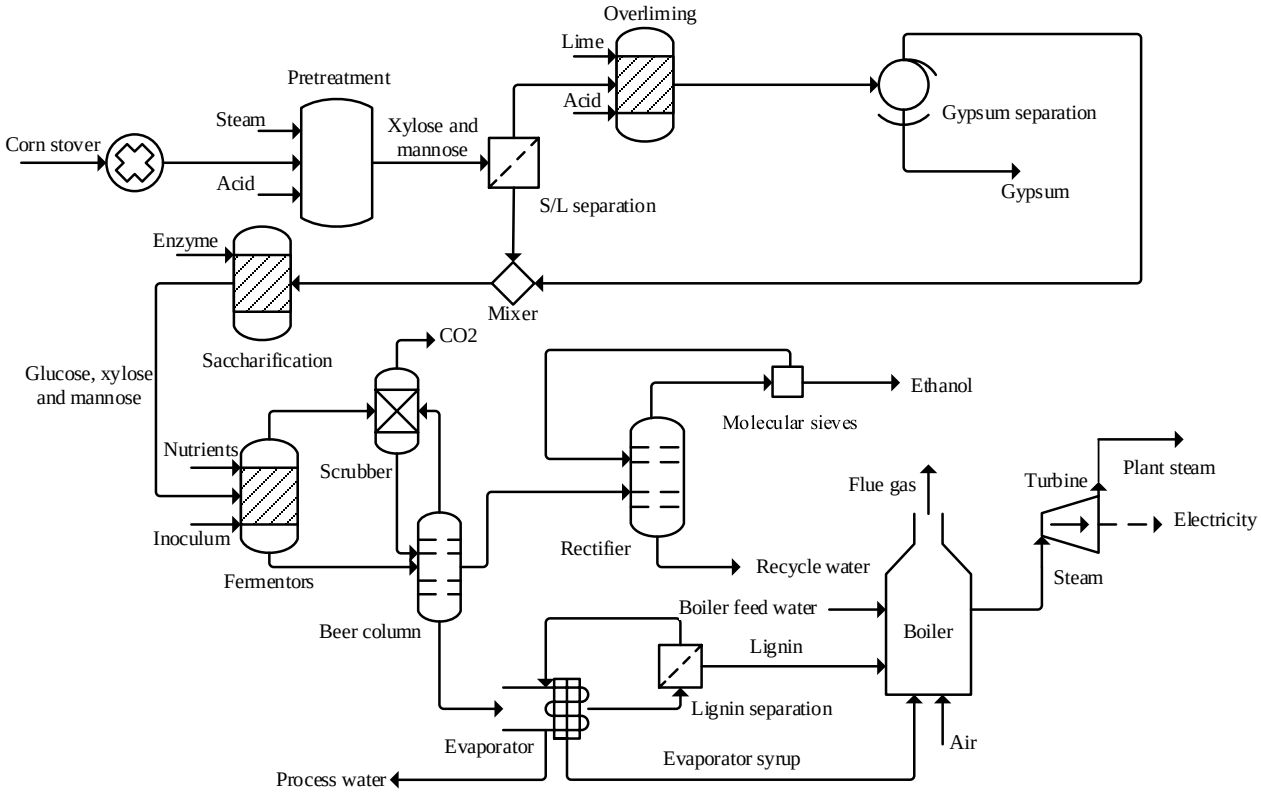

Figure 2 Schematic of a Gen 2 cellulosic ethanol plant.

Figure 2 is a schematic of a Gen 2 ethanol production plant. Corn stover bales are received and delivered to a feed handling area for impurity removal and size reduction. From here, the washed and milled stover is fed to a pre-steamer reactor. Low pressure (LP) steam is added to remove non-condensable gases and reduce the pre-hydrolysis reaction heat requirement. Acid and high pressure (HP) steam are added to hydrolyze most of the hemicellulose to soluble sugars such as xylose, mannose, arabinose and galactose. The liquid portion is overlimed after being separated from the solids. After pH adjustment it is mixed with hydrolyzate solids from the solid/liquid separation step. The conditioned slurry is then mixed with purchased cellulase enzymes to saccharify the cellulose to glucose. The resulting glucose together with the sugars released in the hydrolysis of hemicellulose are co-fermented to ethanol and carbon dioxide by the action of recombinant Z. mobilis, which is grown in a seed fermentation train of vessels in the process area. The beer from fermentation is fed into the beer column where almost all of the CO2 and about 90% of water are removed. The vapor side draw from beer column then enters a rectifier to capture more than 99% of the ethanol. The distillate from the rectifier goes to molecular sieves to produce 99.5% pure ethanol by removing 95% of the water. The CO2 produced in fermentation and the vent of the beer column pass through a water scrubber before venting the gas. The water effluent from the scrubber is fed to the beer column. The bottoms of the beer column, which contains insoluble solids, are sent to a multi-effect evaporator. Lignin is separated from the slurry from the first stage of the evaporator by solid-liquid separation. The liquid portion is then returned to the second stage of the evaporator. The concentrated syrup from the evaporator is mixed with lignin and sent to a boiler, which supplies all the thermal energy required in the Gen 2 plant for pretreatment of stover, saccharification of cellulose

and hemicellulose, distillation of ethanol, and recovery of lignin and syrup from the distillation bottoms. The condensate from the evaporator is recycled to the process as relatively clean water.

Combined heat and power (CHP) plant design for co-located Gen 1 and Gen 2 plants

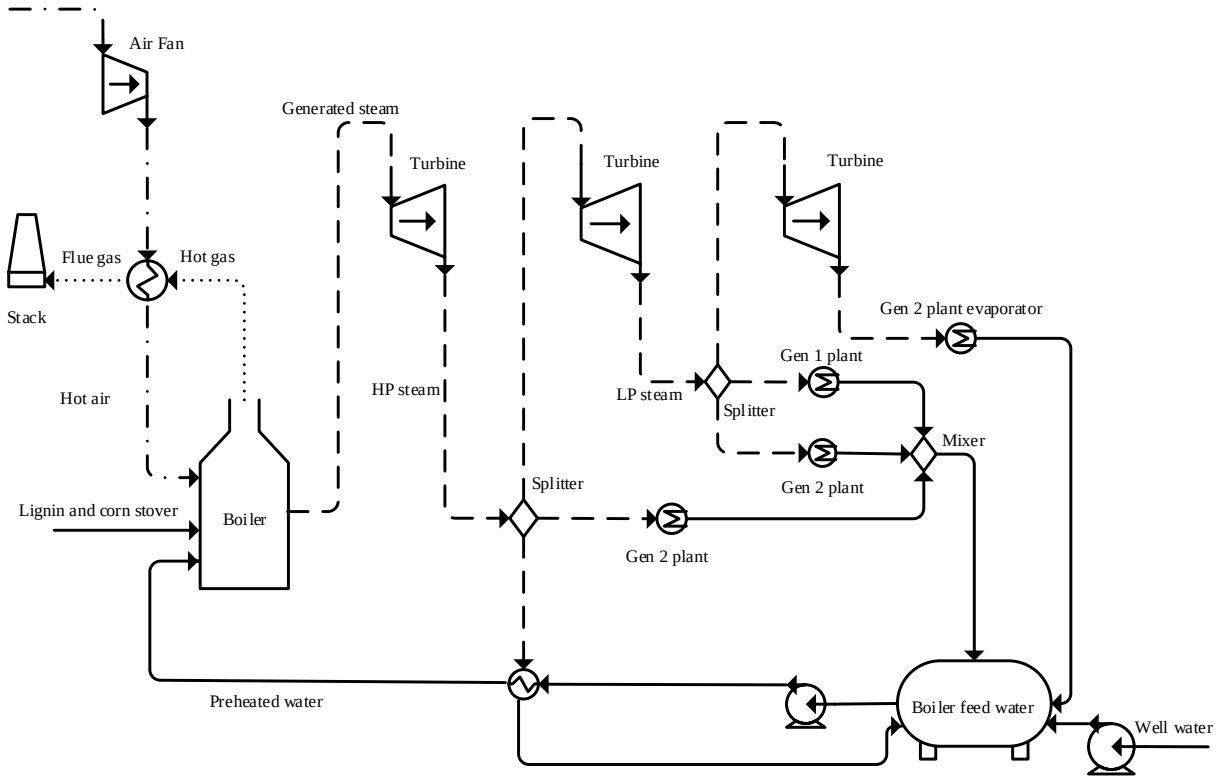

Figure 3 Schematic of the CHP plant. Stream types: steam (dash), water (solid), air (dash dot), flue gas (dot).

Thermal energy for the co-located Gen 1 and Gen 2 plants is provided by a CHP plant, illustrated in **Figure 3**, co-fired by lignin and cornstover instead of natural gas, as is the case for a stand-alone Gen 1 plant. The fraction of corn stover that is combusted depends on the SGM ratio. The CHP plant also produces electricity in excess of plant requirements for power and is sold to the grid. Combustion occurs at 20% excess air to generate superheated steam at 60 atm and 454 ^{o}C. This steam is

expanded through a turbine to 268 ºC, 13 atm, which is split into three streams to meet the HP steam requirement of the Gen 2 plant, preheat boiler feed water to 177 ºC, and supply the second stage of turbine expansion to 164 ºC, 4.42 atm. The LP steam exiting this expansion stage supports thermal energy requirements of both the Gen 1 and Gen 2 plants. Excess LP steam is used to generate additional electricity. Efficiency of the turbine stages is assumed to be 0.85. Flue gas leaves the boiler at 278 ºC and is used to preheat compressed air to 204 ºC.

Economic analysis

The first step in performing economic analyses of the Gen 1 dry mill ethanol and Gen 2 cellulosic ethanol plants are to build process models using ChemCAD™. The process data implemented in ChemCAD™ are obtained from previously published papers [16-19]. The results from the ChemCAD™ simulations are then used to estimate purchased equipment costs. Purchased costs of some simple equipment such as pumps are obtained directly from ChemCAD™. Purchased costs of the remaining equipment are derived from previous reports and publications and scaled according to the sizing results of the ChemCAD™ simulations. The sum of purchased equipment costs is reported as total purchased equipment cost (TPEC). All prices are adjusted to 2012.

Total project investment (TPI) cost is calculated as a function of TPEC. A total Lang factor of 5.03 is recommended for estimating TPI based on TPEC [21]. **Table 3** presents the methodology employed to calculate plant TPI. Operating cost is calculated using the output data from ChemCAD™ and other available resources [16-19]. The results are imported into a Microsoft® Excel discounted cash flow rate of return (DCFROR) spreadsheet developed by NREL [22] in which MESP is calculated as a function of capital cost and operating cost. MESP is determined such that the

net present value equals zero at a 10% internal rate of return (IRR). **Table 4** gives the main assumptions made to obtain the MESPs in this paper. **Table 5** gives the prices of the main pathway input and output commodities, which are used to calculate operating costs and revenue. Since 2011 the prices of corn grain and DDGS have ranged widely from $5/bu to $8/bu and $200/ton to $300/ton, respectively [23]. A corn grain price of $6/bu ($236/metric ton) and a DDGS price of $245/ton ($0.27/kg) are employed in this analysis. Electricity price have ranged from $0.065/kwh to $0.074/kwh since 2011 [24]. An electricity price of $0.070/kwh is employed. The purchased cellulase price is taken such that it contributes $0.50/gal to Gen 2 ethanol production cost [17]. Prices of sulfuric acid, alpha-amylase, glucoamylase, yeast from previous papers [18,19] are adjusted to 2012 prices.

The mass ratio of corn stover to corn grain in the production of a corn crop is estimated to be 1:1 [25]. Therefore, the maximum mass flow rate of corn stover available for ethanol production equals to the mass flow rate of corn if corn stover comes from the same location as corn. However, at least 40% of stover should be left on the field to ensure soil preservation by mitigating erosion.[26] Therefore at most 60% of stover can be sustainably harvested from the same location as the corn. In this paper, four SGM ratios are investigated: 0.4:1, 0.6:1, 0.8:1 and 1:1. Stover that exceeds 60% is either transported from other locations or from the same location on the occasion that it is demonstrated that more than 60% stover removal is agriculturally sustainable. The additional cost incurred either by transporting the exceeding part of stover or preservation of soil quality with more than 60% stover removal is dependent on plant location, feedstock availability and logistics and is difficult to account for. However, these addition costs can be treated as an increase in feedstock cost. Its impact on the overall MESP is discussed in sensitivity analysis.

Table 3 Ratio factors for estimating TPI [21]

Direct Costs	
Total purchased equipment cost (TPEC)	100
Purchased equipment installation	39
Instrumentation and controls (installed)	26
Piping (installed)	31
Electrical systems (installed)	10
Buildings (including services)	29
Yard improvements	12
Service facilities (installed)	55
Total installed cost (TIC)	302
Indirect costs	
Engineering and supervision	32
Construction expenses	34
Legal expenses	4
Contractor's fee	19
Contingency	37
Total indirect cost	126
Fixed capital investment (TIC + indirect plant costs)	428
Working capital (15% of total capital investment)	75
Total project investment (Fixed capital investment + working capital)	503

Summarizing, six different scenarios are developed in the present study: a Gen 1 dry mill corn ethanol plant (Scenario A), a Gen 2 cellulosic ethanol plant using corn stover as feedstock (Scenario B), and a co-located Gen 1+ Gen 2 ethanol plant with SGM ratios of 0.4:1, 0.6:1, 0.8:1, and 1:1 (Scenarios C, D, E and F). This analysis assumes that the two co-located plants have in common only utility-related equipment; that is, steam and electricity generated at the facility are shared by the Gen 1 and Gen 2 plants, making the overall facility self-sufficient in meeting energy

demand, while the process streams are not co-mingled. Due to the fact that the dry mill corn ethanol plant is more energy intensive and requires a larger amount of steam than the Gen 2 plant, a fraction of the stover supply is combusted together with lignin co-product from processing corn stover in the Gen 2 plant to meet the overall steam demand.

Table 4 Main assumptions for economic calculations [17]

Plant Life (Years)	30
Operating Hours per Year	7920
Equity	100%
General Plant Depreciation	200% declining balance (DB)
Steam Plant Depreciation	150% DB
Depreciation Period (Years)	
General Plant	7
Steam/Electricity System	20
Construction Period (Years)	2.5
% Spent in Year -3	8.00%
% Spent in Year -2	60.00%
% Spent in Year -1	32.00%
Start-up Time (Years)	0.5
Revenues (% of Normal)	50%
Variable Costs (% of Normal)	75%
Fixed Cost (% of Normal)	100%
IRR	10.00%
Income Tax Rate	39.00%

Table 5 Raw material price used in simulations

Raw materials	Price
Corn	$236/metric ton ($6/bu)
Corn stover	$83/dry metric ton [18]
Sulfuric acid	$0.28/kg
Alpha-Amylase	$3.96/kg
Glucoamylase	$3.96/kg
Cellulase	$0.39/kg
Yeast	$5.51/kg
DDGS (selling price)	$0.27/kg
Electricity	$0.070/kwh

In order to investigate the effect of SGM ratios on MESP, the capacity of the dry mill corn ethanol plant is fixed at 95.9 million gallons per year, which is a typical capacity of a modern dry mill plant [27], while the mass flow rate of corn stover is varied to account for different SGM ratios. Not all of the harvested stover is converted to ethanol in the co-located plant since a fraction is combusted to provide process heat. The mass of stover combusted is calculated so that the co-located plant is self-sufficient in terms of steam and electricity. The capital costs of the Gen 2 ethanol plant in SGM ratio scenarios C, D, E and F are then scaled from the equipment cost of the stand-alone Gen 2 ethanol plant (Scenario B) based on the mass of stover combusted. The equipment scaling ratio is obtained from previous studies 16-18]. Finally, the capital costs and operating costs of the co-located plant is combined and the MESP for the co-located Gen 1 + Gen 2 facility is obtained. The MESP for cellulosic ethanol for the co-located plant is calculated via the following equation [28]:

$$MESP_{Gen\ 2} = \frac{MESP_{Gen\ 1+Gen\ 2} \cdot Y_{Gen\ 1+Gen\ 2} - MESP_{Gen\ 1} \cdot Y_{Gen\ 1}}{Y_{Gen\ 1+Gen\ 2} - Y_{Gen\ 1}} \qquad (1)$$

Where $MESP_{Gen\ 1+Gen\ 2}$ is the overall MESP, $MESP_{Gen\ 1}$ is the MESP for corn grain ethanol (Scenario A), $Y_{Gen\ 1+Gen\ 2}$ is the volume of Gen 1+ Gen 2 ethanol produced in the co-located plant, and $Y_{Gen\ 1}$ is the volume of ethanol produced in the Gen 1 process.

Results and discussion

Results

Table 6 shows TPEC and TIC of a 95.9 MMgal/yr stand-alone Gen 1 ethanol plant (Scenario A). Coproduct processing comprises the largest portion of installed cost of a Gen 1 ethanol plant, accounting for more than 40% of the total. The cost is

mainly driven by the employment of a multi-effect evaporator, a rotary drum dryer and a centrifuge. Fermentation is the second largest contributor to the total installed cost, accounting for 20% of the total. These results accord with that of other publications [19].

Table 6 TPEC and TIC of a 95.9 MMgal/yr stand-alone Gen 1 ethanol plant (Scenario A)

Area	TPEC (MM$)	TIC (MM$)
Grain handling and milling	2.50	7.54
Starch to sugar conversion	3.28	9.89
Fermentation	7.42	22.42
Ethanol processing	6.58	19.88
Coproduct processing	16.33	49.30
Auxiliaries	1.14	3.43
Total	37.24	112.45

Table 7 shows TPEC and TIC of a 47.7 MMgal/yr stand-alone Gen 2 ethanol plant (Scenario B). Combustor, boiler, and turbogenerator contributes 38% of the total. It is the largest portion of total installed cost and is followed by pretreatment, recovery, saccharification and fermentation. These results also agree with other reports [16,18].

Table 7 TPEC and TIC of a 47.7 MMgal/yr stand-alone Gen 2 ethanol plant (Scenario B)

Area	TPEC (MM$)	TIC (MM$)
Feedstock Handling	5.97	18.04
Pretreatment	21.88	66.08
Saccharification and Fermentation	18.09	54.65
Recovery	20.75	62.67
Wastewater Treatment	4.20	12.67
Storage	1.62	4.90
Combustor, Boiler, and Turbogenerator	46.66	140.91
Utilities	4.38	13.23
Total	**123.56**	**373.16**

Table 8 shows the results of the six scenarios considered. MESPs of a stand-alone 95.9 million gallons per year Gen 1 plant and a stand-alone 47.7 million gallons per year Gen 2 plant are $3.18/ gasoline gallon equivalent (GGE) and $5.64/GGE, respectively. The high MESP of a Gen 2 plant is a major obstacle to its commercialization. It is also noticeable that a significant amount of surplus electricity is produced in a Gen 2 plant while a Gen 1 plant purchases electricity from the grid, making it possible to share the generated electricity in a co-located plant, thus decreasing the production cost.

In a co-located Gen 1 and Gen 2 plant, not all of the stover is used to produce cellulosic ethanol. Part of it is combusted to supply thermal energy to the plant, the amount depending upon the SGM ratio. By comparing scenarios C, D, E and F, it can be seen that for a SGM ratio of 0.4:1 (Scenario C), more than 40% of the corn stover is combusted in order to meet the steam and power demand of the co-located plants while only a small portion of stover is converted to ethanol, producing only 12.8 million gallons per year of cellulosic ethanol. As SGM ratio increases, the fraction of combusted corn stover decreases and cellulosic ethanol production increases. Co-located Gen 1 and Gen 2 plants with SGM ratios of 0.6:1 and 0.8:1 (Scenarios D and E) produce 24.4 and 36.0 million gallons of cellulosic ethanol per year, respectively. When the SGM ratio reaches 1:1 (Scenario F), about 16% of stover is combusted and cellulosic ethanol production reaches 47.7 million gallons per year, about 4 times of that of Scenario C. As a consequence of increased cellulosic ethanol production, the overall MESP of co-located plants goes up as the SGM ratio increases due to higher production cost of cellulosic ethanol. The overall MESP ranges from $3.73/GGE to $3.94/GGE as SGM ratio increases from 0.4:1 and

1:1. Although this value is higher than the MESP of a stand-alone Gen 1 plant, it is still significantly lower than the MESP for a stand-alone Gen 2 ethanol plant, demonstrating the advantage of co-locating a Gen 2 plant with a Gen 1 plant. In spite of the increasing overall MESP, MESP for cellulosic ethanol reduces from \$7.85/GGE to \$5.47/GGE as the SGM goes from 0.4:1 to 1:1, demonstrating the effect of economies of scale. This result indicates that higher SGM ratio favors production of price-competitive cellulosic ethanol. It also can be seen from **Table 8** that more surplus electricity is produced alongside the increase of Gen 2 ethanol yield when the SGM ratio increases since electricity is a main byproduct of Gen 2 ethanol.

Table 8 Summary of analysis of the 6 scenarios

	Scenarios [a]					
	A	B	C	D	E	F
Mass of stover (metric ton per day (MTPD))	—	2233	1067	1600	2133	2667
SMG ratio	—	—	0.4:1	0.6:1	0.8:1	1:1
Mass of stover combusted (MTPD)	—	—	467.5	456.1	444.7	433.3
Ratio of stover combusted	—	—	43.8%	28.5%	20.8%	16.3%
Gen 1 ethanol produced (MM gal / yr)	95.9	—	95.9	95.9	95.9	95.9
Gen 2 ethanol produced (MM gal / yr)	—	47.7	12.8	24.4	36.0	47.7
Electricity produced (MW)	—	34.1	20.3	25.3	30.3	35.4
Electricity Used by Gen 1 process (MW)	6.7	—	6.7	6.7	6.7	6.7
Electricity used by Gen 2 process (MW)	—	13.4	3.6	6.9	10.1	13.4

Table 8 continued

Surplus Electricity (MW)	—	20.7	10.0	11.7	13.5	15.3
Surplus Electricity (kWh/gal Gen 1+Gen 2)	—	3.43	0.72	0.77	0.81	0.84
Overall MESP[b] ($/GGE)	3.18	5.64	3.73	3.84	3.90	3.94
MESP for cellulosic ethanol[c] ($/GGE)	—	—	7.85	6.43	5.82	5.47

[a] Scenario A: stand-alone corn grain ethanol plant; Scenario B: stand-alone cellulosic ethanol plant; Scenario C: co-located Gen 1+ Gen 2 plants with SGM ratio of 0.4:1; Scenario D: co-located Gen 1+ Gen 2 plants with SGM ratio of 0.6:1; Scenario E: co-located Gen 1+ Gen 2 plants with SGM ratio of 0.8:1; Scenario F: co-located Gen 1+ Gen 2 plants with SGM ratio of 1:1.
[b] Overall MESP of Scenarios A and B are MESP for corn grain ethanol and MESP for cellulosic ethanol respectively.
[c] MESP for cellulosic ethanol of Scenarios C, D, E and F are calculated via equation (1).

By comparing the MESP of Scenario B with that of Scenario D, it is found that the co-located plants provide lower MESP for cellulosic ethanol than stand-alone Gen 2 ethanol plants with the same yield. It is expected that if corn price is reduced, the co-located plants will result in even lower MESP for cellulosic ethanol. However, as previously mentioned, around 40% percent of stover should be left in the field to prevent soil erosion; hence a higher SGM ratio may incur additional transportation costs, which are not considered in the calculation.

Sensitivity analysis

The overall MESP for a Gen 1+ Gen 2 facility is very sensitive to the price of the feedstocks (corn grain and corn stover) and to byproduct (DDGS and electricity) selling price; capital cost and yield also have significant impact on overall MESP; thus an analysis of impact of these variables on the overall MESP is performed for scenarios C, D, E, and F. The results are shown in **Figure 4**. It should be noticed that as previously mentioned, the change in feedstock price may be a reflection of

either change in real market price or an increase incurred by additional feedstock transportation cost or soil preservation cost.

The cost of purchasing corn grain accounts for a large proportion of the overall MESP for a Gen 1+ Gen 2 facility. In fact, with the rapid increase of corn price in recent years, corn accounts for a larger proportion of the MESP for grain ethanol than at any time in the past. Corn price has increased by more than 100% since 2010, from about $118/metric ton ($3/bu) to higher than $236/metric ton ($6/bu). Hence, it is expected that corn price has a significant impact on overall MESP for a Gen 1+ Gen 2 facility, as can be seen in **Figure 4**(a). A decrease in corn price by 30% reduces the overall MESP by more than 15% in all scenarios. When corn price reaches a very high value (>$300/metric ton), the overall MESP gets very close in all mass ratio scenarios. The high corn price covers the difference of other variables in this case, thus resulting in a similar overall MESP.

Figure 4(b) shows the impact of corn stover price on the overall MESP for a Gen 1 + Gen 2 facility. Despite the fact that the impact of corn stover price on the overall MESP is very similar to that of corn grain price in trend, the former has much less impact on the overall MESP than the latter does. A decrease in corn stover price by 30% reduces the overall MESP by less than 5%. If more cellulosic ethanol plants are built in the future, the price of corn stover is likely to increase with growing stover demand and overall MESP will go up for a Gen 1 + Gen 2 facility.

The impact of selling price of byproducts on the overall MESP is shown in **Figure 4**(c) and (d). A decrease in DDGS selling price by 30% reduces the overall MESP by about 6% while a decrease in electricity selling price by 40% reduces the overall MESP by about 1%.

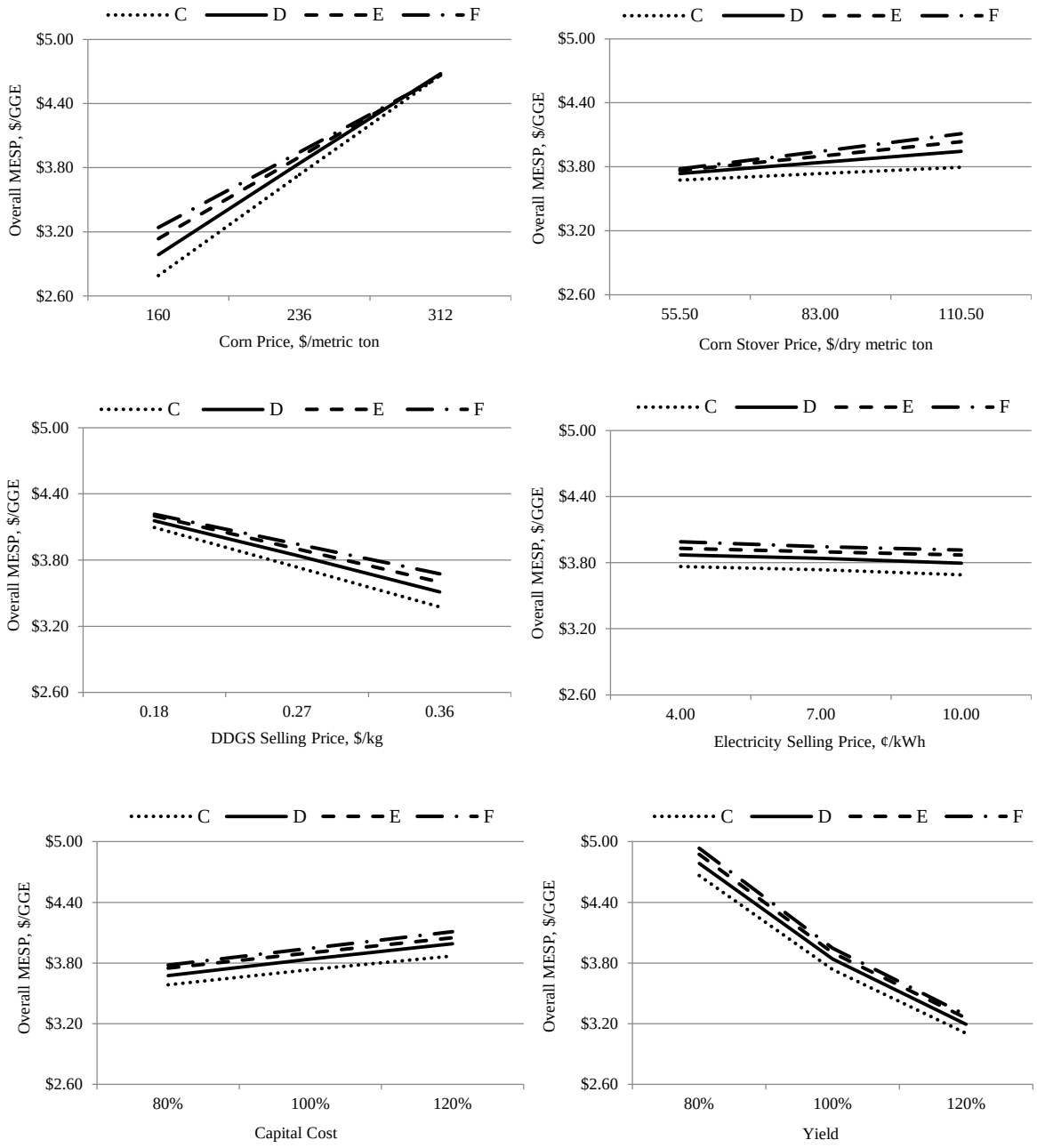

Figure 4 Influence of different variables on the overall MESP for a Gen 1 + Gen 2 ethanol facility.

The impact of capital cost and yield on overall MESP is evaluated by assuming a ±20% change in these parameters from base case for each scenario. The results are shown in **Figure 4**(e) and (f) respectively. A 20% increase (reduction) in capital cost leads to a 4% increase (reduction) in overall MESP. Overall MESP is more sensitive to yield by contrast. A 20% increase in ethanol yield results in approximately 17% reduction in overall MESP. If ethanol yield decreases

by 20%, overall MESP would rise by 25%. It is not likely to increase the yield of Gen 1 ethanol plant due to relative maturity of technology; however, Gen 2 ethanol technology is still under development and it would be highly advantageous to employ new technologies such as 2-stage dilute acid pretreatment and separate C5 and C6 fermentation[18] if these technologies are proved to be able to increase Gen 2 ethanol yield.

Conclusions

Co-location of grain ethanol (Gen 1) and cellulosic ethanol (Gen 2) plants produces lower-cost cellulosic ethanol than stand-alone Gen 2 plants. In general, higher SGM ratio improves the competitiveness of cellulosic ethanol. An increase of SGM ratio from 0.4:1 to 1:1 reduces the MESP for cellulosic ethanol from $7.85/GGE to $5.47/GGE. Overall MESP for a Gen 1 + Gen 2 facility is most sensitive to the price of feedstocks.

With increasing corn price and Gen 1 ethanol production rate approaching the RFS2 capping, co-location of Gen 1 and Gen 2 plants may become even more appealing in the near future. However, MESP of co-located ethanol plants is still higher than ethanol market price.[29] This may be the main obstacle for commercialized co-located ethanol plants. The high MESP is mainly driven by high corn price and high conversion cost of Gen 2 stover ethanol plant. Sensitivity analysis indicates that increasing yield can lower MESP significantly. If new technologies are developed to increase the yield of Gen 2 ethanol plants, it is more likely to see co-located Gen 1 and Gen 2 ethanol plants emerge in the future.

References

[1] Kadam KL, McMillan JD, Availability of corn stover as a sustainable feedstock for bioethanol production. *Bioresour. Technol.* **88**(1):17-25 (2003).

[2] DOE, *U.S. Billion-Ton Update: Biomass Supply for a Bioenergy and Bioproducts Industry*. Oak Ridge National Laboratory, Oak Ridge, TN (2011).

[3] Graham RL, Nelson R, Sheehan J, Perlack RD, Wright LL, Current and potential US corn stover supplies. *Agron. J.* **99**(1):1-11 (2007).

[4] Kauffman N, Hayes D, Brown R, A life cycle assessment of advanced biofuel production from a hectare of corn. *Fuel* **90**(11):3306-14 (2011).

[5] USDA. *U.S. Domestic Corn Use.* http://www.ers.usda.gov/media/866543/cornusetable.html [accessed 24 July 2013]

[6] EIA. *Petroleum & Other Liquids.* http://www.eia.gov/petroleum/data.cfm#refining [accessed 24 July 2013]

[7] Runge CF, Senauer B. How Biofuels Could Starve the Poor. *Foreign Affairs*. (2007 May/June).

[8] Searchinger T, Heimlich R, Hougthon R, Dong F, Elobeid A, Fabiosa J, et al., Use of U.S. Croplands for Biofuels Increases Greenhouse Gases through Emissions from Land-Use Change. *Science* **319**(5867):1238-40 (2008).

[9] Headey D, Was the global food crisis really a crisis? Simulations versus self-reporting. International Conference On Applied Economics - ICOAE, Perugia (2011).

[10] Dumortier J, Hayes DJ, Carriquiry M, Dong F, Du X, Elobeid A, et al., Sensitivity of Carbon Emission Estimates from Indirect Land-Use Change. *Applied Economic Perspectives and Policy* **33**(3):428-48 (2011).

[11] Solomon BD, Barnes JR, Halvorsen KE, Grain and cellulosic ethanol: History, economics, and energy policy. *Biomass Bioenergy* **31**(6):416-25 (2007).

[12] Hill J, Nelson E, Tilman D, Polasky S, Tiffany D, Environmental, economic, and energetic costs and benefits of biodiesel and ethanol biofuels. *Proc. Natl. Acad. Sci. U. S. A.* **103**(30):11206-10 (2006).

[13] Brown TR, Brown RC, A review of cellulosic biofuel commercial-scale projects in the United States. *Biofuels, Bioprod. Biorefin.* **7**(3):235-45 (2013).

[14] Gao J, Qian L, Thelen KD, Hao X, Sousa LdC, Lau MW, et al., Corn Harvest Strategies for Combined Starch and Cellulosic Bioprocessing to Ethanol. *Agron. J.* **103**(3):844-50 (2011).

[15] Wallace R, Ibsen K, McAloon A, Yee W, *Feasibility Study for Co-Locating and Integrating Ethanol Production Plants from Corn Starch and Lignocellulosic Feedstocks (Revised)*. National Renewable Energy Laboratory, Golden, CO (2005).

[16] Aden A, Ruth M, Ibsen K, Jechura J, Neeves K, Sheehan J, et al., *Lignocellulosic biomass to ethanol process design and economics utilizing co-current dilute acid prehydrolysis and enzymatic hydrolysis for corn stover*. National Renewable Energy Laboratory, Golden, CO (2002).

[17] Humbird D, Davis R, Tao L, Kinchin C, Hsu D, Aden A, et al., *Process design and economics for biochemical conversion of lignocellulosic biomass to ethanol dilute-acid pretreatment and enzymatic hydrolysis of corn stover*. National Renewable Energy Laboratory, Golden, CO (2011).

[18] Kazi FK, Fortman J, Anex R, Kothandaraman G, Hsu D, Aden A, et al., *Techno-economic analysis of biochemical scenarios for production of cellulosic ethanol*. National Renewable Energy Laboratory, Golden, CO (2010).
[19] Kwiatkowski JR, McAloon AJ, Taylor F, Johnston DB, Modeling the process and costs of fuel ethanol production by the corn dry-grind process. *Ind. Crops Prod.* **23**(3):288-96 (2006).

[20] DOE, *Multi-year program plan.* U.S. Department of Energy, Washington, DC (2011).

[21] Peters MS, Timmerhaus KD, West RE, *Plant Design and Economics for Chemical Engineers 5th ed*. McGraw-Hill, New York (2003).

[22] Wright MM, Satrio JA, Brown RC, *Techno-economic analysis of biomass fast pyroysis to transportation fuels*. National Renewable Energy Laboratory, Golden, CO (2010).

[23] Hofstrand D, Johanns A, *Weekly Ethanol, Distillers Grain, & Corn Prices.* http://www.extension.iastate.edu/agdm/energy/xls/agmrcethanolplantprices.xlsx [accessed 24 July 2013]

[24] EIA, *Electric Power Monthly with data for April 2013*. U.S. Energy Information Administration (2013).

[25] Gupta SC, Onstad CA, Larson WE, Predicting the Effects of Tillage and Crop Residue Management on Soil Erosion. *J. Soil Water Conserv.* **34**(2):77-9 (1979).

[26] Nielsen RL, *Questions Relative to Harvesting & Storing Corn Stover.* http://www.agry.purdue.edu/ext/corn/pubs/agry9509.htm [accessed 24 July 2013]

[27] RFA, *Biorefinery Locations.* http://www.ethanolrfa.org/bio-refinery-locations/ [accessed 24 July 2013]

[28] Macrelli S, Mogensen J, Zacchi G, Techno-economic evaluation of 2nd generation bioethanol production from sugar cane bagasse and leaves integrated with the sugar-based ethanol process. *Biotechnol. Biofuels* **5** (2012).

[29] USDA, *Fuel ethanol, corn and gasoline prices, by month.* www.ers.usda.gov/datafiles/US_Bioenergy/Prices/table14.xls [accessed 29 December 2013]

CHAPTER 3 TECHNO-ECONOMIC ANALYSIS OF TRANSPORTATION FUELS FROM DEFATTED MICROALGAE VIA HYDROTHERMAL LIQUEFACTION AND HYDROPROCESSING

A paper published in *Biomass and Bioenergy*

Longwen Ou, Rajeeva Thilakaratne, Robert, C. Brown, Mark M. Wright

Abstract

This study describes a techno-economic analysis to evaluate the economic feasibility of transportation fuel production by hydrothermal liquefaction (HTL) of defatted microalgae followed by hydroprocessing of the resulting bio-crude. A 2000 dry metric ton per day biorefinery produces 112 million liters of gasoline-range fuels and 121 million liters of diesel-range fuels per year. We estimate the total project investment is $504 million dollars and the annual operating cost is $158 million dollars. The minimum fuel-selling price (MFSP) is $0.68 per liter assuming a 10% internal rate of return. Sensitivity analysis shows that MFSP is most sensitive to product fuel yield indicating the relative importance of HTL conversion performance. Feedstock cost also strongly influences MFSP, which varied between $0.58 and $0.87 per liter for feedstock cost of $33 and $132 per dry metric ton, respectively. A Monte-Carlo analysis suggests an 80% probability of MFSP being between $0.61 and $0.83 per liter.

Keywords: Defatted microalgae; Hydrothermal liquefaction; Process modeling; Minimum fuel selling price; Uncertainty analysis

Introduction

Environmental concerns and land availability constraints for energy use have prompted the search for clean sources of high-yielding biomass. Microalgae are a potential biomass resource for the production of renewable biofuels with low emissions and reduced land requirements [1-4]. Microalgae present several advantages for biomass production compared to lignocellulosic feedstock. These advantages include low maintenance cultivation, rapid growth, limited need of fresh water, and low nutrient utilization [3]. Microalgae are primarily composed of lipids, carbohydrates, and protein [5]. Their varied composition makes them suitable for multiple applications. They can be employed for ethanol production via fermentation [6] and hydrocarbon fuel synthesis via thermochemical pathways such as fast pyrolysis and gasification [7-9].

Defatted microalgae are a by-product of biodiesel production via lipid extraction from microalgae [10-12]. The defatted microalgae, which can account for as high as 85 wt. % of the whole microalgae on a dry basis [5], has similar carbon and hydrogen content as lipids [13] and could be used for biofuel production [5]. Previous studies identified several applications for defatted microalgae, including animal feeding supplements [14], biogas generation feedstock via anaerobic digestion (AD) [15, 16] and chemical production substrate via fermentation [17]. Defatted microalgae could also be converted into drop-in liquid fuels that are compatible with existing vehicles and transportation fuel infrastructure.

Several thermochemical routes such as pyrolysis, gasification and hydrothermal liquefaction (HTL) [18-20], can convert biomass into biofuels. However, pyrolysis and gasification have a disadvantage with respect to high moisture feedstocks such as

defatted microalgae due to the significant energy losses associated with drying the material [21, 22]. HTL, on the other hand, is considered a promising pathway for processing feedstock with high moisture content [21]. HTL involves processing biomass in pressurized water at temperatures between 250 and 550 °C, and pressures of 5 to 25 MPa. HTL produces a crude oil, an aqueous fraction and a gaseous fraction [21, 23]. HTL crude oil, often called bio-crude, has a relative high heating value (>30 MJ per kg) [23-25] compared to pyrolysis oils (around 20 MJ per kg) [26-28]. HTL has been utilized to process lignocellulosic biomass in the presence of catalyst to produce high-energy content bio-crude [29, 30]. However, the intrinsic characteristics of HTL suggest that it is more economically advantageous for processing feedstock with high water content such as algae, sludge, etc. by eliminating the need to dry feedstock.

The advantages of HTL include: a) avoidance of the costly feedstock drying; b) high yield of bio-crude [31, 32]; c) and the possibility of recycling the high nutrient containing aqueous fraction [33]. However, a significant drawback of HTL is the severe operating condition required (high pressure and high temperature), which incurs high investment and operating cost [1]. There is limited public literature on the costs of biofuel production from the HTL of algae feedstock [1, 5]. Therefore, this study seeks to evaluate the economic feasibility of converting defatted microalgae into biofuels via HTL with the understanding that it is in an early development phase.

To our knowledge, only a limited number of studies investigate the feasibility of producing liquid biofuels from defatted microalgae [5, 32]. Slow pyrolysis and HTL were examined as potential ways of converting defatted microalgae into high-energy content oils [32], which could be subsequently upgraded to liquid fuels via hydrotreating and

hydrocracking. Previous research has shown that HTL has a more attractive energy balance than slow pyrolysis [32].

In this study, we conduct a techno-economic analysis (TEA) to evaluate the potential of producing liquid fuels from defatted microalgae by HTL followed by upgrading of bio-crude. A commercial-scale 2000 dry metric ton per day HTL and hydroprocessing facility is modeled to estimate its total project investment and annual operating costs. The process model assumes that the facility is the n^{th} plant of its kind meaning that major technical challenges have been overcome and requisite equipment is commercially available. The commercialization potential is determined by the competitiveness of the minimum fuel-selling price (MFSP) relative to market alternatives. The MFSP is estimated based on a 10% internal rate of return (IRR) and 30-year facility lifetime.

Materials and Methods

The TEA employs chemical process modeling and economic cost estimates to determine the process profitability. This study employs ChemCAD 6.5 software by Chemstations™ for process modeling. Purchase costs of common equipment such as compressors, pumps, and heat exchangers are appraised using ChemCAD. Purchase costs of custom engineered equipment such as the HTL reactor and hydrogen plant are projected based on a power law with the commonly employed scaling factor of 0.6 for chemical processing equipment [34-37]. The return on investment is evaluated with a 30-year discounted cash flow rate-of-return (DCFROR) spreadsheet. Some major assumptions made in this analysis are listed below:

- Plant capacity is 2000 dry metric ton per day of defatted microalgae.

- The wet feedstock contains 80% moisture.
- Liquid effluent and solids from the HTL reactor are directed to a wastewater treatment plant and solid waste disposal plant, respectively.
- Process off-gases are combusted for heat recovery.
- The cost analysis represents a n^{th} plant design, which assumes that major technical obstacles have been overcome and requisite equipment is commercially available.

Process modeling

The chemical process model comprises 5 areas: hydrothermal liquefaction, hydroprocessing, hydrogen generation, product refining, and a combined heat and power (CHP) plant as illustrated in **Figure 1**. The following sections describe assumptions relevant to each of these areas. Waste handling and disposal facilities are not modeled in this analysis. Instead, we assume that HTL wastewater could be treated by a third-party facility at a fixed price per unit volume ($0.89 per cubic meter) [38], and solid waste can be disposed at a fixed price per unit mass ($36.98 per metric ton) [39]. These costs assume that the waste treatment facilities are capable of handling all potential contaminants without additional capital investment or major infrastructure modifications.

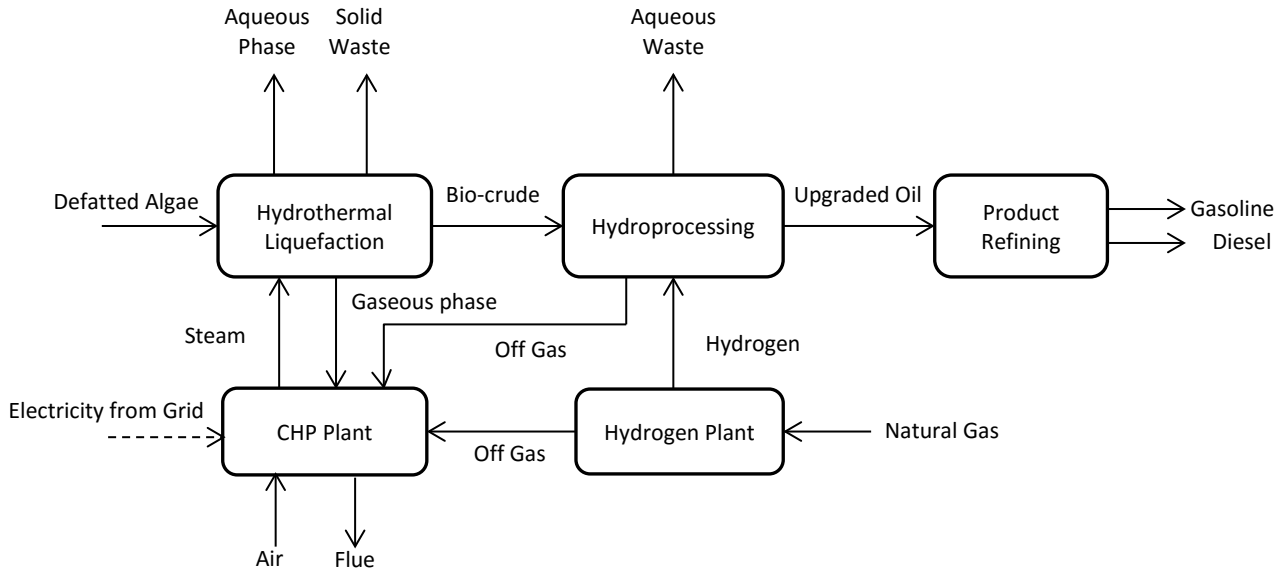

Figure 1 Schematic of the Defatted Microalgae Hydrothermal Liquefaction Process for Gasoline and Diesel Production.

Biomass feedstock

Both raw and defatted microalgae can be used as feedstock of HTL process considering their high moisture content. However, estimated production cost of raw microalgae cultivation can be as high as $3000 per metric ton, impairing the potential of raw microalgae as HTL feedstock [12]. Prices of defatted microalgae, on the other hand, are expected to be in line with wet distiller's grain with solubles (WDGS) considering the fact that they share similar protein and moisture content and can both be used as animal feed supplement. The lower price of defatted microalgae grants it advantage as a potential HTL feedstock.

Vardon et al. [32] reported the elemental composition of raw *Scenedesmus* and defatted *Scenedesmus*, as listed in **Table 1**. The composition of defatted *Scenedesmus* with moisture content of 80% was employed in this analysis. Vardon et al. [32] determined that raw *Scenedesmus* contains 13% lipids while defatted *Scenedesmus*

contains less than 1% lipid. Despite the differences in nutritional profile, the elemental composition of defatted microalgae is comparable to that of raw microalgae, with slightly higher nitrogen content and lower carbon content. The hydrogen and oxygen contents are similar for both materials, and the sulfur content is low in both raw and defatted *Scenedesmus*. The nitrogen content in microalgae (around 8%) is much higher than in lignocellulosic biomass (<1%) [28]. The high nitrogen content in algal biomass can be attributed to protein [32]. A significant portion of the feedstock nitrogen may be retained in the bio-crude products, causing potential problems with direct combustion and bio-crude upgrading [24, 31, 32, 40].

Hydrothermal liquefaction

Purchased wet algae are first pumped to 18 MPa and sent through a pair of heat exchangers to raise the temperature of the algae stream to 350°C. After this process, the state of the water in the stream is slightly below the supercritical point and is then capable of dissolving most of the organic material in the stream. Meanwhile, phosphates and sulfates in the feedstock cease to be soluble and precipitate as solids [41]. The stream then goes through a precipitation tank where the precipitated phosphates and sulfates congregate at the bottom of the tank and get removed so that the catalysts downstream will not be poisoned.

The effluent from the precipitation tank is then fed into the HTL reactor with sodium carbonate to convert the biomass into bio-crude. The effluent from the hydrothermal reactor feeds into a filter to separate unreacted biomass, char and ash as solids waste. Yields of bio-crude, solids waste and aqueous fraction are 36%, 6%, 17%, respectively, as shown in **Table 1** [32]. The rest is converted to gaseous components

[32]. The filtered effluent goes through a heat exchanger to recover heat and leaves at 148 °C. A 3-phase separator follows to split the stream into a gaseous phase, an aqueous phase and an organic phase (bio-crude). The aqueous phase, mainly consisting of water and small polar compounds such as formic and acetic acid, is sent to a wastewater treatment facility [32, 40]. Based on engineering judgment, the aqueous phase does not contain enough carbon to be economically reformed or recovered. The gaseous phase, consisting mostly of hydrogen, carbon dioxide and light alkanes, is sent to the combustor area where it is combusted to supply process heat. The bio-crude is sent to the hydroprocessing process where it is deoxygenated via hydrotreating in reactor with cobalt molybdenum (CoMo) catalysts [35].

Table 1 Process modeling parameters [32]

Elemental Composition			
	Defatted Microalgae	Raw Microalgae	HTL Bio-crude
C	49.9	52.1	72.2
H	7.1	7.4	8.9
N	9.9	8.8	7.8
O[a]	32.1	31.1	10.5
S	0.96	0.48	0.90
HTL Yields (wt%)			
Bio-crude	Solids	Aqueous	Gaseous
36	6	17	41

[a] Oxygen content determined by difference for total mass.

Upgrading

Raw bio-crude material has high oxygen and nitrogen content, which must be reduced to meet transportation fuel standards. This process employs a two-stage hydroprocessing unit where the first stage operates at mild conditions (200 °C, 11.7

MPa) to stabilize the bio-crude, and the second stage operates at more severe conditions (400°C, 11.7 MPa) [42].

There are a few publications on the hydroprocessing of HTL bio-crude [43, 44]. However, there is not enough detailed data for the upgrading of algae-derived HTL oil. This analysis utilizes the same methodology as that used by [42] to estimate the product distribution of hydroprocessing. The model assumes that 85% of the oxygen in the bio-crude is removed as water, and the rest is removed as carbon dioxide. **Table 2** gives the material balance of hydroprocessing.

Table 2 Process baseline material balance of bio-crude hydroprocessing at 200-400 °C, 11.7 MPa [42]

Component	wt% of dry feed
Feed hydrogen[a]	3.9
Upgraded oil[a]	77.9
Gas[a]	16.27
Water	9.75
Gas components	wt% of dry feed
CO_2	2.1
CH_4	2.0
C_2H_6	0.61
C_3H_8	0.55
C_4H_{10}	0.58
NH_3	9.47
H_2S	0.96
Upgraded oil composition	
Aromatics	25.0
Cycloalkanes	50.6
Partially saturated aromatics	7.4
Olefins	2.4
Paraffins	14.6

[a] Calculated from mole balance

The effluent of the upgrading step, which has negligible oxygen content, is then separated into upgraded oil, aqueous waste, and off-gas streams. The aqueous waste is sent to a wastewater treatment plant, while the gases are sent to the cogeneration area and combusted for energy.

The upgraded bio-crude is then stabilized using a debutanizer column by removing butane and other light compounds. The overhead gas containing light organics is sent to cogeneration area and combusted. The debutanizer bottom product is then further separated into gasoline and diesel range fuels using a fractionation column.

Hydrogen generation

In this study, hydrogen is produced by steam reforming of pipeline quality natural gas. The composition of the natural gas is based on National Energy Technology Laboratory (NETL) report [45]. Purchased natural gas is first compressed to 2 MPa, hydrodesulfurized, and then mixed with superheated steam at 335 °C with a steam-to-carbon molar ratio of 3.5 [46, 47]. The mixture is fed to the steam reformer at 2 MPa to produce syngas. High temperature water-gas-shift follows to increase the hydrogen content of syngas by converting carbon monoxide and water into hydrogen and carbon dioxide. After condensing out the water, hydrogen is purified to greater than 99.99% concentration by pressure swing adsorption. The off-gas stream from the hydrogen plant is sent to cogeneration and combusted along with off-gas from other process areas.

2.1.5 Combined heat and power plant

In this area, off-gas streams are combined and combusted to recover process heat. Flue gas from the combustor is used to preheat air feed to the combustor. The primary heat consumers in the process are the HTL reactor, steam reformer and natural gas heater in the hydrogen plant. Superheated steam (450 °C, 6 MPa) [34] is generated to supply heat for the process. The superheated steam is then split into 2 streams. The first stream provides dedicated heat to the HTL reactor. The second stream provides both heat and power by first going through a multistage turbine and power generator. Steam is extracted from the turbine at four different conditions for use in the process. Steam at 335 °C, 2.4 MPa is extracted for hydrogen generation [37]. High pressure steam at 4.2 MPa, medium pressure steam at 1.1 MPa and low pressure steam at 0.6 MPa [48] are also extracted. Part of the high-pressure steam is used to preheat boiler feed water. Plant steam demand consumes the remaining high-pressure steam and all of the medium pressure steam. Low pressure steam is sent to the deaerator to remove dissolved gases from boiler feed water [34]. In the final stage of the turbine, the expanded steam is cooled and condensed to 0.01 MPa and 46 °C [34]. Boiler blowdown is assumed to be 3% of the steam production [34]. The generated electricity is supplied to users of the plant. Purchased electricity supplies the remainder of the plant power demand.

Economic analysis

A process model is built in ChemCAD^{TM} to obtain material and energy balance of the microalgae HTL pathway. Process equipment units are then sized based on the material and energy balances and operating conditions. Purchase costs of common

equipment such as pumps, compressors and vessels are estimated using ChemCAD. Costs of more complex equipment such as reactors and distillation columns are estimated by scaling of publically available data for similar equipment [1, 35]. The installed cost of the hydrogen plant is obtained by volumetric scaling using estimates provided by Stanford Research Institute (SRI) for a natural gas steam-reforming hydrogen plant [37]. Once the Total Purchased Equipment Cost (TPEC) is obtained, Fixed Capital Investment (FCI) and Total Project Investment (TPI) can be determined from Peters and Timmerhaus [49] factors. The parameters used to estimate FCI and TPI from TPEC are listed in **Table 3**. The results were then used as input information into a modified DCFROR analysis spreadsheet to calculate the MFSP. **Table 4** details the main assumptions of the economic analysis. A standard 15% contingency factor was included to account for unforeseen expenses during the startup-period [35]. However, the contingency factor for the hydrogen plant was assumed to be negligible due to the availability of turn-key commercial reforming units [35].

Annual operating costs include costs for feedstock, natural gas, catalysts and chemicals, waste disposal, utilities, fixed costs including labor and equipment maintenance, and capital depreciation. Feedstock cost is a factor that can have great impact on MFSP. Price of defatted microalgae is difficult to predict due to lack of commercial data. In this analysis, feedstock cost is assumed to be $66 per dry metric ton, which is the same as that of WDGS [50]. This assumption is valid if defatted microalgae could substitute WDGS in the animal feed market at a price of $66 per dry metric ton and there are no other higher value markets for defatted microalgae. Prices of natural gas and electricity ($5.59 per 1000 MJ and 7.9 cents per kWh) are taken from

U.S. Energy Information Administration (EIA) database [51, 52]. Prices of other raw materials and catalysts are taken from previous published literature [37, 53]. Catalyst and chemical costs are taken from other similar reports and adjusted to 2011 dollars [35, 37, 53].

Table 3 Total project investment cost factors [49]

Direct Costs	
Total purchased equipment cost (TPEC)	100
Purchased equipment installation	39
Instrumentation and controls (installed)	26
Piping (installed)	31
Electrical systems (installed)	10
Buildings (including services)	29
Yard improvements	12
Service facilities (installed)	55
Total installed cost (TIC)	302
Indirect costs	
Engineering and supervision	32
Construction expenses	34
Legal expenses	4
Contractor's fee	19
Contingency	37
Total indirect cost	126
Fixed capital investment (TIC + indirect plant costs)	428
Working capital (15% of total capital investment)	75
Total project investment (Fixed capital investment + working capital)	**503**

Table 4 Major economic analysis assumptions [34]

Plant Life (Years)	30
Operating Hours per Year	7920
Equity	100%
General Plant Depreciation	200 declining balance (DB)
Steam Plant Depreciation	150 DB
Depreciation Period (Years)	
General Plant	7
Steam/Electricity System	20
Construction Period (Years)	2.5
% Spent in Year -3	8.00%
% Spent in Year -2	60.00%
% Spent in Year -1	32.00%
Start-up Time (Years)	0.5
Revenues (% of Normal)	50%
Variable Costs (% of Normal)	75%
Fixed Cost (% of Normal)	100%
IRR	10.00%
Income Tax Rate	39.00%

Sensitivity and uncertainty analysis

Process parameters may vary during operation of the HTL facility. Therefore, sensitivity analysis is employed to evaluate the impact of parameter changes on the MFSP. This is accomplished by evaluating MFSP after changing one parameter while assuming that all other parameters remain fixed. In this analysis, the parameters considered are product fuel yield, fixed capital investment, IRR, feedstock cost, income tax rate, working capital, and hydrotreating catalyst cost. Sensitivity analysis is conducted by assuming a certain range of key process parameters. In order to account for the high variability potential of feedstock price, a relatively large range (-50% to

+100%) is employed. For other parameters, a ±20% range is employed. MFSP is evaluated for the base case, the high-end, and the low-end values for each parameter.

The sensitivity analysis varies only one parameter change at a time while the rest remain fixed. This approach is valuable for understanding the impact of individual parameters. In practice, values for several of the parameters would vary simultaneously. The impact of this behavior can be captured with a stochastic Monte-Carlo analysis. A multivariate Monte-Carlo analysis was performed to obtain a MFSP probability distribution for the HTL facility. We employed triangular probability distributions with the same ranges assumed in the sensitivity analysis for product fuel yield, feedstock cost, fixed capital investment, and IRR. The stochastic analysis was performed with 10000 trials using Crystal Ball®, and the results were analyzed using MathWorks® Matlab®.

Results and Discussion

Mass and energy balances

The process model estimates that a 2000 dry metric ton feedstock per day plant produces 233 million liters of liquid fuel of which 112 million liters are gasoline and 121 million liters are diesel fuel. These results translate to a fuel yield of 352 liter per dry metric ton feedstock. This is slightly lower than the 367 liters per dry metric ton estimated for fast pyrolysis of corn stover but significantly higher than the 223 liters per dry metric ton estimated for mild catalytic pyrolysis of woody biomass [39, 42]. Major process modeling results are listed in **Table 5**.

Table 5 Process modeling results

Algae feed flow rate (dry metric ton per day)	2000
Natural gas flow rate (kg per hour)	3080
Overall process yields	
Gasoline production rate (million liters per year)	112
Diesel production rate (million liters per year)	121
Hydrogen consumption (kg per kg feed oil)	0.04
Water usage	
Boiler feed water (kg per hour)	13479
Cooling water makeup (kg per hour)	30432
Electricity usage	
Electricity required (MW)	9.1
Electricity generated (MW)	3.0
Purchased Electricity (MW)	6.1

The simulation also provides estimates for utility usage. Cooling make-up water and boiler feed water are the major uses of water in the plant, totaling 43914 kg per hour. Process off-gases are combusted to provide process heat with excess heat used to generate superheated steam. The steam reformer in the hydrogen plant and the HTL reactor consume the most process heat. Generated steam is used for: a) feed to steam reformer in the hydrogen plant; b) heat source in the process; and c) electricity generation. Although electricity is produced in the steam plant, the process is not self-sufficient in electricity. Therefore, the facility is a net importer of electricity. The largest electricity consumer is the upgrading area, where most of the electricity is used for hydrogen compression. HTL is the second largest electricity consumer since pumping algal sludge into the reactor requires a large amount of energy.

Costs analysis

Major economic results are listed in **Tables 6** and **7**. The minimum fuel-selling price is estimated to be $0.68 per liter. The 2000 dry metric ton per day plant requires a TPEC of $99 million and a TIC of $424 million, which are significantly higher than for a biomass pyrolysis facility processing the same amount of biomass [39]. HTL contributes 51% of the fixed capital cost, which is chiefly due to the costs of the pressure vessel for the HTL reactor. Hydroprocessing accounts for 17% of the capital costs, which is due to the presence of two hydrotreaters. The steam and hydrogen generation plants account for 13% and 12% of the installed cost with a value of $54 million and $48 million, respectively.

Table 6 Economic analysis results

Total purchased equipment cost (TPEC)	100% TPEC	$99 million
Direct installed cost (DIC)	302% TPEC	$299 million
Indirect installed cost (TIC)	126% TPEC	$125 million
Fixed Capital investment (FCI)	428% TPEC	$424 million
Working capital	15% FCI	$75 million
Land	6% TPEC	$6 million
Total project investment (TPI)	510% TPEC	$504 million

The HTL and subsequent upgrading technology is still in early development. The technology employed in future commercial plants may require more capital investment than assumed in this analysis. In order to investigate potential risks of building a commercial plant based on this concept, fixed capital investment was varied in the sensitivity analysis to study its impact on the MFSP.

Table 7 Major economic analysis results

Fixed Capital Investment	$ million
Hydrothermal Liquefaction	209
Hydroprocessing	71
Product Refining	6
Hydrogen Generation	52
Steam Plant	63
Auxiliaries	23
Total fixed capital investment	424
Annual Operating Cost	
Feedstock	43.4
Natural Gas	6.7
Catalysts & Chemicals	6.9
Waste Disposal	4.1
Electricity and other utilities	3.9
Fixed Costs	22.8
Capital Depreciation	21.2
Average Income Tax	12.0
Average Return on Investment	37.0
Total annual operating cost	158.0
MFSP, $ per liter	0.68

Total annual operating costs are estimated at $158 million. Feedstock costs account for 28% of operating costs followed by fixed costs (14%) and capital depreciation (13%). Purchased natural gas, catalyst and chemicals constitutes 8% of annual operating costs.

Figure 2 shows area contributions to conversion cost. It can be seen from **Figure 2** that capital cost accounts for about 44% of the conversion cost while operating

cost accounts for 56%. HTL constitutes about 33% of the conversion cost. This result is in accordance with the high capital cost of the HTL reactor. Bio-crude upgrading and refining also contributes to more than 21% of conversion cost.

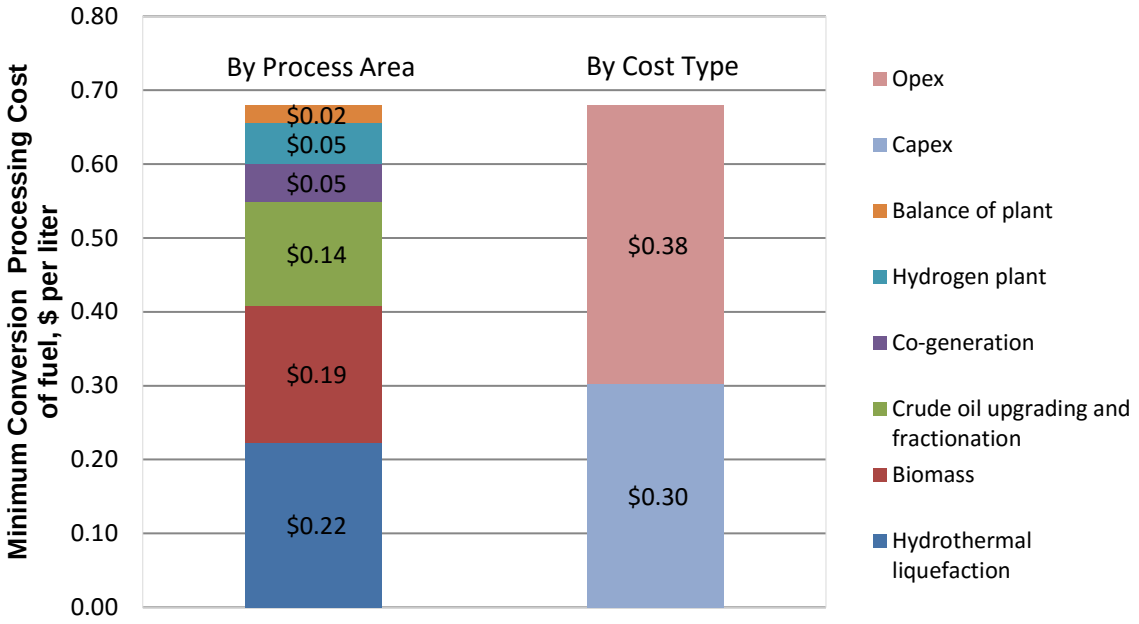

Figure 2 Contributions to the Operating Cost of Hydrothermal Liquefaction of Defatted Microalgae and Upgrading to Transportation Fuels. Operating Costs Grouped by Process Area (Left) and Cost Type (Right). Cost Types Include Opex (Operating Expenditure) and Capex (Capital Expenditure).

Energy flow analysis

Figure 3 shows the energy flows in the facility expressed as the sum of higher heating values (HHV) and sensible heats of the streams [42]. HHV of the streams is obtained from stream properties packages available in ChemCAD. Sensible heat is calculated as the difference between the enthalpy of stream at the process state and the enthalpy at reference state of 25 °C and 1 atm [42].

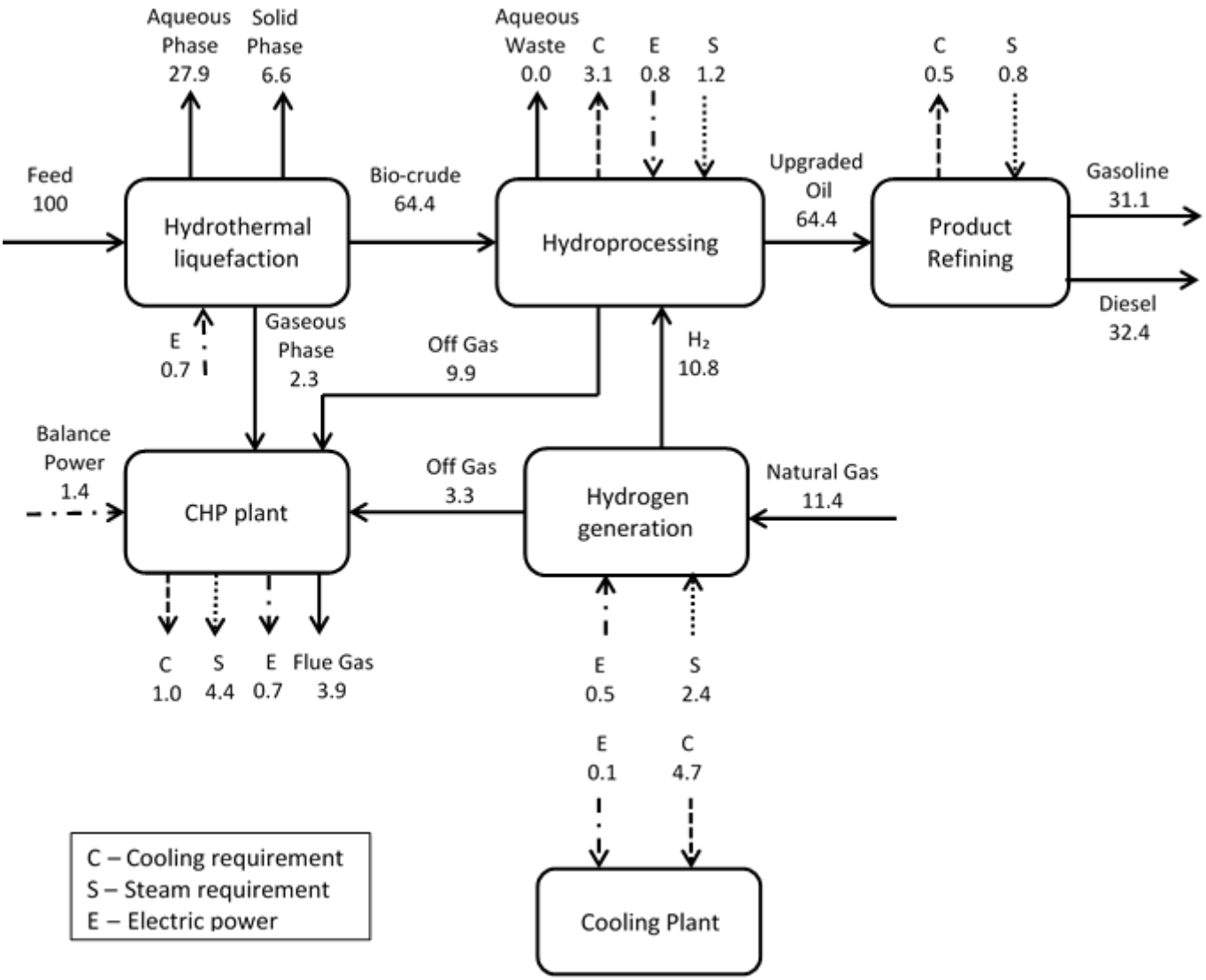

Figure 3 Energy Flow of Process Mass and Energy (sensible + HHV) Streams as a Percentage of Feedstock HHV.

Overall 63.5% of the total energy in the feedstock is retained in the liquid fuel end product. This conversion rate is higher than that of cellulosic ethanol (44%) and mild catalytic pyrolysis of woody biomass (39%) [34, 42]. HTL and upgrading efficiency can be attributed to the high yield and quality of bio-crude. Bio-crude from defatted microalgae would require less intensive hydroprocessing than bio-oil from catalytic

pyrolysis because of its lower oxygen content, and much less energy input for distillation than cellulosic ethanol due to a lower water content. The high energy efficiency for fuel production demonstrates a key advantage of the proposed facility. However, the facility requires significant energy input in the form of electricity and natural gas. **Figure 3** indicates that the facility can only meet 34% of total electricity demand while the rest must be purchased from the grid. If energy input from other sources such as natural gas and electricity are also considered, the proposed facility achieves an overall energy efficiency of 56.3%. Carbon yield of the proposed facility is 52.1%, which represents the percentage of carbon in feedstock and natural gas that is retained in the final product. Overall carbon yield of 49.3% is obtained when carbon input from natural gas is also considered.

Sensitivity analysis

Results of the sensitivity analysis are shown in **Figure 4**. The results are obtained with a ±20% range employed for all the parameters except for feedstock cost, for which a relatively large range (-50% to +100%) is employed to account for its high variability potential. As shown in **Figure 4**, product fuel yield and feedstock cost have the greatest impact on MFSP. A ±20% variation in fuel yields result in a MFSP range of $0.57 per liter to $0.85 per liter. Several factors can impact final product yield, including bio-crude yield, upgrading yield, and separation efficiencies. In this analysis, the yield of hydroprocessing is calculated based on assumptions rather than from existing experimental data. Results of sensitivity analysis demonstrate the necessity of further experiments on the yield of bio-crude upgrading.

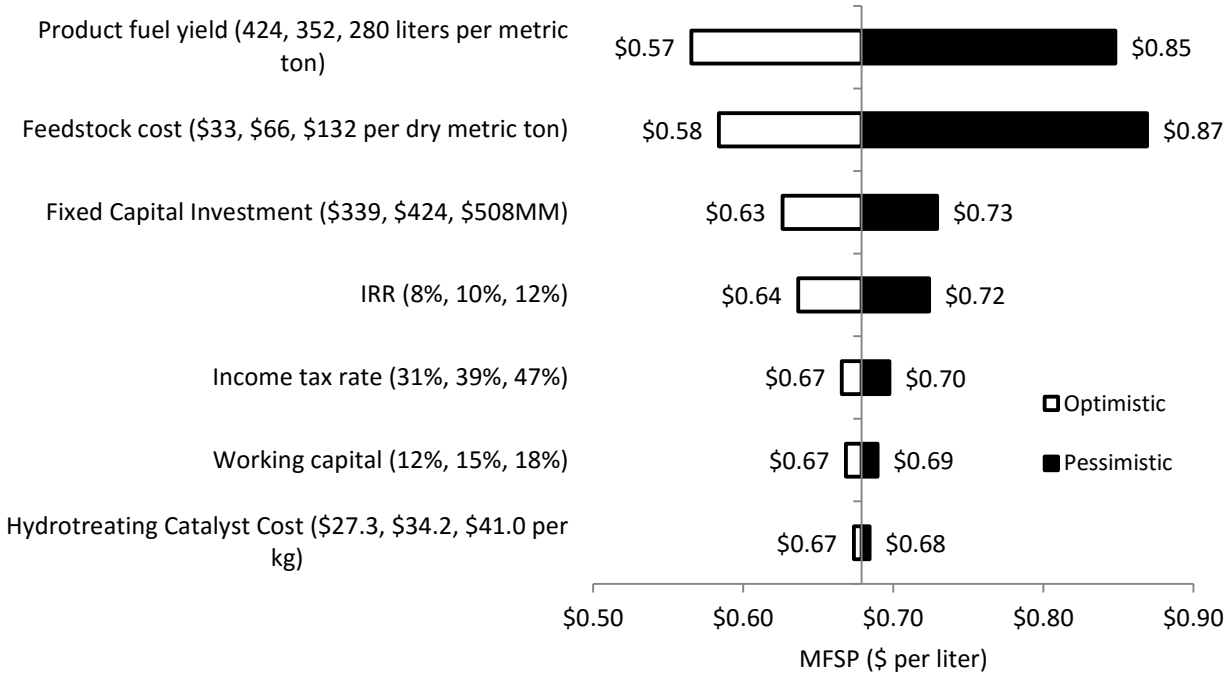

Figure 4 Sensitivity Analysis of the Minimum Fuel-Selling Price to Select Technical and Economic Parameters.

The purchase costs of microalgae remain uncertain and difficult to predict. Therefore, a large value range is considered in this analysis. Sensitivity analysis shows that the MFSP can be as low as $0.58 per liter if the feedstock can be purchased at as low as $33 per dry metric ton. On the other hand, if feedstock costs increase to $132 per dry metric ton, the MFSP would also increase to $0.87 per liter. More research effort should go into determining the market price of defatted algae before this HTL process is commercialized.

The next key parameters in terms of MFSP sensitivity are fixed capital investment and IRR. A 20% increase in fixed capital investment and IRR lead to 8% and 7% increases in MFSP, respectively.

Uncertainty analysis

The uncertainty analysis evaluates the impact of stochastic variations between multiple parameters on the estimated MFSP. Product fuel yield, feedstock cost, fixed capital investment, and IRR were identified as the key parameters to which MFSP is most sensitive. To understand the interactions among these parameters, we conducted a Monte-Carlo analysis to evaluate the MFSP distribution for the process assuming triangular distributions for these parameters. Triangular distributions are often employed in the absence of detailed statistical data [54]. Triangular distributions in this study are constructed based on the expected parameter value and ±20% limits except for feedstock cost, for which larger limits between -50% and +100% are assumed. The resulting MFSP ranges from $0.48 per liter to $1.03 per liter, with a 50% probability of the MFSP being less than $0.72 per liter (**Figure 5**(a)). This fuel price is competitive with the 20-year average of historical gasoline prices, suggesting that the pathway evaluated in this analysis is a promising process for transportation fuel production [55]. The probability distribution of the MFSP based on variations in the product fuel yield, feedstock cost, fixed capital investment, and IRR is shown in **Figure 5**(b), which reveals an 80% probability of the MFSP falling within $0.61 per liter to $0.83 per liter.

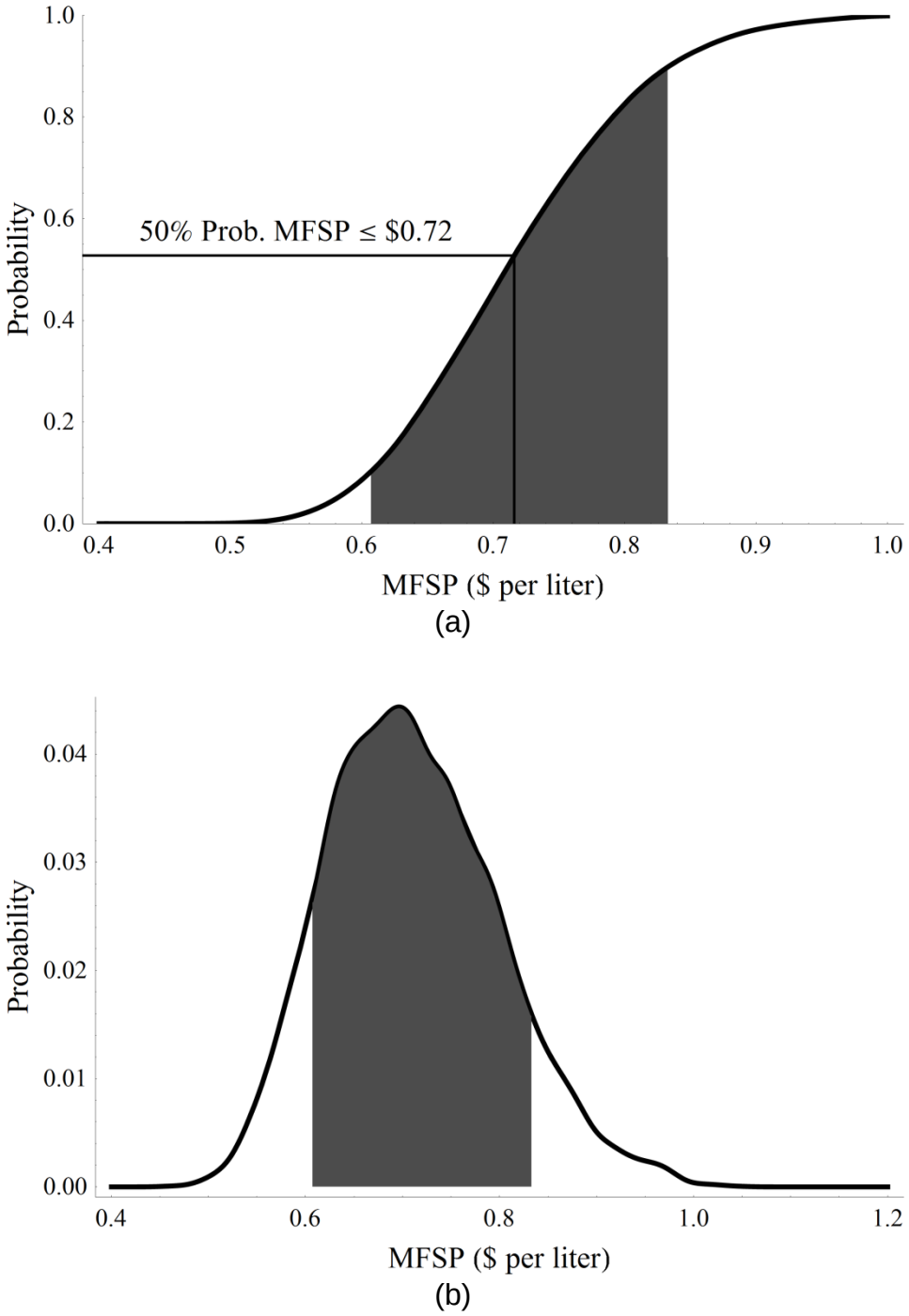

Figure 5 (a) Cumulative Probability of Minimum Fuel-Selling Price (MFSP); (b) MFSP Probabilities Based on Triangular Distributions for Feedstock Cost, Fixed Capital Investment, And Internal Rate of Return. Shaded Region Indicates Confidence Interval Between 0.1 and 0.9.

Conclusions

This techno-economic analysis evaluated the minimum fuel selling price for gasoline- and diesel-range fuels from HTP of defatted microalgae followed by bio-crude upgrading. The process yielded 352 liters per metric ton of dry biomass approximately equally divided between gasoline and diesel fuel.

The 2000 dry metric ton per day facility had a total project investment cost of $489 million, 50% of which was associated with the HTL reactor due to the high-pressure and high-temperature operating conditions. The MFSP was estimated to be $0.68 per liter. Sensitivity analysis showed MFSP to be most sensitive to product fuel yield. Fixed capital investment, IRR and feedstock also greatly influenced MFSP. Monte-Carlo analysis revealed a 50% probability of MFSP being lower than $0.72 per liter, which is comparable to the twenty-year average for gasoline price [55]. These results indicate that HTP of defatted microalgae followed by bio-crude upgrading is a promising pathway for producing advanced biofuels.

References

[1] Delrue F, Li-Beisson Y, Setier PA, Sahut C, Roubaud A, Froment AK, et al. Comparison of various microalgae liquid biofuel production pathways based on energetic, economic and environmental criteria. Bioresour Technol 2013;136:205-12.

[2] Gao X, Yu Y, Wu H. Life Cycle Energy and Carbon Footprints of Microalgal Biodiesel Production in Western Australia: A Comparison of Byproducts Utilization Strategies. ACS Sustainable Chem Eng 2013;1(11):1371-80.

[3] Mata TM, Martins AA, Caetano NS. Microalgae for biodiesel production and other applications: A review. Renew Sustain Energy Rev 2010;14(1):217-32.

[4] Rashid N, Rehman MSU, Han J-I. Recycling and reuse of spent microalgal biomass for sustainable biofuels. Biochem Eng J 2013;75:101-7.

[5] Zhu Y, Albrecht KO, Elliott DC, Hallen RT, Jones SB. Development of hydrothermal liquefaction and upgrading technologies for lipid-extracted algae conversion to liquid fuels. Algal Res 2013;2(4):455-64.

[6] Harun R, Danquah MK, Forde GM. Microalgal biomass as a fermentation feedstock for bioethanol production. J Chem Technol Biotechnol 2010;85(2):199-203.

[7] Hirano A, Hon-Nami K, Kunito S, Hada M, Ogushi Y. Temperature effect on continuous gasification of microalgal biomass: theoretical yield of methanol production and its energy balance. Catal Today 1998;45(1–4):399-404.

[8] Li Y, Horsman M, Wu N, Lan CQ, Dubois-Calero N. Biofuels from Microalgae. Biotechnol Prog 2008;24(4):815-20.

[9] Wang K, Brown RC. Catalytic pyrolysis of microalgae for production of aromatics and ammonia. Green Chem 2013;15(3):675-81.

[10] Amin S. Review on biofuel oil and gas production processes from microalgae. Energy Convers Manag 2009;50(7):1834-40.

[11] Brennan L, Owende P. Biofuels from microalgae—A review of technologies for production, processing, and extractions of biofuels and co-products. Renew Sustain Energy Rev 2010;14(2):557-77.

[12] Chisti Y. Biodiesel from microalgae. Biotechnol Adv 2007;25(3):294-306.

[13] Williams PJlB, Laurens LML. Microalgae as biodiesel & biomass feedstocks: Review & analysis of the biochemistry, energetics & economics. Energy Environ Sci 2010;3(5):554-90.

[14] Bryant HL, Gogichaishvili I, Anderson D, Richardson JW, Sawyer J, Wickersham T, et al. The value of post-extracted algae residue. Algal Res 2012;1(2):185-93.

[15] Davis R, Aden A, Pienkos PT. Techno-economic analysis of autotrophic microalgae for fuel production. Appl Energy 2011;88(10):3524-31.

[16] Yang Z, Guo R, Xu X, Fan X, Luo S. Fermentative hydrogen production from lipid-extracted microalgal biomass residues. Appl Energy 2011;88(10):3468-72.

[17] Talukder MMR, Das P, Wu JC. Microalgae (*Nannochloropsis salina*) biomass to lactic acid and lipid. Biochem Eng J 2012;68:109-13.

[18] Elliott DC, Beckman D, Bridgwater AV, Diebold JP, Gevert SB, Solantausta Y. Developments in direct thermochemical liquefaction of biomass: 1983-1990. Energy Fuels 1991;5(3):399-410.

[19] Matsumura Y, Minowa T, Potic B, Kersten SRA, Prins W, van Swaaij WPM, et al. Biomass gasification in near- and super-critical water: Status and prospects. Biomass Bioenergy 2005;29(4):269-92.

[20] Peterson AA, Vogel F, Lachance RP, Froling M, Antal JMJ, Tester JW. Thermochemical biofuel production in hydrothermal media: A review of sub- and supercritical water technologies. Energy Environ Sci 2008;1(1):32-65.

[21] Akhtar J, Amin NAS. A review on process conditions for optimum bio-oil yield in hydrothermal liquefaction of biomass. Renew Sustain Energy Rev 2011;15(3):1615-24.

[22] Thilakaratne R, Wright MM, Brown RC. A techno-economic analysis of microalgae remnant catalytic pyrolysis and upgrading to fuels. Fuel 2014;128:104-12.

[23] Ross AB, Biller P, Kubacki ML, Li H, Lea-Langton A, Jones JM. Hydrothermal processing of microalgae using alkali and organic acids. Fuel 2010;89(9):2234-43.

[24] Brown TM, Duan P, Savage PE. Hydrothermal Liquefaction and Gasification of Nannochloropsis sp. Energy Fuels 2010;24(6):3639-46.

[25] Toor SS, Rosendahl L, Rudolf A. Hydrothermal liquefaction of biomass: A review of subcritical water technologies. Energy 2011;36(5):2328-42.

[26] Bridgwater AV. Review of fast pyrolysis of biomass and product upgrading. Biomass Bioenergy 2012;38:68-94.

[27] Meier D, Faix O. State of the art of applied fast pyrolysis of lignocellulosic materials — a review. Bioresour Technol 1999;68(1):71-7.

[28] Mohan D, Pittman CU, Steele PH. Pyrolysis of Wood/Biomass for Bio-oil: A Critical Review. Energy Fuels 2006;20(3):848-89.

[29] Maldas D, Shiraishi N. Liquefaction of biomass in the presence of phenol and H_2O using alkalies and salts as the catalyst. Biomass Bioenergy 1997;12(4):273-9.

[30] Meier D, Larimer DR, Faix O. Direct liquefaction of different lignocellulosics and their constituents: 1. Fractionation, elemental composition. Fuel 1986;65(7):910-5.

[31] Jena U, Das KC, Kastner JR. Effect of operating conditions of thermochemical liquefaction on biocrude production from Spirulina platensis. Bioresour Technol 2011;102(10):6221-9.

[32] Vardon DR, Sharma BK, Blazina GV, Rajagopalan K, Strathmann TJ. Thermochemical conversion of raw and defatted algal biomass via hydrothermal liquefaction and slow pyrolysis. Bioresour Technol 2012;109:178-87.

[33] Biller P, Ross AB, Skill SC, Lea-Langton A, Balasundaram B, Hall C, et al. Nutrient recycling of aqueous phase for microalgae cultivation from the hydrothermal liquefaction process. Algal Res 2012;1(1):70-6.

[34] Humbird D, Davis R, Tao L, Kinchin C, Hsu D, Aden A, et al. Process design and economics for biochemical conversion of lignocellulosic biomass to ethanol dilute-acid pretreatment and enzymatic hydrolysis of corn stover. Golden (CO): National Renewable Energy Laboratory; 2011. Report No.: NREL/TP-5100-47764. Contract No.: DE-AC36-08GO28308. Sponsored by the Department of Energy.

[35] Jones SB, Valkenburg C, Walton CW, Elliott DC, Holladay JE, Stevens DJ, et al. Production of gasoline and diesel from biomass via fast pyrolysis, hydrotreating and hydrocracking: a design case. Richland (WA): Pacific Northwest National Laboratory; 2009. Report No.: PNNL-18284. Contract No.: DE-AC05-76RL01830. Sponsored by the Department of Energy.

[36] Kazi FK, Fortman J, Anex R, Kothandaraman G, Hsu D, Aden A, et al. Techno-economic analysis of biochemical scenarios for production of cellulosic ethanol. Golden (CO): National Renewable Energy Laboratory; 2010. Report No.: NREL/TP 6A2-46588. Contract No.: DE-AC36-08-GO28308. Sponsored by the Department of Energy.

[37] SRI. PEP Yearbook International 2007. Menlo Park (CA): SRI International; 2007.

[38] Jones SB, Zhu Y. Techno-economic analysis for the conversion of lignocellulosic biomass to gasoline via the methanol-to-gasoline (MTG) process. Richland (WA): Pacific Northwest National Laboratory; 2009. Report No.: PNNL-18481. Contract No.: DE-AC05-76RL01830. Sponsored by the Department of Energy.

[39] Wright MM, Daugaard DE, Satrio JA, Brown RC. Techno-economic analysis of biomass fast pyrolysis to transportation fuels. Fuel 2010;89 Suppl 1:S2-10.

[40] Biller P, Ross AB. Potential yields and properties of oil from the hydrothermal liquefaction of microalgae with different biochemical content. Bioresour Technol 2011;102(1):215-25.

[41] Elliott DC, Neuenschwander GG, Hart TR, Rotness L, Zacher AH, Santosa D, et al. Catalytic hydrothermal gasification of lignin-rich biorefinery residues and algae. Richland (WA): Pacific Northwest National Laboratory; 2009. Report No.: PNNL-18944. Contract No.: DE-AC06-76RL01830. Sponsored by the Department of Energy.

[42] Thilakaratne R, Brown T, Li Y, Hu G, Brown R. Mild catalytic pyrolysis of biomass for production of transportation fuels: a techno-economic analysis. Green Chem 2014;16(2):627-36.

[43] Elliott DC. Historical Developments in Hydroprocessing Bio-oils. Energy Fuels 2007;21(3):1792-815.

[44] Elliott DC, Hart TR, Schmidt AJ, Neuenschwander GG, Rotness LJ, Olarte MV, et al. Process development for hydrothermal liquefaction of algae feedstocks in a continuous-flow reactor. Algal Res 2013;2(4):445-54.

[45] Skone TJ. Role of Alternative Energy Sources: Natural Gas Technology Assessment. Pittsburgh (PA): National Energy Technology Laboratory; 2012. Report No.: DOE/NETL-2012/1539. Contract No.: DE-FE0004001. Sponsored by the Department of Energy.

[46] Molburg JC, Doctor RD. Hydrogen from steam-methane reforming with CO_2 capture. Proceedings of the 20th Annual international Pittsburgh coal conference; 2003 Sep 15-19; Pittsburgh PA.

[47] Spath PL, Mann MK. Life cycle assessment of hydrogen production via natural gas steam reforming. Golden (CO): National Renewable Energy Laboratory; 2000. Report No.: NREL/TP-570-27637. Contract No.: DE-AC36-99-GO10337. Sponsored by the Department of Energy.

[48] Turton R, Bailie RC, Whiting WB, Shaeiwitz JA. Analysis, synthesis and design of chemical processes. 3rd ed. Boston: Pearson Education; 2008.

[49] Peters MS, Timmerhaus KD, West RE. Plant Design and Economics for Chemical Engineers. 5th ed. New York: McGraw-Hill; 2003.

[50] Hofstrand D, Johanns A. Weekly Ethanol, Distillers Grain, & Corn Prices. http://www.extension.iastate.edu/agdm/energy/xls/agmrcethanolplantprices.xlsx [accessed 7 June 2014].

[51] EIA. United States Natural Gas Industrial Price. http://www.eia.gov/dnav/ng/hist/n3035us3m.htm [accessed 7 June 2014].

[52] EIA. Electric Power Monthly with data for April 2013. Independent Statistics & Analysis. Washington (DC): U.S. Energy Information Administration; 2013.

[53] Aden A. Biochemical production of ethanol from corn stover: 2007 state of technology model. Golden (CO): National Renewable Energy Laboratory; 2008. Report No.: NREL/TP-510-43205. Contract No.: DE-AC36-99-GO10337. Sponsored by the Department of Energy.

[54] Glantz M, Henderson B. Scientific Financial Management: Advances in Financial Intelligence Capabilities for Corporate Valuation and Risk Assessment. 1st ed. New York: AMACOM; 2000.

[55] EIA. Annual Energy Outlook 2011. Independent Statistics & Analysis. Washington (DC): U.S. Energy Information Administration; 2011. Report No.: DOE/EIA-0383(2011).

CHAPTER 4 UNDERSTANDING UNCERTAINTIES IN THE ECONOMIC FEASIBILITY OF TRANSPORTATION FUEL PRODUCTION USING BIOMASS GASIFICATION AND MIXED ALCOHOL SYNTHESIS

A paper published in *Energy Technology*

Longwen Ou, Boyan Li, Qi Dang, Susanne Jones, Robert Brown, Mark M Wright

Abstract

This study evaluates uncertainties in the techno-economic analysis of transportation fuel production from biomass gasification and mixed alcohol synthesis. Two scenarios are considered: a state-of-technology scenario and a target scenario with projected technological advances. Uncertainties of more than 10 parameters are investigated. The probability distributions of these parameters are estimated based on historical price data and experimental data. Data samples generated from the corresponding distribution are then utilized to run a Monte Carlo simulation. The results yield minimum fuel-selling prices of $\$ 1.85\ L^{-1}$ with a standard deviation of 0.13 for the state-of-technology scenario and $\$ 1.14\ L^{-1}$ with a standard deviation of 0.11 for the target scenario, respectively. The feedstock price and internal rate of return (IRR) have significant impacts on the minimum fuel-selling price in both scenarios. These findings are indicative of the reduction in biofuel cost and uncertainty achievable with increasing technology maturity.

Introduction

Growing demand for fossil fuels and increasing emphasis on the environment have made biofuels an attractive substitute of petroleum derived transportation fuels.[1-3]

Ethanol remains the biofuel most widely available commercially although a wide variety of pathways have been investigated including gasification, fast pyrolysis, and hydrothermal liquefaction.[4-8] These pathways have the potential to be scaled up commercially, but they require large capital investment at a significant financial risk.[9] Therefore, it is imperative that the uncertainty in the profitability of these pathways is investigated before investments are made to minimize risks.

Biomass gasification is a mature technology recognized for its ability to deliver a wide range of fuels through several catalytic upgrading routes. Biomass gasification generates a synthetic gas that can be upgraded to hydrocarbons via Fischer-Tropsch[10, 11] or Methanol-to-Gasoline synthesis,[12] alcohols through mixed alcohol synthesis[13] and fermentation.[14] Although gasification is a mature technology, the catalytic upgrading pathways are at varying levels of development and few have achieved large industrial scale in the biofuel sector. Several commercialization ventures have pursued gasification-based biofuel production in recent years. [15]

Biomass gasification and mixed alcohol synthesis is an attractive option for biofuel production because of its ability to produce ethanol at a high yield (350 L/MT [13]) from a wide range of feedstock. However, barriers to commercial success are the high capital cost, limited market for higher alcohol co-products, and challenges with tar removal. The sensitivity of the minimum ethanol selling price (MESP) to various techno-economic parameters has been evaluated in a previous study by Dutta et al. [13] That study found potential changes of up to +38.6%/-34.5% to the MESP for variations in individual parameters. However, the range of potential MESP values could be greater if more than one parameter deviates from expected values.

Techno-economic analysis (TEA) has been used widely to evaluate economic feasibility of various biofuel pathways, including mature first generation ethanol biorefineries, and relatively novel fast pyrolysis, gasification, and hydrothermal liquefaction. [16-20] Immaturity of these processes dictate their intrinsic risk, which result from uncertainties of the parameters chosen to conduct the TEA such as feedstock price, internal rate of return (IRR), etc. These uncertainties can be accounted for by incorporating variability in commodity prices, experimental measurements, and financing parameters among others. In a previous study, Brown and Wright demonstrated that these uncertainties have a significant influence on the predicted profitability of biofuel pathways. [9] Therefore, TEAs with single point estimates [21] could be enhanced by addressing the uncertainties in the analyses.

Monte-Carlo simulation has been adopted in recent TEAs as an effort to account for the uncertainties within the analyses. [17, 22, 23] The sequence proceeds as follows: several key parameters with potential for significant impact on the results are first identified, a predetermined distribution is then assigned for each parameter, and large data sets (usually 10,000 data) are generated according to the assigned distributions. These data sets are then incorporated into the financial spreadsheet to run a Monte-Carlo simulation so that each iteration utilizes a unique combination of data for each parameter in the data set. [24] It allows more than one parameter to vary at the same time so that the impacts of multiple parameters on the result can be evaluated. It also provides distribution information on the result of TEA.

This paper contributes a detailed uncertainty analysis of two biomass gasification and mixed alcohol synthesis scenarios: a state-of-technology scenario and a target

scenario. More than ten parameters that may have significant impact on the Minimum Fuel Selling Prices (MFSP) are investigated. Distributions of each parameter are determined from historical data, which are then used to generate data sets for Monte-Carlo simulations.

Methodology

Process design of biomass gasification and alcohol synthesis for diesel fuel production

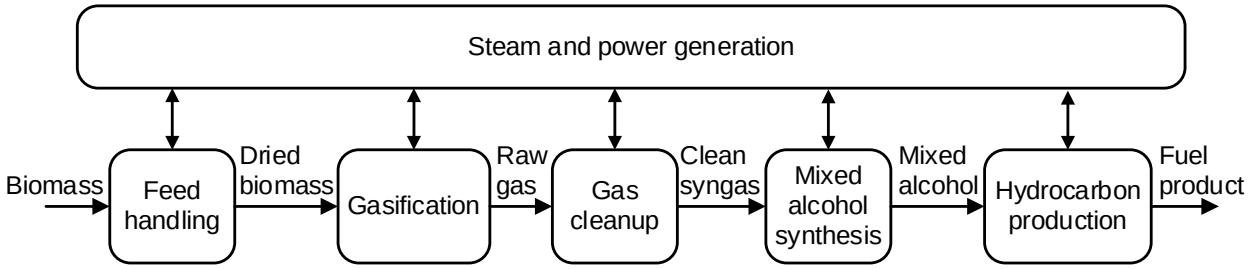

Figure 1 Schematic of biomass gasification and alcohol synthesis for diesel fuel production.

The process evaluated in this analysis is transportation fuel production via biomass gasification and subsequent alcohol synthesis and conversion to distillates. Six areas are involved in this process: feed handling and preparation, gasification, syngas cleanup, mixed alcohol synthesis, hydrocarbon production, and steam and power generation, as shown in **Figure 1**. The design of feedstock handling, gasification, syngas cleanup, and mixed alcohol synthesis is based on previous work by NREL. [25] The design of hydrocarbon production is based on related patents.

Feed handling and preparation involves feedstock drying to below 10 wt. % moisture content. The dried biomass is then gasified at 870 °C and 2 bar. A relatively small fraction of biomass is converted into tars, which are comprised mostly of aromatic

and poly-aromatic hydrocarbons. The nitrogen in the feedstock is primarily converted to ammonia. The raw producer gas from the gasifier is sent to a catalytic tar reformer to convert a portion of tar, methane and other light hydrocarbons to CO and H_2. Part of the ammonia is converted to nitrogen and hydrogen. The syngas is then cooled and sent to a wet scrubber to remove impurities such as particulates, remaining ammonia and residual tars.

The conditioned syngas is then compressed to 207 bar using a six-stage compressor system with inter-stage cooling. The compressed syngas is mixed with recycled syngas and recycled methanol and preheated to 313 °C before entering for mixed alcohols reactor. The gas entering the alcohol synthesis reactor has a H_2/CO molar ratio of 1.5. Steam is generated using the heat released from the exothermic alcohol synthesis reactions. The effluent gases from the reactor are cooled and flashed to remove alcohols as a liquid stream. The gaseous stream is recycled to the reactor after removal of CO_2 and H_2S with a physical solvent: dimethyl ethers of polyethylene glycol (DEPG). The solvent from the absorber is then flashed at a lower pressure to expel less soluble compounds such as H_2, CO, and CH_4, which is then recycled to the tar reformer and fuel combustor. The liquid effluent is directed to a distillation column for methanol removal before dehydration. Overhead product of the methanol removal column, consisting of essentially all of the feed methanol and other light compounds such as CO_2 and H_2, is then cooled and flashed. The gaseous stream of the flash drum goes to fuel combustor with the liquid stream, which consists mostly of methanol and a small amount of ethanol, recycled to the mixed alcohol synthesis reactors.

Dehydration of mixed alcohols is designed based on US patent 4396789 and US patent application 20130190547. The synthesized alcohols are pumped to 20 bar and dehydrated in a series of three adiabatic reactors to produce small molecular weight olefins. After heat recovery, the olefin product from the dehydration reactors goes through a water scrubber for removal of methanol and other residual alcohols. The olefin stream undergoes oligomerization in the presence of organic solvent, toluene, at 32 bar to produce linear alpha olefins including *1*-decene and *1*-dodecene. This process is based on patent DE4338414C1.

The product stream is depressurized and cooled in a flash separator. The gaseous stream is recycled to the oligomerization reactor while the liquid stream is directed to a distillation column to separate solvent from olefins. The solvent is recycled to the oligomerization reactor. The olefins are hydrogenated at 29 bar to produce saturated hydrocarbons product.

The process also includes a steam cycle that generates steam through recovering waste heat from the hot process streams throughout the plant. The steam cycle also generates power for plant operations through a multi-stage steam turbine. A fuel combustor is also included to recover energy from plant off-gases.

State-of-technology scenario and target scenario

This analysis involves two scenarios: a state-of-technology scenario and a target scenario. These scenarios are distinguished primarily by assumptions in Lang Factor and oligomerization technology. The state-of-technology scenario assumes a Lang Factor (total investment divided by bare equipment costs) of 4.15 to account for the high degree of uncertainty in the process equipment needed and costs for a pioneer technology

implementation. In the target scenario, a lower Lang factor and equipment costs are assumed to account for technological and process improvements. A mean value of 4 is assumed for Lang factor which is lower than the fixed value in the state-of-technology scenario. Ethylene per pass conversion to butene and hexene is estimated to be approximately 11 wt. %. A low per-pass conversion of 0.11% was considered in order to understand the potential impact on long-term profitability. Per-pass conversion affects the amount of olefin recycle and the yield of the desired products.

Uncertainty analysis

This analysis evaluates TEA uncertainties of a biomass gasification and mixed alcohol synthesis process design for ethanol production. Uncertainties of the TEAs result from various factors including variability in parameters such as IRR, capital costs, and volatility of feedstock and product prices. Uncertainties of more than ten parameters are considered in this analysis to gain a better understanding of the economic performance of the proposed process including feedstock price, IRR, capital cost, Lang Factor, catalyst cost, electricity price, conversion factors of key reactions such as mixed alcohol synthesis and olefin oligomerization. The analysis proceeds as follows: data for the parameters mentioned above are first collected and categorized. [25-28] The data are then fitted to an appropriate distribution. Several candidate distributions are considered: Normal, Lognormal, Exponential, Chi-Square, Cauchy, Laplace, and Logistic. The best fit distributions are determined from the Anderson-Darling goodness-of-fit test. [29] In some cases, the best-fit distributions are adjusted to account for differences in the expected mean value, variance, or distribution type. For example, the mean of feedstock price is shifted from $28/dry MT from the original data set to $80/dry ton in order to account for

additional costs associated with transportation, handling, and grower payments. Data sets with 10,000 unique samples are gathered from the best-fit probability distributions.

The parameters investigated in this analysis can be divided into two categories. The first category includes all parameters except for reaction conversion factors. These parameters are incorporated directly into the financial spreadsheet to run the Monte-Carlo analysis. Reaction conversion parameters fall into the second category, whose impact on the final MFSP is evaluated indirectly via the biofuel production rate. That is, a relationship between the biofuel production rate and reaction conversions was first determined through a surrogate model of the CHEMCAD process model. A predetermined triangular distribution was assigned to the conversion of each alcohol synthesis and olefin oligomerization reaction. For example, the mixed alcohol reactor converts syngas and recycled methanol into alcohols, hydrocarbons and carbon dioxide. Each reaction is modeled by a stoichiometric equation with fixed conversion rates. The conversion rates were varied and a simple yield correlation developed. The built-in CHEMCAD sensitivity analysis tool is then used to investigate the impact of each conversion yield factor on the diesel biofuel production rate. The sensitivity analysis data is employed to develop a linear regression, and it appears that alcohol and hydrocarbon synthesis yields have a linear relationship with biofuel production. This linear relationship is employed to generate 10,000 product fuel production rates based on the conversion yield distributions. The results of the fuel production rate data, along with other key parameters are integrated into financial spreadsheets to calculate the minimum fuel-selling price (MFSP) of biofuels. Uncertainty analysis results are reported as error bars and distributions of the MFSP, and

the relative impacts of the key input parameters. **Figure 2** shows a flowchart of the research methodology.

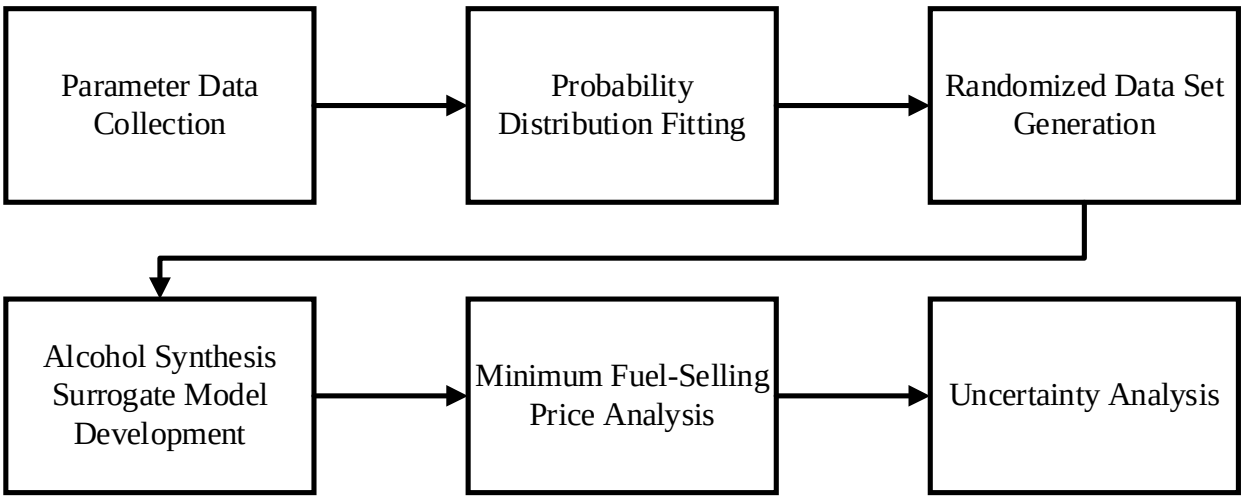

Figure 2 Flowchart of the uncertainty methodology for biomass gasification and mixed alcohol synthesis.

Historical price data for feedstock and various fuels from 2007 to 2012 are collected from several sources. U.S. average wholesale prices for gasoline and diesel and industrial natural gas and electricity prices are taken from Energy Information Administration (EIA).[27] Feedstock price data are collected from pine pulpwood prices from the Texas A&M Forestry Service.[26]

The parameters investigated in this analysis are shown in **Table 1**. The mixed alcohol synthesis reactor conversions shown in **Table 1** are taken from the data given in.[25] Uncertainties of several parameters such as Lang Factor and catalysts costs are only investigated in the target scenario to see how they affect the MFSP. Oligomerization conversion yields differ as well based on the assumption of improving ethanol yields.

Table 1 Mean, 10% and 90% confidence levels, and best-fit distributions of selected techno-economic analysis parameters

Parameter	Mean	10% Confidence / Min[a]	90% Confidence / Max[a]	Distribution
Industrial Natural Gas Price ($/m3)	0.22	0.14	0.32	Lognormal
Industrial Electricity Price (¢/kwh)	6.05	5.00	7.09	Normal
Pine pulpwood ($/MT)	78.69	67.21	90.18	Lognormal
Gasoline Wholesale ($/L)	0.47	0.24	0.76	Lognormal
Diesel Wholesale ($/L)	0.46	0.16	0.77	Lognormal
Gasifier uninstalled capex (MM$)	9.80	7.35	12.93	Triangular
Tar reformer uninstalled capex (MM$)	4.90	4.90	9.70	Triangular
Installation factor	2.31	1.50	2.80	Triangular
Methanol to Ethanol Conv. Frac	0.44	0.46	0.48	Triangular
CO to Methanol Conv. Frac.	0.059	0.062	0.065	Triangular
CO to Ethanol Conv. Frac.	0.040	0.042	0.044	Triangular
CO to N-Propanol Conv. Frac.	0.015	0.016	0.016	Triangular
CO to Methane Conv. Frac.	0.039	0.042	0.044	Triangular
CO to Ethane Conv. Frac.	0.0029	0.0030	0.0032	Triangular
CO to Propane Conv. Frac.	0.0010	0.0011	0.0012	Triangular
Butene to Hexadecene Conv. Frac.	0.86	0.90	0.95	Triangular
Ethylene to Butene Conv. Frac.	0.10 (0.0011)[b]	0.11 (0.11)	0.12 (0.12)	Triangular
Ethylene to Hexene Conv. Frac.	NA[c] (0.0011)	NA (0.11)	NA (0.11)	Triangular
Syngas compressors capex[c]	100% (90%)	80% (50%)	140% (140%)	Triangular
Synthesis reactor capex[c]	100% (90%)	90% (50%)	140% (140%)	Triangular
Purge gas expanders capex[c]	100% (90%)	90% (50%)	140% (140%)	Triangular
acid gas system capex[c]	100% (90%)	100% (50%)	140% (140%)	Triangular
heat integration capex[c]	100% (90%)	100% (50%)	140% (140%)	Triangular
Compression duty (MW)[c]	100% (90%)	80% (50%)	100% (100%)	Triangular
Expander duty (MW)[c]	100% (90%)	50% (50%)	100% (100%)	Triangular
Alcohol to hydrocarbon fuels capex, MM$	NA (160)	NA (120)	NA (280)	Triangular
Catalysts Costs, MM$/year	NA (3.20)	NA (1.00)	NA (7.50)	Triangular
Lang Factor	NA (4.00)	NA (3.00)	NA (5.00)	Triangular

[a] For lognormal distribution, 10% / 90% confidence interval is given. For triangular distribution, minimum / maximum values are given. [b] Values in parentheses are used in the analysis of the target scenario. [c] NA: not available. [c] Values are given as percentage of the base case values.

Results and discussion

Distribution fitting

Figure 3 shows fitted Probability Density Functions (PDF) of historical feedstock and energy prices. The fitted distribution for each variable is listed in **Table 1**. They reflect the historical trends of these commodities. Lognormal distribution best fitted historical price data for all commodities. Triangular distributions are used for variables with limited sample data.

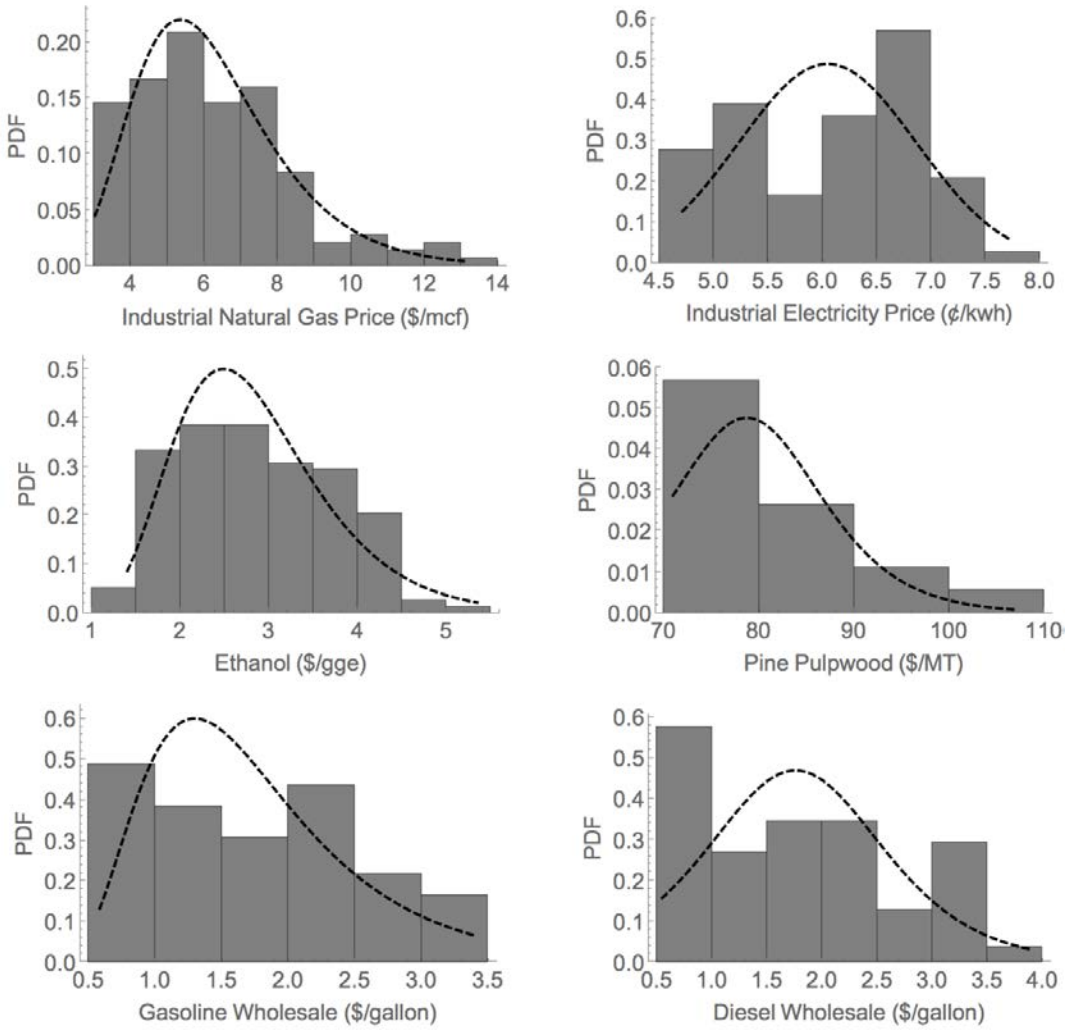

Figure 3 Fitted Probability Density Functions (PDF) of Historical Feedstock and Energy Prices.

State-of-technology scenario

Tables 2-4 show the base case results of the state-of-technology scenario. The results are obtained by assuming the most probable values for all input variables. The estimated MFSP is high due to immaturity of some process areas such as mixed alcohol synthesis and diesel fuel production. High capital costs and heavy utility demand of these areas contribute to the high MFSP.

Table 2 Process modeling results

Scenario	MFSP ($/L)	Fuel production rate (MM L/year)	Fuel product yield (L/dry MT feedstock)
SOT	1.79	159	246
Target	1.04	178	269

Table 3 Breakdown of Installed equipment cost in million dollars

Scenario	Feed Handling	Gasification	Syngas Cleanup	Mixed Alcohol Synthesis	Diesel Fuel Production	Power & Heat Plant	Balance of Plant	Total
SOT	0	48.2	106.5	83.8	118.8	30.8	9.0	397.1
Target	0	48.2	83.5	58.7	59.4	27.7	9.0	286.5

Table 4 Breakdown of operating costs in million dollars

Scenario	Feedstock	Catalysts & Chemicals	Waste Disposal	Electricity and other utilities	Fixed Costs	Capital Depreciation	Average Income Tax	Average Return on Investment	Total
SOT	57.9	19.8	0.7	11.6	44.6	47.4	25.4	79.3	286.7
Target	57.9	5.4	0.7	2.4	28.5	27.3	14.8	46.3	183.3

Figure 4 shows the probability and cumulative MFSP distributions for the high Lang Factor syngas to distillates case scenario. It can be seen that the base case MFSP lies on the left of the most probable region. The most probable MFSP value is slightly higher than the base case value. There is an 80% probability that the MFSP falls between \$1.69/L and \$2.02/L for the given assumptions.

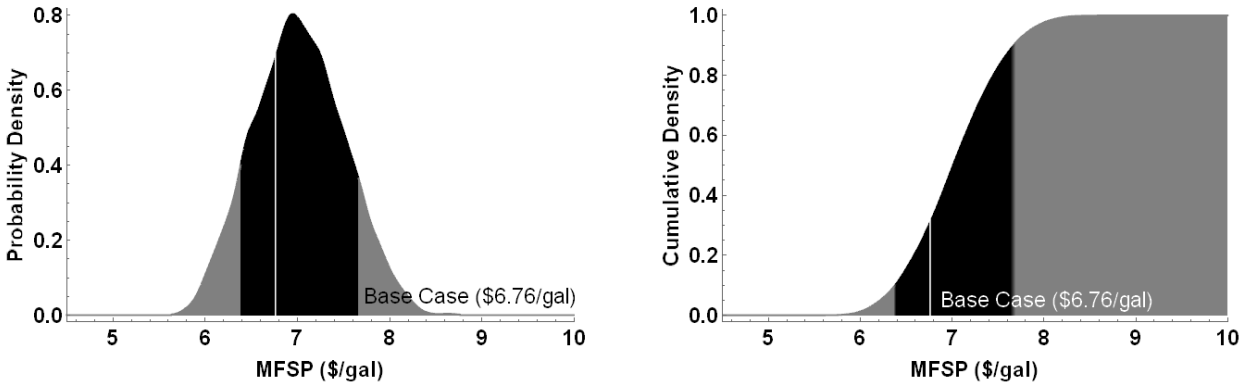

Figure 4 Minimum Fuel-Selling Price (MFSP) probability (left) and cumulative (right) distributions for syngas to distillates with high Lang factor.

Figure 5 shows the parameter uncertainty impact on the syngas to distillate MFSP for the state-of-technology scenario. This figure is more informative than traditional sensitivity analysis. It gives not only the range of the MFSP, but also the 0.25/0.75 quartile values for each parameter investigated. In some cases, the parameter that generates the largest MFSP range does not necessarily give the largest range of 0.25/0.75 quartile values, as will be shown later in **Figure 7**. **Figure 5** also provides the median value for each parameter in contrast to the sensitivity analysis in which only the base case value is provided for each parameter. For instance, the median value of feedstock price in **Figure 5** is skewed leftward, indicating that the uncertainty of feedstock price is likely to result in a lower MFSP than the base case. **Figure 5** presents the parameters investigated in such a way that the parameter with the greatest direct influence (a larger value of the

parameter generates a higher MFSP) comes first while those with the greatest inverse influence (a larger value of the parameter generates a lower MFSP) come last. For example, feedstock has a positive influence on the MFSP since higher feedstock price would increase the MFSP. In contrast, higher gas hourly space velocity reduces the size of the reactors and thus capital cost; therefore it has an inverse influence on the MFSP. As is shown in **Figure 5**, IRR has the most significant impact on MFSP, followed by feedstock price. However, the latter has a smaller range of expected (0.25/0.75 quartile) values. This result agrees with other research regarding biomass gasification and methanol-to-gasoline.[12] The relatively low impact of process parameters, installation factors and equipment costs indicates that this process is mature.

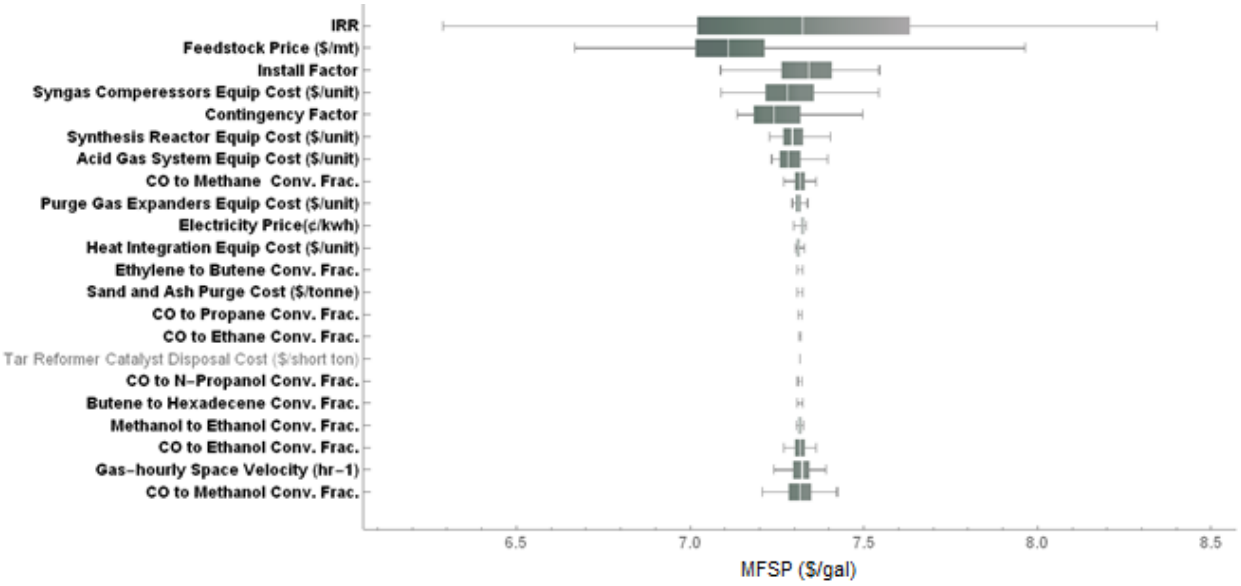

Figure 5 Syngas to distillates high Lang factor parameter uncertainty impact on the MFSP. Gates indicate min/max MFSP range; boxes indicate 0.25-0.75 quantiles of the MFSP; white vertical lines show the median MFSP value. Bold legends indicate significant ($p<0.05$) parameters.

Target scenario

Base case results of the target scenario are shown in **Tables 2-4**. The main difference from the state-of-technology scenario is that installed equipment costs related to mixed alcohol synthesis, and fuel production are lower due to improved maturity of the target scenario concept design. Installed equipment costs of steam plant are also reduced to account for lower energy demand in the target scenario. Other improvements include higher product yield and lower catalyst load in mixed alcohol synthesis, alcohol dehydration, and alkene hydrogenation reactions.

Figure 6 shows the target scenario MFSP distribution. In the target scenario, the uncertainty of Lang Factor impact are also investigated. It can be seen from **Figure 6** that the base case MFSP lies on the left half of the probability density curve, while the most probable value for MFSP (~$1.12/L) is actually higher than the base case value of $1.04/L. It is shown in **Figure 6** that there is 80% probability that the MFSP lies between $1.01/L and $1.29/L.

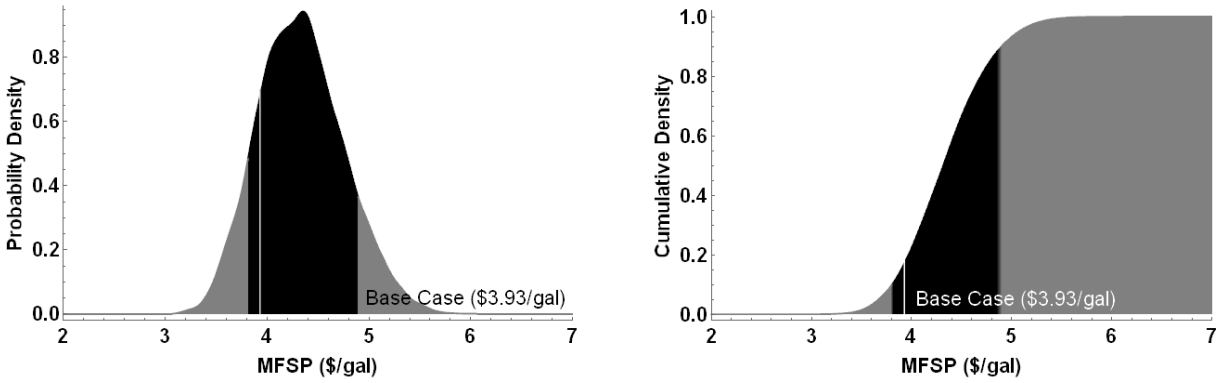

Figure 6 Minimum Fuel-Selling Price (MFSP) probability (left) and cumulative (right) distributions for syngas to distillates with low Lang factor target scenario.

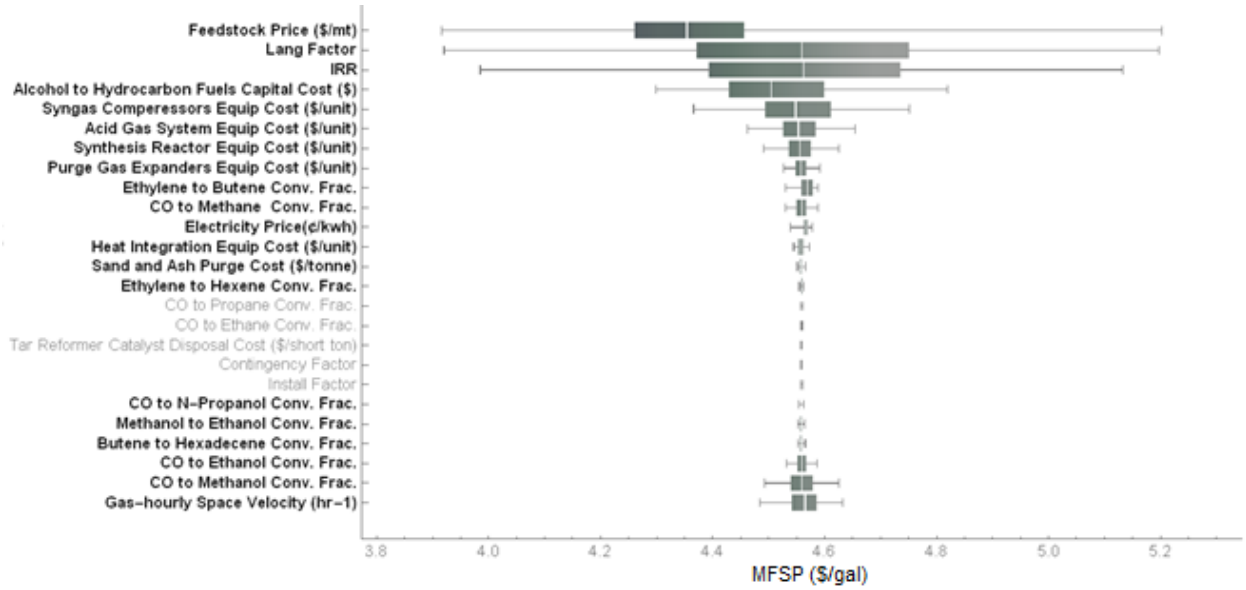

Figure 7 Syngas to distillates target scenario with low Lang factor parameter uncertainty impact on the MFSP. Gates indicate min/max MFSP range; boxes indicate 0.25-0.75 quantiles of the MFSP; white vertical lines show the median MFSP value. Bold legends indicate significant ($p<0.05$) parameters.

Figure 7 shows the impactful parameters for the target scenario. Feedstock price has the widest range of MFSP suggesting it might have the greatest impact on MFSP. However, the range of most probable feedstock prices lying between the 0.25-0.75 quantiles suggest it has a smaller influence than Lang factor and IRR. This result highlights how uncertainty analysis can enhance sensitivity analysis by identifying not only potential values but also their likelihood.

Comparison of state-of-technology and target scenarios

Figure 8 shows a comparison of the MFSP for the state-of-technology and target scenarios. The results indicate that the state-of-technology scenario has a high expected MFSP of $1.85/L. With the capital cost being lowered in the target scenario, a lower mean MFSP ($1.14/L) was obtained. Capital costs are the main contributing factors to the higher cost for the base case scenario. However, the standard deviation of the target

scenario (10% of the mean MFSP) is higher than that of the state-of-technology scenario (7% of the mean MFSP).

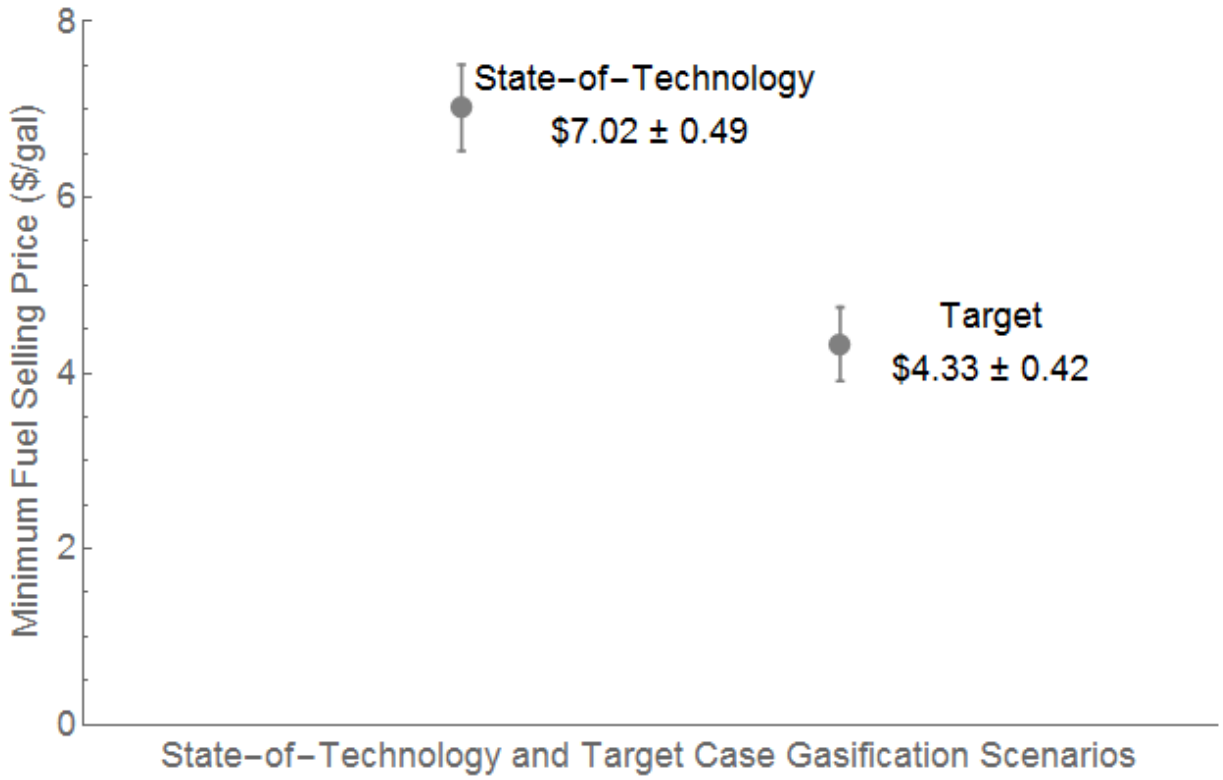

Figure 8 Syngas to distillates target scenario with low Lang factor parameter.

Conclusions

This analysis investigated the uncertainty of biomass gasification and subsequent diesel fuel production process by comparing with a state-of-technology and a target scenario. Impacts of more than ten parameters on the MFSP were explored by Monte-Carlo simulation, consisting of 10,000 runs. The state-of-technology scenario yielded a MFSP of $1.85/L with a standard deviation of 0.13; the target scenario presented a MFSP

of $1.14/L with a standard deviation of 0.11. The analysis gave a 10% to 90% probability interval of the two scenarios of $1.69/L to $2.02/L, and $1.01/L to $1.29/L respectively.

Feedstock price and IRR were the most impactful parameters on the MFSP in both scenarios. Uncertainty of Lang Factor was investigated in the target scenario. The results indicated that it had significant impact on the MFSP. The results of this analysis justified the need to better understand uncertainties of these parameters.

References

[1] Escobar JC, Lora ES, Venturini OJ, Yáñez EE, Castillo EF, Almazan O. Biofuels: Environment, technology and food security. Renew Sustain Energy Rev 2009;13(6–7):1275-87.

[2] Hill J, Nelson E, Tilman D, Polasky S, Tiffany D. Environmental, economic, and energetic costs and benefits of biodiesel and ethanol biofuels. Proceedings of the National Academy of Sciences 2006;103(30):11206-10.

[3] Peters J, Thielmann S. Promoting biofuels: Implications for developing countries. Energ Policy 2008;36(4):1538-44.

[4] Huber GW, Chheda JN, Barrett CJ, Dumesic JA. Production of liquid alkanes by aqueous-phase processing of biomass-derived carbohydrates. Science 2005;308(5727):1446-50.

[5] Meier D, Faix O. State of the art of applied fast pyrolysis of lignocellulosic materials — a review. Bioresour Technol 1999;68(1):71-7.

[6] Richardson Y, Blin J, Julbe A. A short overview on purification and conditioning of syngas produced by biomass gasification: Catalytic strategies, process intensification and new concepts. Prog Energ Combust 2012;38(6):765-81.

[7] Toor SS, Rosendahl L, Rudolf A. Hydrothermal liquefaction of biomass: A review of subcritical water technologies. Energy 2011;36(5):2328-42.

[8] Wang K, Brown RC. Catalytic pyrolysis of microalgae for production of aromatics and ammonia. Green Chem 2013;15(3):675-81.

[9] Brown TR, Wright MM. A Framework for Defining the Economic Feasibility of Cellulosic Biofuel Pathways. Biofuels 2014;5(5):579-90.

[10] Floudas CA, Elia JA, Baliban RC. Hybrid and single feedstock energy processes for liquid transportation fuels: A critical review. Comput Chem Eng 2012;41:24-51.

[11] Swanson RM, Platon A, Satrio JA, Brown RC. Techno-economic analysis of biomass-to-liquids production based on gasification. Fuel 2010;89, Supplement 1:S11-S9.

[12] Phillips SD, Tarud JK, Biddy MJ, Dutta A. Gasoline from Woody Biomass via Thermochemical Gasification, Methanol Synthesis, and Methanol-to-Gasoline Technologies: A Technoeconomic Analysis. Ind Eng Chem Res 2011;50(20):11734-45.

[13] Dutta A, Talmadge M, Hensley J, Worley M, Dudgeon D, Barton D, et al. Techno-economics for conversion of lignocellulosic biomass to ethanol by indirect gasification and mixed alcohol synthesis. Environ Prog Sustain 2012;31(2):182-90.

[14] Jarboe L, Wen Z, Choi D, Brown R. Hybrid thermochemical processing: fermentation of pyrolysis-derived bio-oil. Appl Microbiol Biotechnol 2011;91(6):1519-23.

[15] Brown TR, Brown RC. A review of cellulosic biofuel commercial-scale projects in the United States. Biofuel Bioprod Bior 2013;7(3):235-45.

[16] Ou L, Brown TR, Thilakaratne R, Hu G, Brown RC. Techno-economic analysis of co-located corn grain and corn stover ethanol plants. Biofuel Bioprod Bior 2014;8(3):412-22.

[17] Ou L, Thilakaratne R, Brown RC, Wright MM. Techno-economic analysis of transportation fuels from defatted microalgae via hydrothermal liquefaction and hydroprocessing. Biomass Bioenergy 2015;72(0):45-54.

[18] Thilakaratne R, Wright MM, Brown RC. A techno-economic analysis of microalgae remnant catalytic pyrolysis and upgrading to fuels. Fuel 2014;128:104-12.

[19] Wang K, Ou L, Brown T, Brown RC. Beyond ethanol: a techno-economic analysis of an integrated corn biorefinery for the production of hydrocarbon fuels and chemicals. Biofuels, Bioprod Biorefin 2015;9(2):190-200.

[20] Wright MM, Daugaard DE, Satrio JA, Brown RC. Techno-economic analysis of biomass fast pyrolysis to transportation fuels. Fuel 2010;89:S2-S10.

[21] Brown TR. A techno-economic review of thermochemical cellulosic biofuel pathways. Bioresour Technol 2015;178(0):166-76.

[22] Brown TR, Wright MM. Techno-economic impacts of shale gas on cellulosic biofuel pathways. Fuel 2014;117, Part B(0):989-95.

[23] Thilakaratne R, Brown T, Li Y, Hu G, Brown R. Mild catalytic pyrolysis of biomass for production of transportation fuels: a techno-economic analysis. Green Chem 2014;16(2):627-36.

[24] Spinney PJ, Watkins GC. Monte Carlo simulation techniques and electric utility resource decisions. Energ Policy 1996;24(2):155-63.

[25] Dutta A, Talmadge M, Hensley J, Worley M, Dudgeon D, Barton D, et al. Process design and economics for conversion of lignocellulosic biomass to ethanol. Contract; 2011, p. 275-3000.

[26] Service TAMF. Timber Price Trends. 2015.

[27] EIA. Short-term Energy Outlook. 2015.

[28] Jones SB, Zhu Y. Techno-economic analysis for the conversion of lignocellulosic biomass to gasoline via the methanol-to-gasoline (MTG) process. Report No PNNL-18481 Pacific Northwest National Laboratory, Richland, WA; 2009.

[29] Stephens MA. EDF statistics for goodness of fit and some comparisons. J Am Stat Assoc 1974;69(347):730-7.

CHAPTER 5 ENVIRONMENTAL IMPACTS OF CO-FIRING BIO-OIL IN COAL-FIRED POWER PLANTS

A paper in preparation for submission to *Environmental Science & Technology*

Abstract

This study evaluates the environmental impacts of using bio-oil co-firing fuel (BCF) for power generation. Life cycle emissions of hazardous air pollutants are estimated and broken down based where the emissions occur. A case study is also conducted to evaluate the environmental and health impacts of replacing 10% of coal electricity with BCF electricity in the United States. The results show that BCF electricity decreases the emissions of SOx and primary $PM_{2.5}$ compared to coal electricity, but in the same time increases the emission of NH_3 from farming activities. Air quality simulation results suggest that replacing 10% of coal electricity with BCF electricity results in lower annual average concentration of $PM_{2.5}$ in most areas in the United States. Exceptions are the Midwest corn-belt and the southern coast where fertilizer plants are located. Overall $PM_{2.5}$ exposures are reduced by 11 tonne/yr. Total death attributable to $PM_{2.5}$ exposures is reduced by 709 deaths/year.

Introduction

Biofuels have attracted tremendous attention in recent years due to the fact that climate change resulting from greenhouse gases emitted from combustion of fossil fuels becomes a major social concern [1-3]. In order for biofuel to succeed in the competition between fossil fuels, it is important to understand not only its economics, but also its

environmental and social impacts. Life cycle analysis (LCA) has been extensively used to quantify the environmental impacts of biofuel production systems [4, 5]. Greenhouse gas (GHG) emissions is one of the major environmental concerns associated with transportation fuel consumption. Significant research has been done to quantify the net GHG emission for a variety of biofuel production pathways [6-8]. The GHG emissions, together with the result of techno-economic analysis, gives the decision makers a more comprehensive understanding of the particular biofuel production system under investigation.

There are also impacts that biofuel production and consumption has on the society and the environment as well, among which is Hazardous Air Pollutant (HAP) emissions. HAP, also known as toxic air pollutants, are suspected to cause cancer or other serious health effects such as reproductive effects or birth defects, or adverse environmental effects [9]. HAP emissions are regulated by EPA through National Emission Standards for Hazardous Air Pollutants (NESHAP) [10].

Particulate Matter (PM) refers to particles found in air, including dust, dirt, soot, smoke, and liquid droplets [11]. Particles less than 2.5 micrometers in diameter ($PM_{2.5}$) are referred to as “fine” particles and are believed to pose the greatest health risks due to the fact that their small size enables them to lodge deeply into the lungs [11].

$PM_{2.5}$ may result from direct emission; it may also derive from other pollutants such as Volatile Organic Compounds (VOC), SO_x, NO_x, and Ammonia (NH_3) [12]. The particles formed from chemical reactions of other pollutants are also called “secondary $PM_{2.5}$”. In order to quantify $PM_{2.5}$ emissions from biofuel production and consumption, it is essential that both directly emitted and secondary $PM_{2.5}$ are taken into account.

Distinct from GHGs which are stable after emission and can stay in the atmosphere for many years, these HAPs ($PM_{2.5}$, VOC, SO_x, NO_x, NH_3) evolves via chemical reactions [13]. Hence it is important to consider the location of emissions so that meteorological and geographical information can be integrated when considering evolution of the emissions.

Although biofuels have advantage in GHG emissions over traditional petroleum fuels when considering the CO_2 fixed during plant growth. It is still worth investigation whether biofuels also cause less emissions of other HAPs. Tessum et al. [14] developed a spatially and temporally explicit life cycle inventory of air pollutants and analyzed the emissions from gasoline, first generation ethanol produced from corn grain, and second generation ethanol produced from corn stover. It is concluded that life cycle $PM_{2.5}$ emissions are higher for ethanol from corn grain than for ethanol from corn stover. Hill, et al. quantified the life cycle $PM_{2.5}$ emissions from gasoline, corn ethanol and cellulosic ethanol and concluded that cellulosic ethanol provides health benefits from $PM_{2.5}$ reduction [15].

Fast pyrolysis is regarded a promising way to convert biomass into useful end products including biofuels and biochemicals. It refers to the process in which biomass is converted to liquid (bio-oil), soilds (bio-char) and gas products in the absence of oxygen at medium temperature [16]. Brown et al. [17, 18] developed a system that recovers bio-oil as five stage fractions (SF) with distinctive physical and chemical properties to facilitate further upgrading of the fractions according to their unique composition and properties. The high-boiling-point heavy ends, which consists mostly of phenolic oligomers and sugars, can then be used to form a bio-oil co-firing fuel (BCF)

after treating at 105 ^{o}C to remove water contents [19, 20]. Dang et al. [21] analyzed economics and GHG emissions of co-firing BCF and coal for power generation, concluding that it is promising in reducing GHG emission from electricity produced from coal power plants [21]. It is also economically competitive to conventional coal electricity if carbon price reach is higher than $67 per metric ton.

However, emissions of other HAPs that may result from burning BCF with coal has not been reported. It is necessary to evaluate HAPs emissions from BCF electricity generation with coal electricity to quantify the impact of replacing part of coal with BCF for power generation. Coal has been the primary energy source in the United States in the past decades. It is only until recently has coal been overtaken by natural gas in the power generation sector [22, 23]. Coal-generated power emits more pollutant than electricity generated from other sources such as natural gas and other renewable energy sources [24]. Despite the advantage of reduced CO_2 emission, it is also important to quantify emission of other pollutants involved in the process of electricity generation from BCF combustion.

This analysis quantifies life cycle HAPs emission from power generation by combusting BCF. The results are compared with emissions from electricity generation from coal power plants. The emissions of electricity generation from both BCF and coal combustion are broken down into subprocesses according to where the emissions occur. A case study is then developed to quantify the HAPs emissions across the contiguous United States by allocated emissions of each subprocess to corresponding locations.

Methodology

Life cycle assessment of BCF production and electricity generation

This analysis utilized the same system described in [21]. Corn stover is employed as the feedstock. It is then pyrolyzed and recovered as heavy, middle, and light ends with decreasing boiling point. The heavy ends are then treated at 105 ^{o}C for 1.75 hours to form BCF which is then combusted for electricity generation. **Figure 1** shows the process diagram. In this analysis, the middle ends are also combusted for increased power generation. However, it may be used for other purposes such as hydrogen production via steam reforming. The Greenhouse Gases, Regulated Emissions, and Energy Use in Transportation Model (GREET) developed by the Argonne National Laboratory was used to conduct LCA for the process [25].

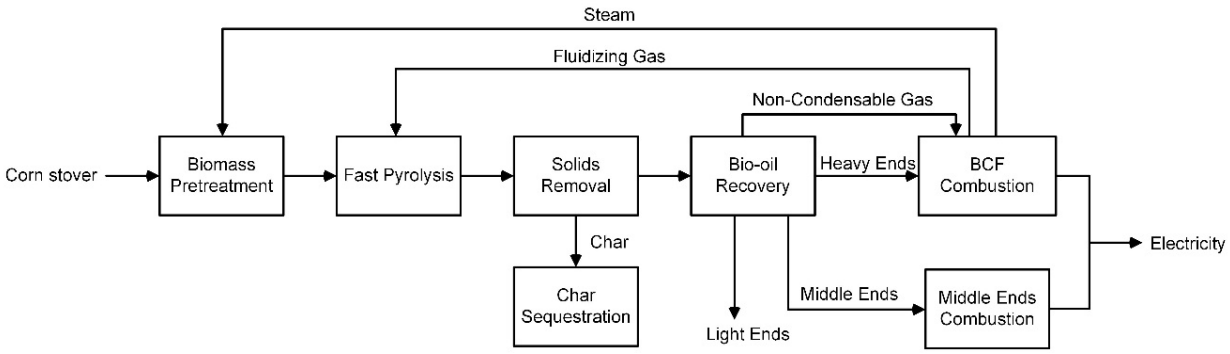

Figure 1 Process diagram of coal generation from BCF combustion.

Emission from combustion of BCF is not available in literature. It is estimated based on the composition of BCF. **Table 1** shows properties of BCF in comparison with various types of coal [20, 26]. BCF has much lower ash, sulfur and nitrogen content than coal. It is thus assumed that BCF combustion emits much lower SO_x and NO_x. Emissions of $PM_{2.5}$ from BCF combustion is also assumed low since it is found that

$PM_{2.5}$ emissions is correlated to the ash content of fuel. To be more specific, it is assumed BCF combustion emits one fourth of NO_x from combustion of coal and one tenth of $PM_{2.5}$. SO_x emission is calculated by GREET model based on the sulfur content in BCF. NH_3 emission is not included in the GREET model. Hence NH_3 emission from each subprocess is calculated separately [15, 27]. It is assumed that electricity is generated from coal or BCF combustion using steam turbine, which accounts for 99% of the electricity generated from coal-fired power plant [28]. Mass balance and energy balance data from Aspen Plus model is used as input to the GREET model. The main inputs to the GREET model is summarized in **Table 2**.

Case study

A case study is analyzed to see how BCF utilization may impact the emission pattern of the United States. In 2015, 4 trillion kWh of electricity was generated in the United States, among which around 33% was generated from coal combustion [23]. This case study evaluates the emission structure If 10% of electricity generated from coal combustion is replaced with that generated from fast pyrolysis and BCF combustion. It is done by process breakdown and emission allocation. Details about these steps are provided below.

Process breakdown

In order to track down the location of emission sources of HAPs, the GREET model is then broken down to more than 30 subprocesses based on the location of emission source, including corn farming, fast pyrolysis and electricity generation, production of ammonia, transportation of coal, etc. Overall over 92% of total emission is included in these subprocesses. Onsite emission (emission that excludes all upstream

and downstream process emissions) is evaluated for each subprocess and is later allocated according to capacity and locations of emission sources.

Table 1 Comparison between BCF and different types of coal

Fuel type	Moisture (wt%)	Ash (wt%)	Sulfur (wt%)	Nitrogen (wt%)	Calorific value (Btu/lb)
Anthracite (Pennsylvania)	4.3	9.6	0.8	0.9	12880
Low-volatile Bituminous (West Virginia)	2.6	5.4	0.8	1.3	14400
Medium-volatile Bituminous (Pennsylvania)	2.1	6.1	1.0	1.4	14310
High-volatile A Bituminous (West Virginia)	2.3	5.2	0.8	1.6	14040
High-volatile B Bituminous (Kentucky)	8.5	10.8	2.8	1.3	11680
High-volatile C Bituminous (Illinois)	14.4	9.6	3.8	1.0	10810
Subbituminous A (Wyoming)	16.9	3.6	1.4	1.2	10650
Subbituminous B (Wyoming)	22.2	4.3	0.5	1.0	9610
Subbituminous C (Wyoming)	26.6	5.8	0.6	0.9	8630
Lignite (North Dakota)	36.8	5.9	0.9	0.6	7000
BCF	0.72	0.47	0.01	0.3	12264

Table 2 Input and out for the fast pyrolysis and BCF electricity generation

Input	Output	
Corn stover	Electricity	Biochar
0.2962 kg	1 MJ	38.6840 g

Spatial allocation of emission

Geographical information of the locations of emission sources are collected for each subprocess, including the location of coal mines [29], coal power plants [30], corn farms, petroleum refineries [30], natural gas processing facilities [30], fertilizer production facilities [31], sulfuric acid production facilities [32], oil and gas fields [33] etc. Production capacity information is also collected for these emission sources. The emission results for each subprocess is then allocated to each facility according to their relative capacity. For instance, a coal power plants producing 1% of total coal electricity in the United States would be allocated 1% of total emission of the coal mining subprocess.

In order to account for only domestic emissions occurred in contiguous U.S., import of major resources is taken into account to exclude emissions outside contiguous U.S. Domestic fraction of resources such as crude oil, sulfuric acid, fertilizers are listed in **Table 3**. Alaska and Hawaii production is excluded from the total domestic production.

Table 3 Domestic fraction of major resources

Resource	Domestic fraction (%)
Natural gas [34-36]	83.5
Crude oil [37, 38]	47.5
Sulfuric acid [14]	72.0
Phosphoric acid and rock [14]	85.0
All nitrogen fertilizers [14]	56.5
Potassium [14]	17.0

Transportation emission allocation

Emission from truck transportation is allocated using linear programming. First the shortest possible route between each pair of supplier and market are identified. The amount of transportation between each pair of supplier and market is then decided based on the optimal results of linear programming. In some cases, the numbers of suppliers and demands are so large (>1000), leading to more than a million pairs of suppliers and demands. In order to save running time, the suppliers and demands are grouped by states due to the constraint of computing power.

Air quality simulation

In order to simulate formation of secondary $PM_{2.5}$, detailed air quality simulation was performed with InMAP (Intervention Model for Air Pollution) [39]. InMAP is a reduced complexity air quality model for estimating the air pollution health impacts of emission reductions [39]. It was chosen in this study over detailed Chemical Transportation Models (CTMs) for the reason that it provides several desirable features. First of all, InMAP provides estimates of air pollution health impacts resulting from

marginal changes in pollutant emissions, which suits the goal of this study. Secondly, InMAP significantly reduces computational cost relative to traditional CTMs while providing good predictive accuracy. Running InMAP also does not require expertise in air pollution models, facilitating utilization by non-experts such as scientists and policymakers. In order to focus on human exposures, InMAP features a variable resolution grid according to population density. High resolution grids are used in high-population areas while lower resolution grids are used in less densely populated areas. The output of InMAP is a shapefile with a number of attribute columns including estimated annual-average changes in primary and secondary $PM_{2.5}$ concentrations attributable to annual changes in precursor (primary $PM_{2.5}$, SO_x, NO_x, VOCs, and NH_3) emissions, and number of deaths attributable to $PM_{2.5}$. A detailed introduction of InMAP and its performance compared to traditional CTMs can be found in [39].

Results and discussion

Life cycle assessment and process breakdown

Table 4 shows life cycle inventory results of electricity generation from BCF combustion. Life cycle inventory results of coal electricity is also listed for comparison. It can be seen that electricity from BCF combustion emits significantly less SO_x and $PM_{2.5}$. NO_x emissions are quite similar to coal electricity. VOC and NH_3 emissions are increased by generating electricity from BCF. **Figure 2** shows the result of LCA of electricity generated from BCF and coal. It can be seen that each subprocess contribute differently to HAP emissions. Corn farming is the major contributor of NO_x and emission. Around 30% of NO_x and more than 90% of NH_3 are emitted on corn farms. Major source of SO_x emission comes from sulfuric acid production. Fast pyrolysis and combustion of

BCF also leads to some NOx and SO_x emissions. For traditional coal electricity, coal combustion is the major source of emission for NO_x, SO_x, and $PM_{2.5}$, while coal mining emits most part of VOC and NH_3. In general, using BCF as a fuel for electricity generation mitigates onsite emission of electricity generation, at the cost of increasing upstream emissions. NO_x emission from the two processes are roughly the same (<1% difference). BCF electricity incurs much lower SO_x emission in its life cycle (<20% of coal electricity), with the most significant contributor being sulfuric acid production. The low SO_x emission from BCF electricity is mainly because the low S content in BCF. BCF electricity causes 30% higher VOC emission than coal electricity. It is worth noting that the majority of VOC emission comes from the upstream process including fertilizer production and farming activities. The actual onsite VOC emission is pretty close with <1% difference. Emission of fine particulate matter from BCF electricity is 66% higher than that from coal electricity. The actual onsite emission of $PM_{2.5}$ is more than 10 times higher than that from coal electricity.

Table 4 Life cycle inventory results (g/MJ)

	VOC	NO_x	$PM_{2.5}$	SO_x	NH_3
BCF electricity	0.02932	0.1387	0.01033	0.1237	0.1072
Coal electricity	0.02258	0.1399	0.01714	0.6688	4.554e-4

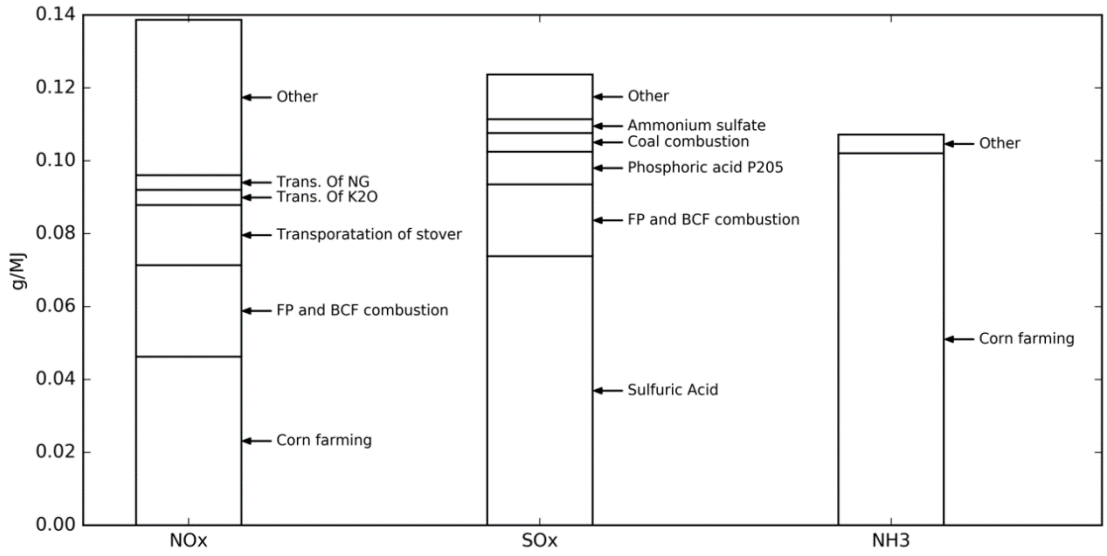

(a)

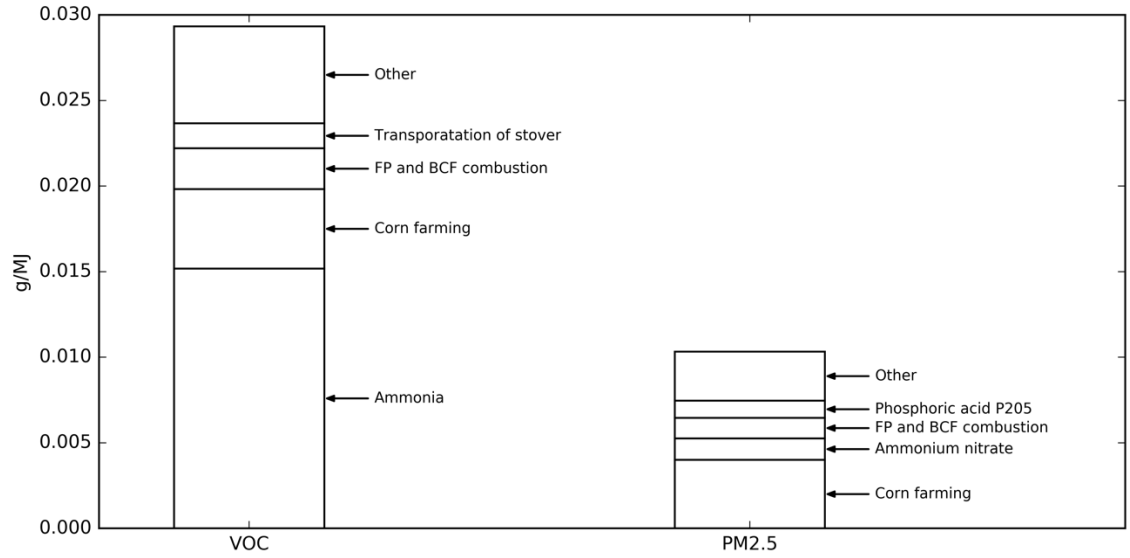

(b)

Figure 2 Breakdown of BCF electricity emissions and coal electricity emissions. (a) and (b) shows life cycle inventory results of BCF electricity generation; (c), (d) and (e) shows life cycle inventory results of coal electricity generation.

Figure 2 continued

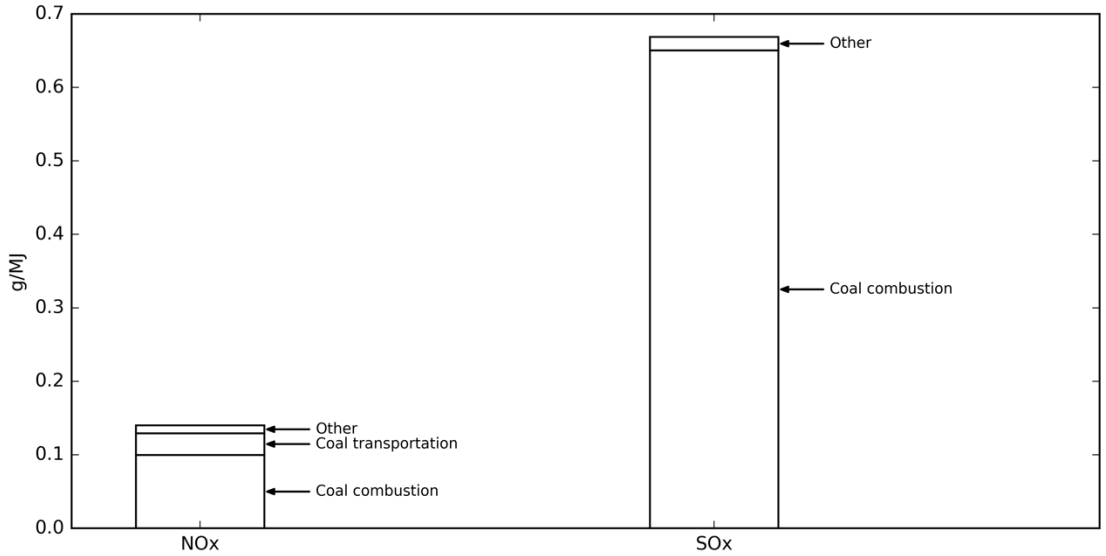

(c)

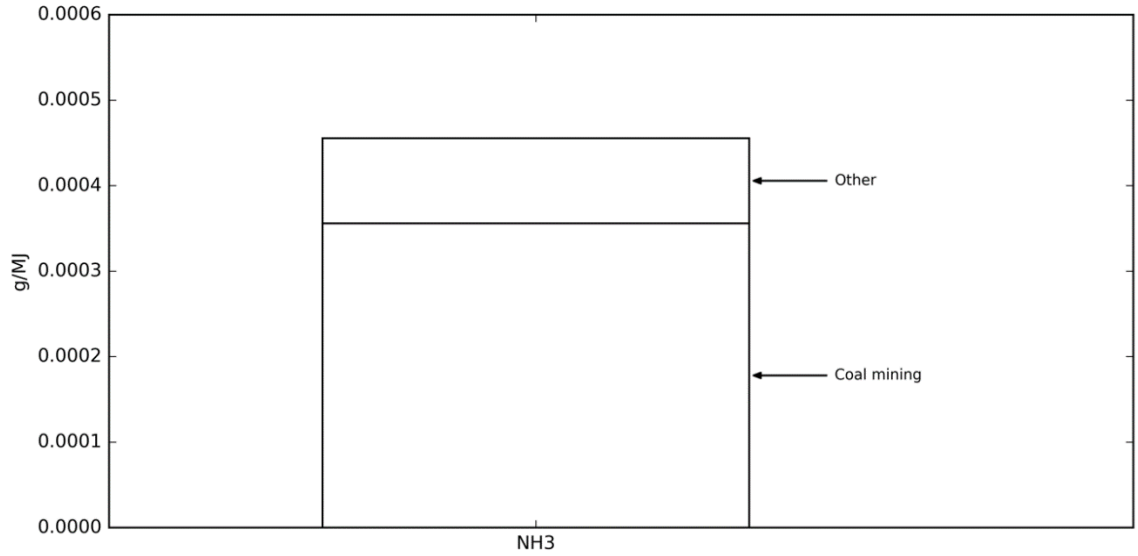

(d)

Figure 2 continued

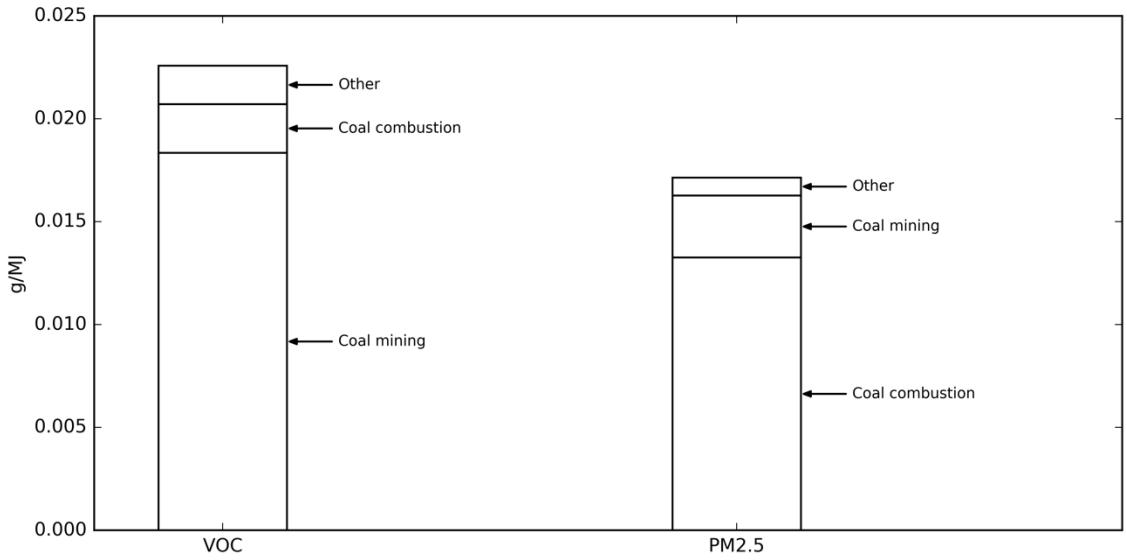

(e)

Case study

HAPs evolve into other pollutants after being emitted. The evolution involves chemical reactions that are affected by reactant concentration (amount of emission) and meteorological conditions such as temperature, wind speed, etc. It is therefore crucial to identify both the amount and location of the emissions. In this case study, it is assumed that 10% of coal electricity is replaced with BCF electricity in order to evaluate the impact of BCF utilization in power sector on the emission pattern in the United States.

Allocation of emissions

Emissions of each of the subprocess of the life cycle is associated with location of the emission sources. For instance, emissions from coal mining take place at coal mines; emissions from fertilizer production happen in the fertilizer plants; emissions related to fertilizer production and other farming activities occur at corn farms. Total emissions of each subprocess is first calculated, and then allocated to each location

based on their capacities. For instance, a plant producing 1% of ammonia of the total production of the country is allocated 1% of the total emissions from ammonia production. The emission allocated to each source is then further distributed to a staggered grid of 36 km by 36 km. This grid is one of the standard grids used in the air quality modeling software CMAQ [40]. Emissions of all the subprocesses is then added together to obtain the total emissions for each grid.

Figure 3 shows the subprocesses with the highest emissions for each pollutant. The center of the circles indicates the location of the emission sources and the area of the circles indicate the relative emission amount (i.e., the capacity of the source). Amount of emissions of each pollutant is also shown in the bar chart. It is clear that coal mines are concentrated in states of Wyoming, West Virginia, and Pennsylvania. The major emissions associated with coal electricity generation is coal mining and coal combustion, causing locations of coal mines and coal power plants the major victim of HAP emissions. Especially considering that most coal power plants are built close to coal mines to minimize transportation cost, the emission locations of coal mining and coal combustion is highly related. Emissions from corn farming activities are highly concentrated in the corn-belt, with the major pollutants being NO_x and NH_3. **Figure 3**(d) shows the emission from transportation of corn stover from corn farms to fast pyrolysis plants that are co-located with existing coal power plants. Transportation routes with darker lines have higher transportation loads, meaning that more corn stover is transported in this route. SO_x emission is mainly from sulfuric acid production facilities, which are located in Florida, and Louisiana.

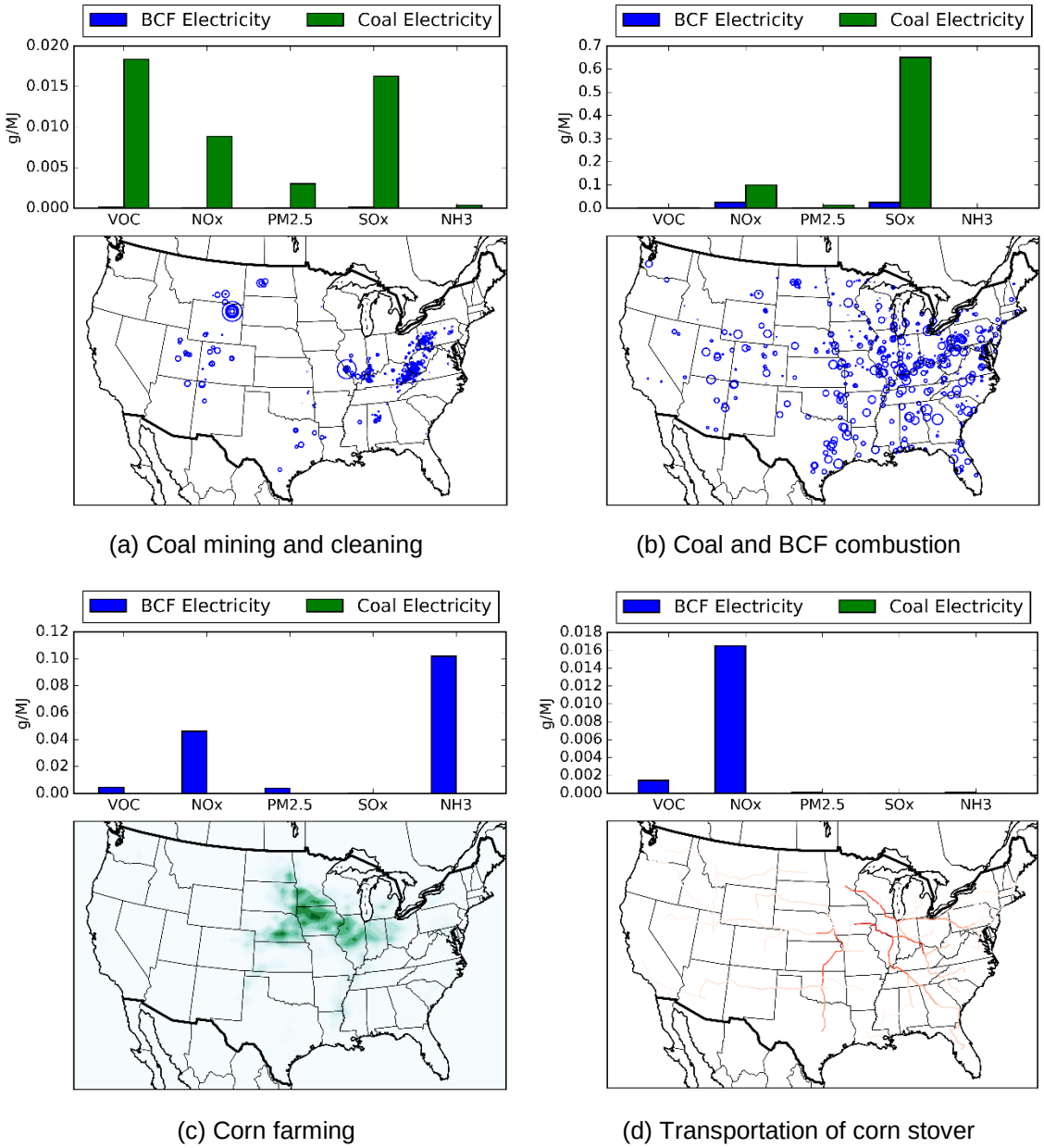

(a) Coal mining and cleaning

(b) Coal and BCF combustion

(c) Corn farming

(d) Transportation of corn stover

Figure 3 Emission allocation of some subprocesses.

Figure 3 continued

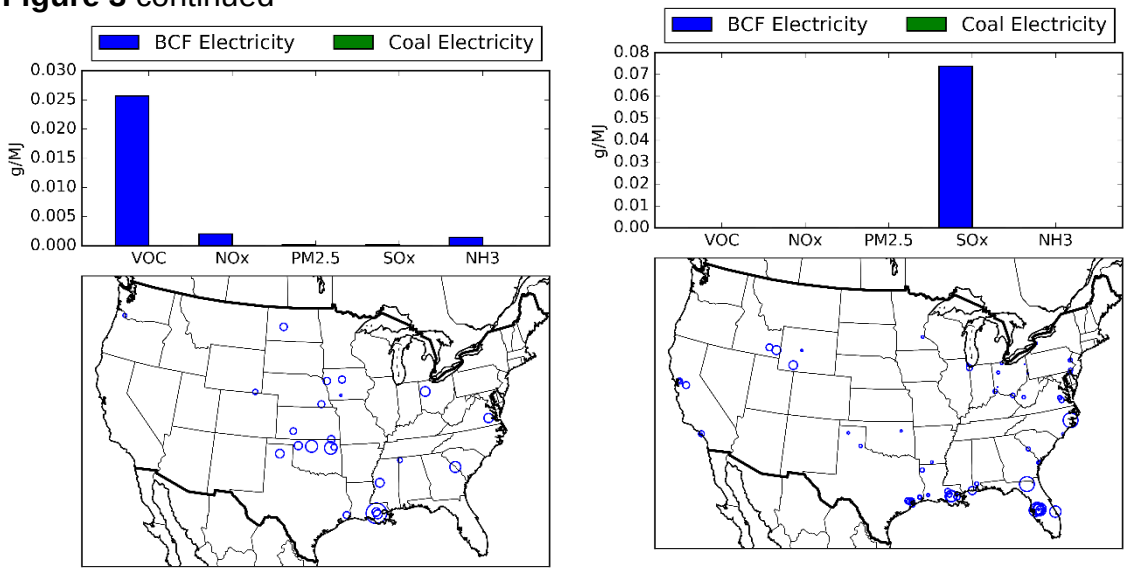

(e) Ammonia production

(f) Sulfuric acid production

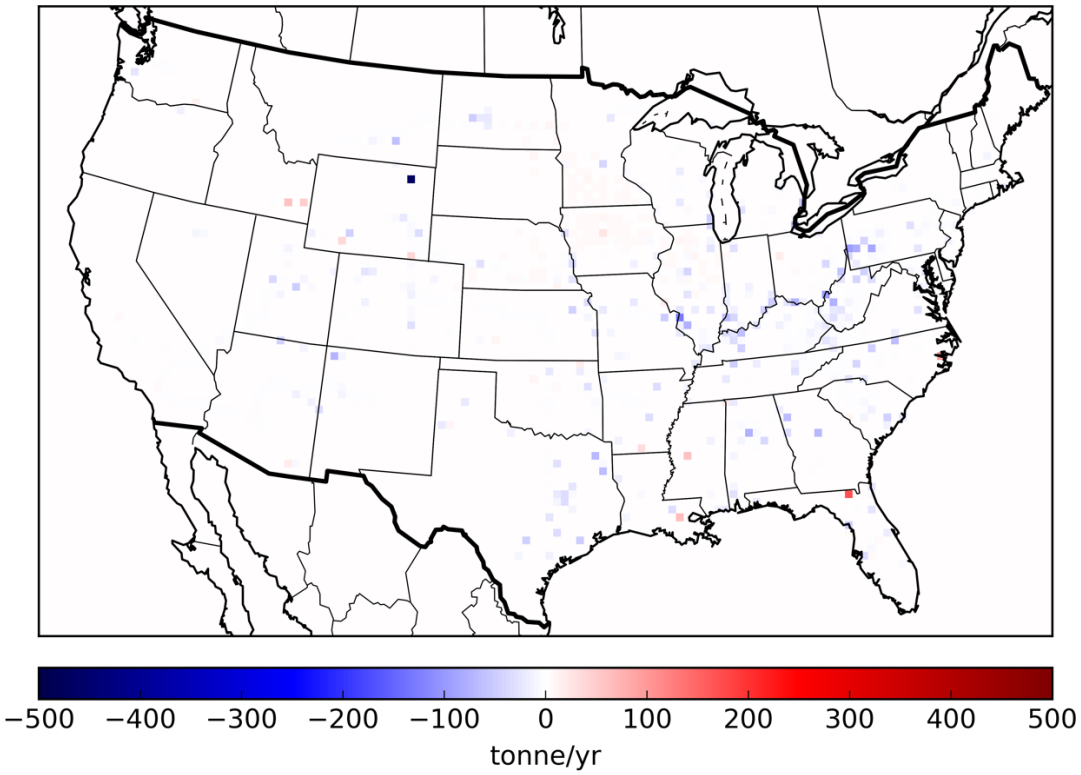

(a) PM2.5 emissions. Total net emission change = -4232 tonne/yr

Figure 4 Net emission change results of case study.

Figure 4 continued

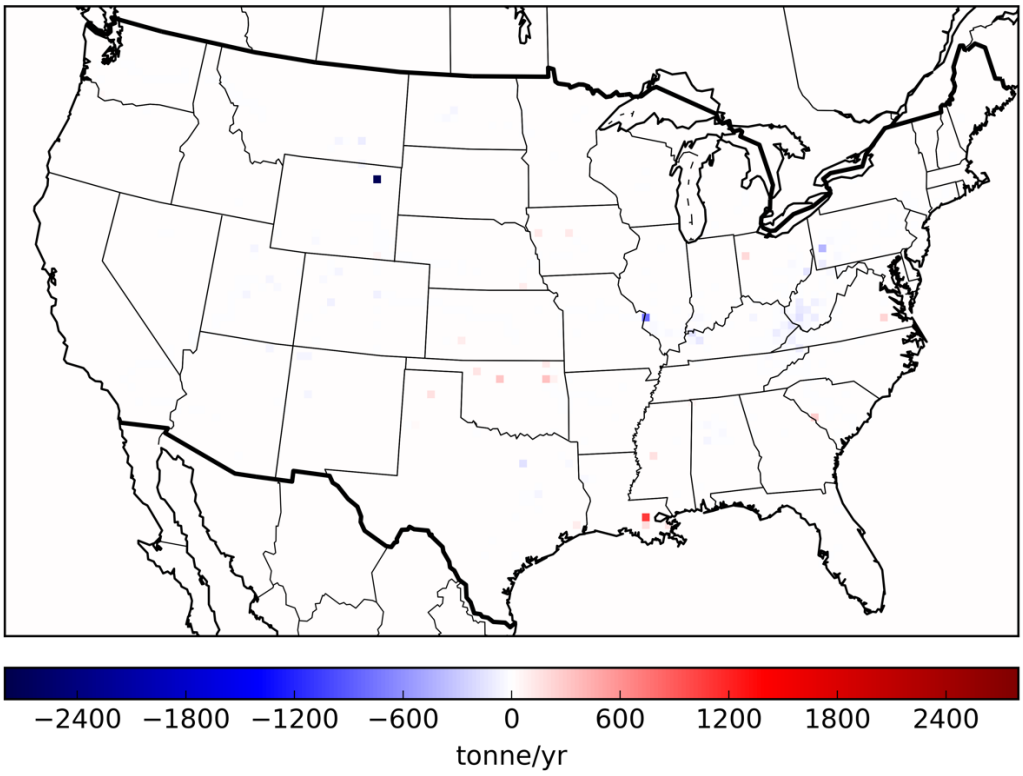

(b) VOC emissions. Total net emission change = -878 tonne/yr

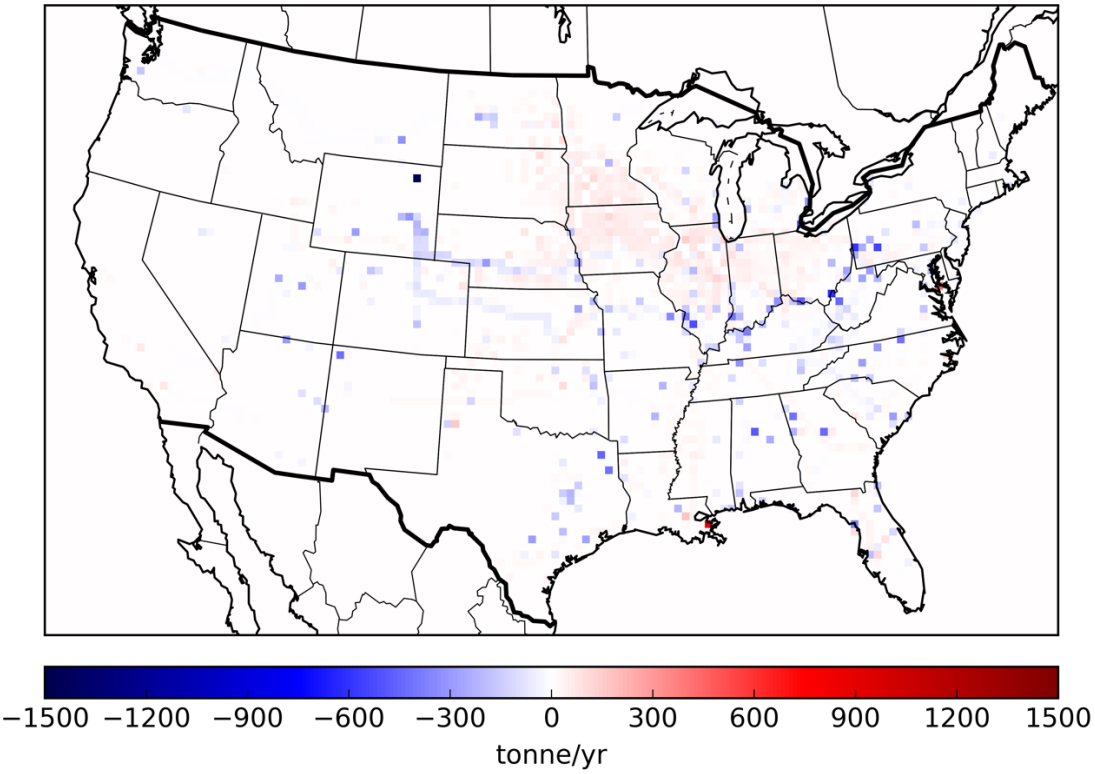

(c) NOx emissions. Total net emission change = -13,106 tonne/yr

Figure 4 continued

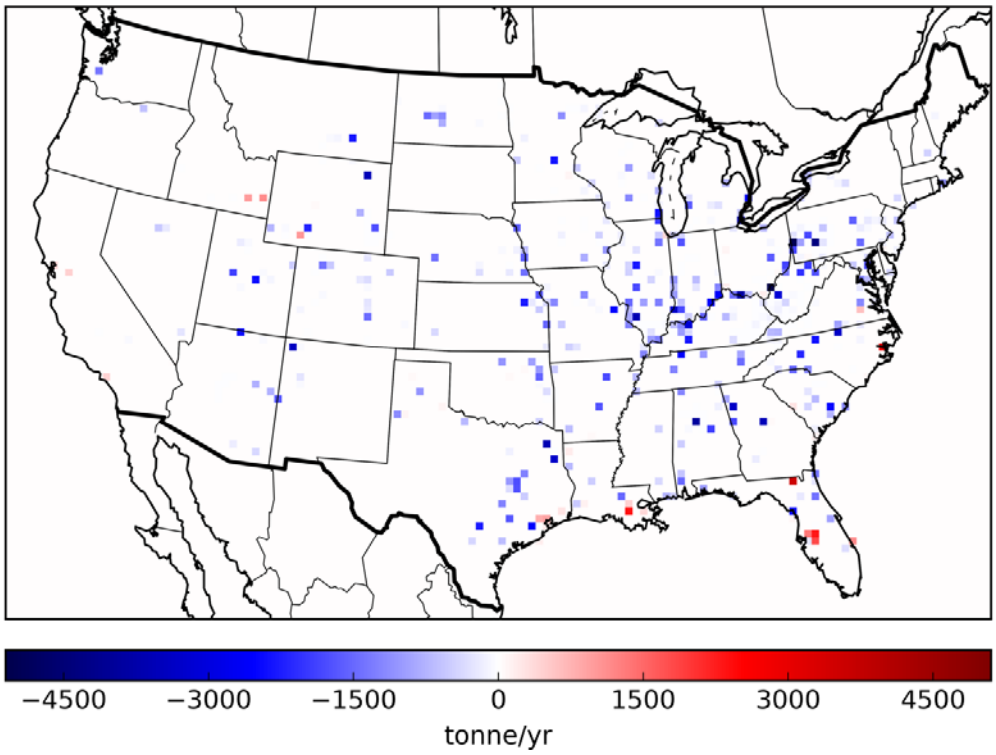

(d) SO_x emissions. Total net emission change = -270,886 tonne/yr

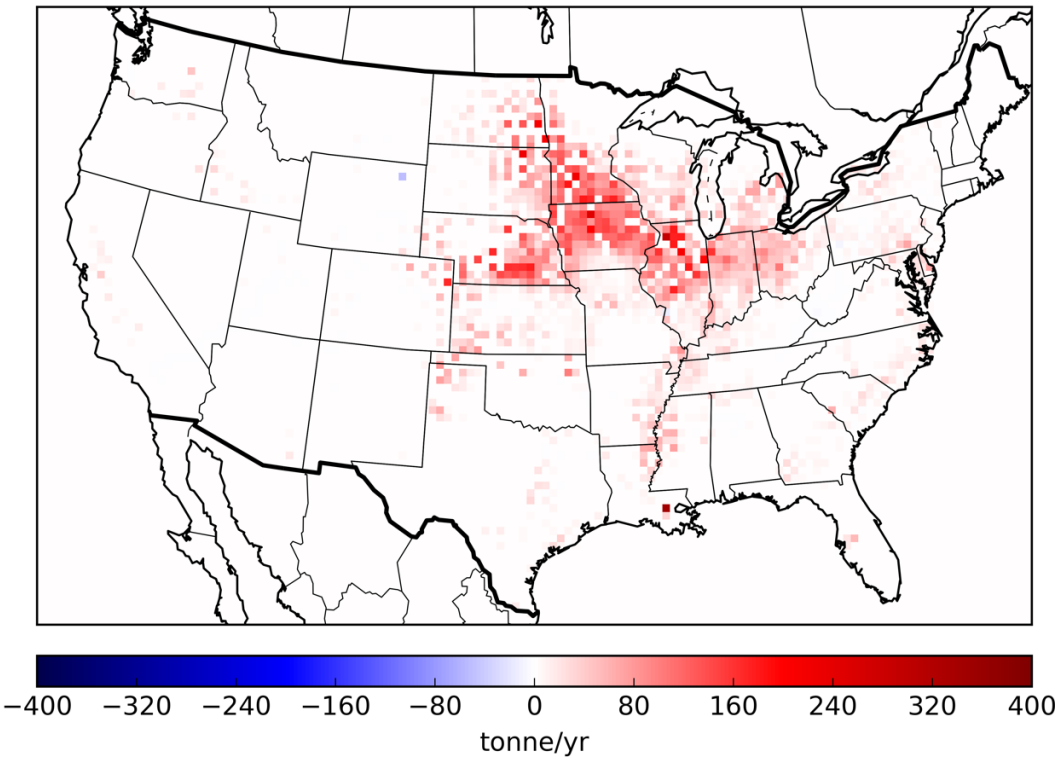

(e) NH_3 emissions. Total net emission change = 49,749 tonne/yr

Figure 4 shows the net change of air pollutant emissions under the assumption that 10% of U.S. coal power is replaced with BCF power. It shows that replacing coal electricity with BCF electricity reduces emissions of SO_x significantly and $PM_{2.5}$, VOC, and NO_x slightly. Nonetheless emission of NH_3 increases drastically as a consequence of fertilizer nitrification. To be more specific, most areas see reduction of $PM_{2.5}$ emission owing to reduction in emissions related to coal mining and coal combustion. However, $PM_{2.5}$ emissions in corn-belt slightly increases as a result of intensified farming activities. Areas where sulfuric acid plants are located also see increased $PM_{2.5}$ emissions since more sulfuric acid is used for fertilizer production.

NO_x emission also shows similar trends. Since life cycle emission of NO_x is similar for coal and BCF electricity, change of NO_x emission may be interpreted in a way that emission from coal combustion is transferred to corn farming, BCF combustion, and transportation of corn stover. Major increase in NO_x is seen in the Midwest where a large amount of corn is produced. Areas where fertilizer plants are located also see increase in NO_x emission while other areas benefit from BCF electricity thanks to its lower demand of fossil fuels such as petroleum, natural gas, and coal.

Replacement of coal electricity by BCF electricity causes drastic increase in NH_3 emission. The most significant contributor to NH_3 emission is farming activities. Emission of NH_3 in the process of fertilizer production is another reason of increased NH_3 emission. The only exception is that NH_3 emissions decrease in the northeastern corner of Wyoming where several large coal mines are located as seen in **Figure 3** Wyoming is the largest coal producer in the U.S., producing about 40% of coal in the U.S. [41]. Therefore, BCF electricity generation causes significant reduction of coal

mining activities and thus leads to decreased NH_3 emission in this area. As a matter of fact, emissions of all the five categories of pollutants decrease in this area.

Air quality simulation and health impact evaluation

The results of emission allocation serve as input to InMAP. The results of InMAP simulation is shown in **Figure 5**. It is obvious that replacing coal with BCF changes the emission pattern of the United States. Reduction in total annual average $PM_{2.5}$ concentrations is seen in most areas, especially where coal mines and coal power plants are located. Slight reduction is also seen in Mountain West region due to abatement of coal mining activities. Increase in total annual average $PM_{2.5}$ concentrations mainly occurs in the corn-belt, which is attributable to increased farming-activity-related emissions, especially NH_3 emissions as seen in **Figure 4**(e). $PM_{2.5}$ concentrations also increase in some areas in the southern States including Florida, Louisiana, and Texas where large sulfuric acid plants are located. Overall $PM_{2.5}$ exposures are reduced by 11 tonne/yr.

InMAP also reports the health impacts of the emissions in the form of number of deaths attributable to exposures to $PM_{2.5}$. The results are shown in Figure 6. The death distribution displays a pretty similar profile as $PM_{2.5}$. Total death attributable to $PM_{2.5}$ exposures is reduced by 709 deaths/year.

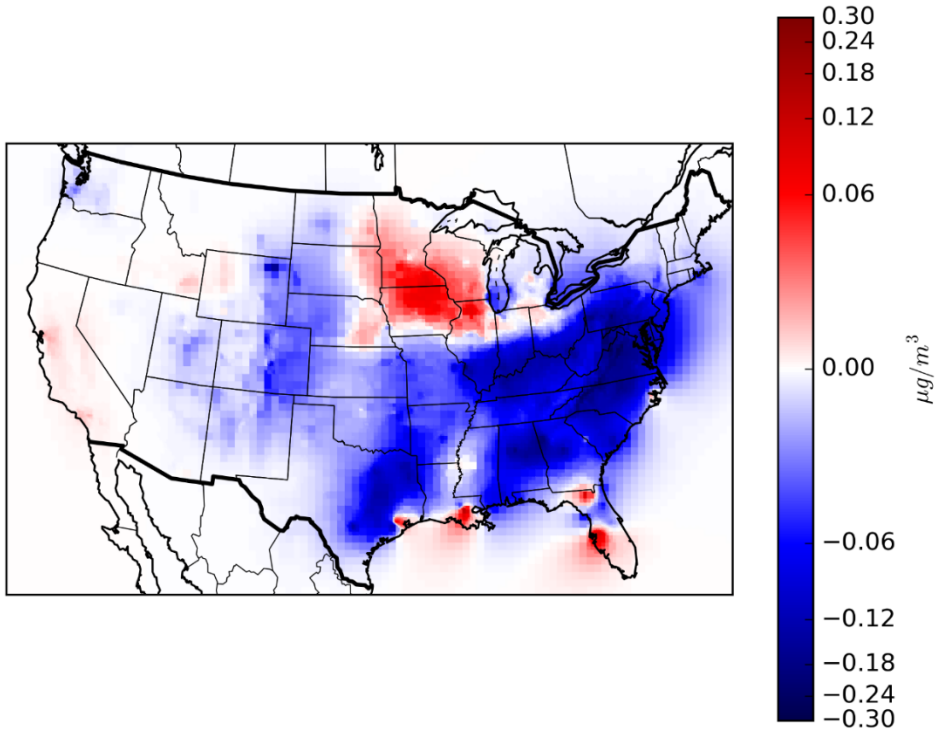

Figure 5 Simulated marginal change in annual average $PM_{2.5}$ concentrations.

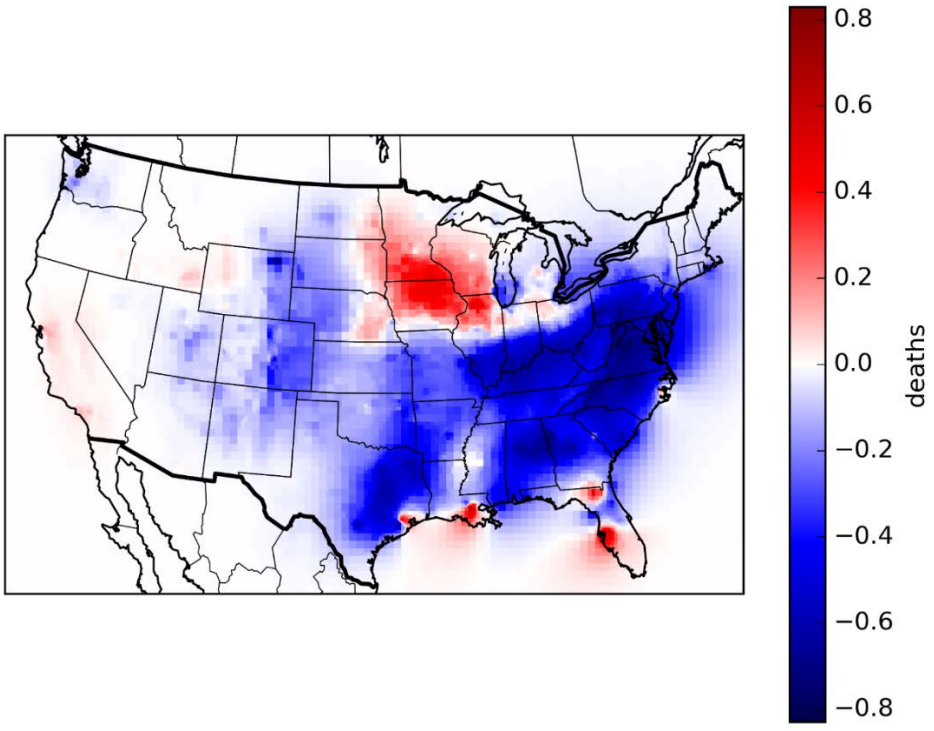

Figure 6 Simulated deaths attributable to exposures to $PM_{2.5}$.

Conclusion

BCF electricity generation has great potential of replacing part of coal electricity with the benefit of reduced emission of air pollutants such as SO_x and $PM_{2.5}$. However, it also causes increased emission of NH_3 due to more intense farming activities. Actually this is also a common downside for all biofuels derived from agricultural crops. Reduction of NH_3 emissions from fertilizer nitrification may reduce life cycle NH_3 emissions of BCF electricity significantly. The results of the case study show the extra information obtained from including geographical information into LCA results. The results indicate that the major beneficiaries of BCF electricity are the areas where coal mines and coal power plants are located. On the contrary, corn farms and fertilizer producing areas will see increased emissions. A topic for future research would be to evaluate annual emission concentrations by run air quality models using these results.

Annual average concentration of $PM_{2.5}$ was simulated with InMAP. The results show reductions in the eastern and southern regions where coal mines and coal power plants are located. Exceptions include areas in Florida, Louisiana, and Texas, where large fertilizer plants are located. Major increase in $PM_{2.5}$ is seen in the Midwest corn-belt, contributed by intensified farming activities. Distribution of deaths attributable to $PM_{2.5}$ exposures also shows a similar profile as $PM_{2.5}$ concentrations. Overall replacing coal with BCF results in reductions in both $PM_{2.5}$ exposures and related deaths.

References

[1] Cherubini F, Bird ND, Cowie A, Jungmeier G, Schlamadinger B, Woess-Gallasch S. Energy- and greenhouse gas-based LCA of biofuel and bioenergy systems: Key issues, ranges and recommendations. Resources, Conservation and Recycling 2009;53(8):434-47.

[2] Schneider UA, McCarl BA. Economic Potential of Biomass Based Fuels for Greenhouse Gas Emission Mitigation. Environmental and Resource Economics 2003;24(4):291-312.

[3] Tilman D, Socolow R, Foley JA, Hill J, Larson E, Lynd L, et al. Beneficial Biofuels—The Food, Energy, and Environment Trilemma. Science 2009;325(5938):270-1.

[4] Curran MA. Environmental life-cycle assessment. Int J Life Cycle Assess 1996;1(3):179-.

[5] Klöpffer W. Life cycle assessment. Environ Sci & Pollut Res 1997;4(4):223-8.

[6] Dang Q, Yu C, Luo Z. Environmental life cycle assessment of bio-fuel production via fast pyrolysis of corn stover and hydroprocessing. Fuel 2014;131:36-42.

[7] Han J, Elgowainy A, Dunn JB, Wang MQ. Life cycle analysis of fuel production from fast pyrolysis of biomass. Bioresour Technol 2013;133:421-8.

[8] Zhang Y, Hu G, Brown RC. Life cycle assessment of commodity chemical production from forest residue via fast pyrolysis. Int J Life Cycle Assess 2014;19(7):1371-81.

[9] EPA. What are Hazardous Air Pollutants? 2015. (Available at: https://www.epa.gov/haps/what-are-hazardous-air-pollutants)

[10] EPA. Asbestos NESHAP. 2016. (Available at: https://www.epa.gov/asbestos/asbestos-neshap)

[11] EPA. Fine Particle (PM2.5) Designations. 2016. (Available at: https://www3.epa.gov/pmdesignations/basicinfo.htm)

[12] Hodan WM, Barnard WR. Evaluating the Contribution of PM2. 5 Precursor Gases and Re-entrained Road Emissions to Mobile Source PM2. 5 Particulate Matter Emissions. 2004.

[13] Hallquist M, Wenger JC, Baltensperger U, Rudich Y, Simpson D, Claeys M, et al. The formation, properties and impact of secondary organic aerosol: current and emerging issues. Atmos Chem Phys 2009;9(14):5155-236.

[14] Tessum CW, Marshall JD, Hill JD. A Spatially and Temporally Explicit Life Cycle Inventory of Air Pollutants from Gasoline and Ethanol in the United States. Environmental Science & Technology 2012;46(20):11408-17.

[15] Hill J, Polasky S, Nelson E, Tilman D, Huo H, Ludwig L, et al. Climate change and health costs of air emissions from biofuels and gasoline. Proceedings of the National Academy of Sciences 2009;106(6):2077-82.

[16] Brown RC, Stevens C. Thermochemical processing of biomass: conversion into fuels, chemicals and power: John Wiley & Sons; 2011.

[17] Pollard AS, Rover MR, Brown RC. Characterization of bio-oil recovered as stage fractions with unique chemical and physical properties. J Anal Appl Pyrol 2012;93:129-38.

[18] Rover MR, Johnston PA, Whitmer LE, Smith RG, Brown RC. The effect of pyrolysis temperature on recovery of bio-oil as distinctive stage fractions. J Anal Appl Pyrol 2014;105:262-8.

[19] Zhang Y, Brown TR, Hu G, Brown RC. Techno-economic analysis of monosaccharide production via fast pyrolysis of lignocellulose. Bioresour Technol 2013;127(0):358-65.

[20] Rover M. Personal Communication. 2016.

[21] Dang Q, Mba Wright M, Brown RC. Ultra-Low Carbon Emissions from Coal-Fired Power Plants through Bio-Oil Co-Firing and Biochar Sequestration. Environmental Science & Technology 2015;49(24):14688-95.

[22] Mathiesen K. Gas surges ahead of coal in US power generation. 2015. (Available at: https://www.theguardian.com/environment/2015/jul/14/gas-surges-ahead-of-coal-in-us-power-generation)

[23] EIA. What is U.S. electricity generation by energy source? 2016. (Available at: https://www.eia.gov/tools/faqs/faq.cfm?id=427&t=3)

[24] Jaramillo P, Griffin WM, Matthews HS. Comparative Life-Cycle Air Emissions of Coal, Domestic Natural Gas, LNG, and SNG for Electricity Generation. Environmental Science & Technology 2007;41(17):6290-6.

[25] Argonne National Laboratory. GREET Model. 2015. (Available at: https://greet.es.anl.gov)

[26] EIA. Coal Data: A Reference. 1995. (Available at: http://webapp1.dlib.indiana.edu/virtual_disk_library/index.cgi/4265704/FID1578/pdf/coal_nuc/006493.pdf)

[27] Ergudenler A, Jennejohn D, Edwards W. Heavy-Duty Diesel Vehicle Emissions in Greater Vancouver. Greater Vancouver Regional District and Levelton Consultants Ltd; 2005.

[28] Cai H, Wang M, Elgowainy A, Han J. Updated greenhouse gas and criteria air pollutant emission factors and their probability distribution functions for electricity generating units. Argonne National Laboratory (ANL); 2012.

[29] Laboratory NRE. Coal Production by MSHA ID, Mine Operation, Union Status, and Average Number of Employees and Hours, 2008. 2015/08/26 ed: National Renewable Energy Laboratory; 2015.

[30] EIA. Layer Information for Interactive State Maps. 2016. (Available at: https://www.eia.gov/maps/layer_info-m.cfm)

[31] IFDC. North America Fertilizer Capacity. 2015.

[32] ICIS. Chemical Profile Sulfuric Acid (virgin). 2005. (Available at: http://www.icis.com/resources/news/2005/12/08/189337/chemical-profile-sulfuric-acid-virgin-/)

[33] EIA. Top 100 U.S. Oil and Gas Fields. 2015. (Available at: https://www.eia.gov/naturalgas/crudeoilreserves/top100/)

[34] EIA. Natural Gas Gross Withdrawals and Production - Alaska. 2016. (Available at: https://www.eia.gov/dnav/ng/ng_prod_sum_dcu_sak_m.htm)

[35] EIA. Natural Gas Gross Withdrawals and Production. 2016.

[36] EIA. U.S. Natural Gas Imports by Country. 2016. (Available at: https://www.eia.gov/dnav/ng/ng_prod_sum_dcu_NUS_m.htm)

[37] EIA. Petroleum & Other Liquids. 2016. (Available at: http://www.eia.gov/petroleum/

[38] EIA. U.S. Imports by Country of Origin. 2016. (Available at: https://www.eia.gov/dnav/pet/pet_move_impcus_a2_nus_ep00_im0_mbbl_m.htm)

[39] Tessum C, Hill J, Marshall J. InMAP: a new model for air pollution interventions. Geoscientific Model Development Discussions (Online) 2015;8(10).

[40] EPA. Community Multi-scale Air Quality (CMAQ) Modeling System for Air Quality Management. 2016. (Available at: https://www.epa.gov/air-research/community-multi-scale-air-quality-cmaq-modeling-system-air-quality-management)

[41] EIA. Rankings: Coal Production, 2014. 2016. (Available at: https://www.eia.gov/state/rankings/#/series/48)

CHAPTER 6 CONCLUDING REMARKS AND FUTURE WORK

Summary

This dissertation displays a systematic platform for evaluating performance of biofuel production systems by considering both economic and environmental metrics. It also demonstrates the necessity of incorporating uncertainty analysis into the results.

Techno-economic analysis is helpful in identifying pathways that have great potential of producing economically competitive end products. It also assists in understanding cost structure and thus guiding research efforts to effectively reducing costs of investigated pathway.

Life cycle assessment on the other hand comprehensively evaluate life cycle environmental impact of a biofuel pathway. Greenhouse gas emission has been a hot topic in biofuel LCA. The results of Chapter 5 show that emission of other air pollutants should also be considered in biofuel LCA. Furthermore, it is important to also consider the locations of the emission sources. One important conclusion from Chapter 4 is that upstream emission from biomass cultivation is a major source of the life cycle emission of biofuels produced from agricultural crops.

The results of LCA and TEA provides policy makers valuable information in identifying the optimal pathway to stimulate. Nevertheless, inherent uncertainty is present in TEA and LCA results. Hence uncertainty analysis is necessary in order to provide robust results as well as to give the readers more comprehensive understanding of the results.

Future work

The pathway that TEA and LCA tackles is usually still at very early development stage and hence uncertainty of the results may be significant. It is thus necessary to develop a standard procedure to incorporate uncertainty analysis and to devise techniques to effectively reduce uncertainty. These techniques may include more effective and accurate data collection, or improved mathematical models of the process as more experience is gained and better understanding is achieved.

Monte Carlo simulation with random sampling is so far the most popular method of uncertainty analysis. It depends on the computing power of modern computers. However, cases still exist where a single run may take such long time that a simulation with tens of thousands of run would take too long to run. For instance, when a detailed process model is used to provide mass and energy balance for TEA and some process parameters are in the interested uncertain parameters. A single run would take too long if the process model is complex. On these occasions, it becomes imperative to adopt more efficient sampling methods such as Latin Hypercube Sampling. It would also be necessary to develop judgment when convergence of Monte Carlo simulation is reached.

The results of Chapter 5 also demonstrate the importance of geographical information incorporated LCA when considering HAPs emissions. Future research effort could work on using the results for detailed air quality simulation to better compare the two pathways.